

QUANTIFICATION OF VIRTUAL CHEMICAL PROPERTIES:
STRAIN, HYPERCONJUGATION, CONJUGATION, AND AROMATICITY

by

JUDY I-CHIA WU

(Under the Direction of Paul von Ragué Schleyer)

ABSTRACT

Highly important chemical concepts, like strain, hyperconjugation, conjugation, and aromaticity, are widely used to interpret the behavior of organic molecules, but are *virtual* (i.e., not directly measurable). This dissertation focuses on validating reliable quantum mechanical approaches for quantitative estimates of these virtual chemical properties and applying them to solve significant chemical problems. We are concerned with the simplest iconic organic molecules: cyclopropane, benzene, cyclobutadiene, cyclooctatetraene, and the polybenzenoid hydrocarbons. Cyclopropane's unexpectedly low ring strain (almost the same as that of cyclobutane) is due to substantial CCC geminal delocalization. Cyclooctatetraene (COT) is not representative of an unconjugated cyclic polyene. Instead, double hyperconjugation stabilizes the tub-shaped COT (D_{2d}), as well as other non-planar conjugated systems, and compensates for their diminished π conjugation. On the other hand, planar D_{4h} COT is net stabilized by π conjugation and only weakly anti-aromatic destabilized. Planar [4]annulenes in general are not very destabilized antiaromatically. Even cyclobutadiene is only modestly destabilized by antiaromaticity; its high heat of formation is mainly due to significant angle strain and Pauli repulsion between the pairs of C=C π bonds. Large $4n$ π electron polycyclic benzenoids and the higher dihydrodiazacenes

benefit from substantial π conjugation and can even display aromatic stabilization energies (ASE), of equal or greater magnitude, than their $4n+2$ π electron analogs. Aromaticity is very robust towards electronic and geometric perturbations. Hence, perfluorobenzene (C_6F_6) is as aromatic as benzene, while perfluorocyclobutadiene (C_4F_4) has only reduced antiaromaticity compared to cyclobutadiene, due to the twisting of its π system. This work further shows the effectiveness of the nucleus independent chemical shifts (NICS) as a “local” probe of aromaticity for substituted and fused-ring aromatic systems. Our computational findings provide valuable insight to the development of fundamental organic concepts.

INDEX WORDS: computational chemistry, hyperconjugation, electron delocalization, resonance energy, aromatic stabilization energy (ASE), substituent effects, nucleus independent chemical shifts (NICS), block-localized wave function (BLW)

QUANTIFICATION OF VIRTUAL CHEMICAL PROPERTIES:
STRAIN, CONJUGATION, HYPERCONJUGATION, AND AROMATICITY

by

JUDY I-CHIA WU

B.S., Tung-Hai University, Taichung, Taiwan, 2004

A Dissertation Submitted to the Graduate Faculty of The University of Georgia in Partial
Fulfillment of the Requirements for the Degree

DOCTOR OF PHILISOPHY

ATHENS, GEORGIA

2011

© 2011

Judy I-Chia Wu

All Rights Reserved

QUANTIFICATION OF VIRTUAL CHEMICAL PROPERTIES:
STRAIN, CONJUGATION, HYPERCONJUGATION, AND AROMATICITY

by

JUDY I-CHIA WU

Major Professor:	Paul von Ragué Schleyer
Committee:	Henry F. Schaefer III
	Robert J. Woods

Electronic Version Approved:

Maureen Grasso
Dean of the Graduate School
The University of Georgia
May 2011

DEDICATION

*To Keigo, Paul, my Parents,
and in memory of Gnocchi*

“It has often been said
there’s so much to be read,
you never can cram
all those words in your head.

So the writer who breeds
more words than he needs
is making a chore
for the reader who reads.

That's why my belief is
the briefer the brief is,
the greater the sigh
of the reader's relief is.

And that's why your books
have such power and strength.
You publish with shorth!
(Shorth is better than length.)”

-Theodor Seuss Giesel

a.k.a. “Dr. Seuss”

“All Hyperconjugation, All the Time.”

ACKNOWLEDGEMENTS

My deepest appreciation goes to many people who have helped me greatly in personal and scientific growth during the past six years. Most of all, I am in debt to Prof. Schleyer for the fine education he has given me. I thank him especially for changing my mind about chemistry. His nurturing of a good appetite for chemical discoveries as well as for elegant scientific writing has made a world of difference for me.

I thank my parents for the love, time, “goodie boxes,” and resources they have devoted to supporting my ups and downs all the time. Special thanks go to my Dad, whose guidance and 3M tips has been an essential part to my accomplishment. I also thank Keigo and Chad for wonderful friendship and many cheerful scientific and philosophical conversations. I’ve enjoyed so much learning and exploring chemistry (and Germany) together with them. I thank Keigo especially for being a great companion through many difficult times, for sharing my excitement for every new discovery, and for being a great mentor in helping me improve many presentations. I am grateful to Prof. Schaefer for his cheerful encouragements and for the valuable opportunities of meeting and observing many distinguished scientists at the CCQC. Clémence has been a wonderful role model. I would like to thank her for the time she has spent guiding me in many ways when I first joined the Schleyer group. I also thank Prof. Mo for many friendly and insightful discussions. Finally, I want to acknowledge Nattoh, Gnocchi, and Dexter for being my Athens family. They do a (almost) perfect job of distracting me from work when stubborn problems and a stubborn mind prevent me from going to bed on time.

TABLE OF CONTENTS

	Page
ACKNOWLEDGEMENTS	vi
LIST OF TABLES	xi
LIST OF FIGURES	xiii
 CHAPTER	
1 INTRODUCTION	1
2 WHY CYCLOOCTATETRAENE IS HIGHLY STABILIZED: THE IMPORTANCE OF “TWO-FOLD” (DOUBLE) HYPERCONJUGATION	5
2.1 ABSTRACT	6
2.2 INTRODUCTION	7
2.3 METHODS	17
2.4 ELECTRON DELOCALIZATION IN D_{2D} AND D_{4H} CYCLOOCTATETRAENE	20
2.5 THE INVERSION BARRIER OF CYCLOOCTATETRAENE	22
2.6 ANTIAROMATICITY IN D_{4H} CYCLOOCTATETRAENE	24
2.7 1,3-BUTADIENE ROTATION	26
2.8 OTHER MOLECULES WITH “TWO-FOLD” (DOUBLE) HYPERCONJUGATION	32
2.9 CONCLUSIONS	36
2.10 REFERENCES	39

3	IS CYCLOBUTADIENE REALLY DESTABILIZED BY ANTIAROMATIVITY?	
	AN ALTERNATIVE EXPLANATION BASED ON SIMPLE STRAIN	
	CONSIDERATIONS	47
	3.1 ABSTRACT	48
	3.2 INTRODUCTION	48
	3.3 EVIDENCE FOR HIGH RING STRAIN IN THE SIGMA-FRAMEWORK	
	OF CBD	52
	3.4 BLOCK-LOCALIZED WAVEFUNCTION ANALYSES	55
	3.5 DISCUSSIONS	56
	3.6 CONCLUSIONS	58
	3.7 REFERENCES	59
4	WHY IS THE STRAIN ENERGY OF CYCLOPROPANE SO LOW?	61
	4.1 ABSTRACT	62
	4.2 INTRODUCTION	62
	4.3 METHODS	70
	4.4 THE MISSING STRAIN IN CYCLOPROPANE	71
	4.5 GEMINAL DELOCALIZATION AND SUBSTITUENT EFFECTS	75
	4.6 NUCLEUS INDEPENDENT CHEMICAL SHIFTS	79
	4.7 CONCLUSIONS	82
	4.8 REFERENCES	83
5	THE EFFECT OF PERFLUORINATION ON THE AROMATICITY OF BENZENE	
	AND HETEROCYCLIC SIX MEMBERED RINGS	86
	5.1 ABSTRACT	87

5.2 INTRODUCTION	87
5.3 COMPUTATIONAL DETAILS	90
5.4 NUCLEUS INDEPENDENT CHEMICAL SHIFTS	91
5.5 EXTRA CYCLIC RESONANCE ENERGY	96
5.6 CONCLUSIONS.....	99
5.7 REFERENCES	101
6 WHY ARE PERFLUOROCYCLOBUTADIENE AND SOME OTHER (CF) _n ^q RINGS NON-PLANAR?.....	106
6.1 ABSTRACT.....	107
6.2 INTRODUCTION	107
6.3 RESULTS AND DISCUSSION.....	110
6.4 CONCLUSIONS.....	118
6.5 REFERENCES	119
7 4N PI ELECTRONS BUT STABLE: N,N-DIHYDRODIAZAPENTACENES	122
7.1 ABSTRACT.....	123
7.2 INTRODUCTION	123
7.3 HEATS OF HYDROGENATION.....	127
7.4 RESONANCE ENERGY	129
7.5 EXTRA CYCLIC RESONANCE ENERGY	132
7.6 NUCLEUS INDEPENDENT CHEMICAL SHIFTS	135
7.7 CONCLUSIONS.....	138
7.8 METHODS	139
7.9 REFERENCES	144

8 CONCLUSIONS.....	149
LIST OF PUBLICATIONS	152

LIST OF TABLES

	Page
TABLE 2-1: Computed BLW-RE's and ASE's of benzene and cyclooctatetraene at HF/6-31G* and B3LYP/6-31G*. The ASE's are derived by the BLW-RE's of COT (and benzene) minus four (and three) times the computed BLW-RE of <i>syn</i> -butadiene. Positive ASE's indicate aromaticity; negative ASE's indicate antiaromaticity.....	25
TABLE 2-2: BLW computed (HF/6-31G*) total electron delocalization energies (DE's) for various butadiene conformers (cf., Fig. 2-7).....	29
TABLE 2-3: B3LYP/6-311+G** geometries for D_{4h} COT, benzene, <i>syn</i> -butadiene, <i>anti</i> -butadiene, and diacetylene with and without π conjugation (i.e. under BLW constraints, in italics in parenthesis). Geometries for ethane and ethylene, computed at the same level, are listed for comparison.....	30
TABLE 2-4: π Conjugation and “two-fold” double hyperconjugative (HPC) interactions (in kcal/mol) in the planar and perpendicular forms of biphenyl, styrene, butadiene, as well as radical stabilization in the planar (C_{2v}) and perpendicular (C_s) forms of allyl radical. All vertical BLW computations are at the HF/6-31G*//HF/6-31G* level	36
TABLE 3-1: Conventional estimates for the strain energy, π resonance energy, and π antiaromaticity of CBD based on homodesmotic and isodesmic equations and new BLW estimates.....	58
TABLE 4-1: Literature estimates of the σ -aromaticity of cyclopropane	67

TABLE 4-2: Strain estimates for C_nH_{2n} ($n = 3$ to 6) rings based on various equations: (1) $n C_3H_8 \rightarrow n C_2H_6 + C_nH_{2n}$ and (2) $n C_2H_6 \rightarrow n CH_4 + C_nH_{2n}$ (evaluated by experimental heats of formation). Equation (1) evaluates the conventional strain energies (CSE) of cycloalkanes. Equation (2) gives the bond separation equation (BSE) strain, and includes protobranching stabilization.....	73
TABLE 4-3: Interaction per geminal $\sigma_{cc} \rightarrow \sigma_{cc}^*$ hyperconjugation (HPC) for the cycloalkanes C_nH_{2n} , C_nF_{2n} , $C_n(BeH)_{2n}$, and silacycloalkanes Si_nH_{2n} , $n = 3$ to 6 series. (NBO data computed at the HF/6-311+G**//HF/6-311+G** level)	78
TABLE 5-1: CMO and LMO NICS(0) $_{\pi zz}$ data for the $C_6F_nH_{(6-n)}$ compounds (both computed at the PW91/IGLOIII level).....	93
TABLE 5-2: Ring LMO-NICS(0) $_{\pi zz}$ values for C_5X_5Y compounds ($X = H$ or F ; $Y = BH^+$, CH , N , NH^+ , O^+) NICS data computed at the PW91/IGLOIII level.....	96
TABLE 6-1: GIAO-Nucleus Independent Chemical Shifts (NICS) data for D_{2h} and C_{2h} C_4F_4 and cyclobutadiene (CBD) (PW91/IGLOIII//B3LYP/6-311+G**), all units are in ppm	109
TABLE 6-2: Energy components (nuclear-nuclear, electron-electron, nuclear-electron, potential, kinetic and total energy) of D_{2h} and C_{2h} C_4F_4 (at B3LYP/6-311+G**//B3LYP/6-311+G* and MP2/6-311+G**//MP2/6-311+G*, italics).....	113
TABLE 7-1: PWRE's and ECRE's of the azaacenes (1 to 7) and dihydroazaacenes (1-H₂ to 7). All BLW data are computed at the B3LYP/6-31G* level	133
TABLE 7-2: PWRE's of acyclic references (9-14) used for evaluating ECRE. All BLW data are computed at the B3LYP/6-31G* level.....	142

LIST OF FIGURES

	Page
FIGURE 2-1: Schematic representation of the COT potential energy surface (adapted from ref. 34 with permission). Note that the singlet D_{8h} and D_{4h} TS's connect directly without an intervening intermediate and that the entire triplet PES, including the aromatic D_{8h} minimum, is higher in energy	10
FIGURE 2-2: Schematic representation of “two-fold” (double hyperconjugation) in <i>perp</i> -butadiene	16
FIGURE 2-3: Schematic representation of the imposed BLW constraints for D_{4h} COT (16 blocks), D_{2d} COT (16 blocks), and C_{2v} <i>syn</i> -butadiene (nine blocks). The CH and CC “blocks” are circled in blue. When this BLW scheme is imposed, both the σ (CC, CH) as well as the π (CC) bonds are fully localized	19
FIGURE 2-4: Hyperconjugation (HPC) and conjugation interactions in D_{2d} and D_{4h} COT, across the C–C single bond.....	20
FIGURE 2-5: Schematic representations of geminal (HCH) and vicinal (HCCH) hyperconjugation (HPC) as well as π conjugation (CCCC) in ethylene, ethane, and <i>anti</i> -butadiene, respectively.....	21
FIGURE 2-6: Various 1,3-butadiene conformations and the numbers of conjugation and hyperconjugations (HPC) involved.....	27
FIGURE 2-7: Computed (HF/6-31G*) BLW-DEs (dashed line) and total energies (solid line) of various butadiene conformers at 30° CCCC dihedral angle intervals relative to <i>anti</i> -1,3-	

butadiene. Note the rather close correspondence except at 0° and 30° (due to steric effects).....	28
FIGURE 2-8: Schematic representations of “two-fold” (double) hyperconjugation in biphenyl (D_2), styrene (C_1), allene (D_{2d}), triplet ethylene (D_{2d}), ethylene dication (D_{2d}), diboryl (D_{2d})	32
FIGURE 2-9: $\pi_{\text{rad}} \rightarrow \pi^*$ ($\pi \rightarrow \pi_{\text{rad}}^*$) conjugation and $\text{CH} \rightarrow \pi^*$ ($\pi \rightarrow \text{CH}^*$) hyperconjugation in the planar (C_{2v}) and perpendicular (C_s) conformations of the allyl radical; the planar C_{2v} form is stabilized by conjugation between the radical and double bond by 20.4 kcal/mol, the perpendicular C_s form is stabilized to a lesser extent by hyperconjugation between the CH's and double bond by 6.8 kcal/mol. The vertical BLW delocalization energies were computed at the UHF/6-31G* level.....	34
FIGURE 3-1: Potential energy surface for CBD (computed at Mk-MRCCSD(T)/cc-PVQZ).....	53
FIGURE 3-2: Crude angle strain estimates for cyclobutane, cyclobutene, and CBD via deformed methane and methyl radicals (at B3LYP/PVTZ).....	54
FIGURE 4-1: Strain energy vs. the number of carbons for cycloalkanes ($n = 3$ to 6) at their the assumed <i>planar</i> geometries (black dashed lines) and at their equilibrium geometries (black solid line). The strain energies are evaluated by $n \text{ C}_3\text{H}_8 \rightarrow n \text{ C}_2\text{H}_6 + \text{C}_n\text{H}_{2n}$, at MP2/6-311+G** (no ZPE correction). The dotted grey line indicates the expected strain energy relationship between cyclopropane and cyclobutane based on Baeyer's angle strain theory	63
FIGURE 4-2: Strain energy vs. the number of silicons for silacycloalkanes ($n = 3$ to 6) at their the assumed <i>planar</i> geometries (black dashed lines) and at their equilibrium geometries	

(black solid line). The strain energies are evaluated by $n \text{ Si}_3\text{H}_8 \rightarrow n \text{ Si}_2\text{H}_6 + \text{Si}_n\text{H}_{2n}$, at MP2/6-311+G** (no ZPE correction)	64
FIGURE 4-3: Contours of the Laplacian, $\nabla^2\rho(r)$, for cyclopropane (reproduced with permission from ref. 9). Bond paths are marked by thick solid lines, bond critical points are indicated by dots; $\nabla^2\rho(r) < 0$ (dashed lines) indicate a concentration of electron density	65
FIGURE 4-4: Conventional strain energy (based on $n \text{ C}_3\text{H}_8 \rightarrow n \text{ C}_2\text{H}_6 + \text{C}_n\text{H}_{2n}$, expt.) vs. the average ring CCC bonds angles (geometries computed at MP2/6-311+G**) of cyclopropane (D_{3h}), cyclobutane (D_{2d}), cyclopentane (C_2), and cyclohexane (D_{3d}). The expected cyclopropane ring strain (extrapolated by the CSE's of cyclobutane, cyclopentane, and cyclohexane) is ca. 30 kcal/mol higher than its CSE	72
FIGURE 4-5: Geminal $\sigma_{cc} \rightarrow \sigma_{cc}^*$ interactions in cyclopropane (C_3H_6), cyclobutane (C_4H_8 , D_{4h}), C_3F_6 , and $\text{C}_3(\text{BeH})_6$. Note the visibly more “bent” C–C bonding orbitals of the three membered rings (greater coefficients that extent to the center of the ring) compared to C_4H_8	77
FIGURE 4-6: Computed strain energy vs. average ring CCC bond angles for perfluorocycloalkanes, All geometries and energies were computed at the MP2/6-31+G* level	78
FIGURE 4-7: Dissected canonical molecular orbital (CMO)-NICS(0) _{zz} for cyclopropane, computed at the ring center (at PW91/IGLOIII); NICS(0) = –42.9 ppm, NICS(0) _{zz} = –30.2 ppm (including core orbital contributions), NICS(0) _{πzz} = –0.5 ppm (includes contributions from MO's 7, 9, 10), NICS(0) _{Walshzz} = +15.5 ppm (includes contributions from the Walsh-type MO's 8, 11, 12)	80

FIGURE 4-8: Dissected canonical molecular orbital (CMO)-NICS(0) of tetrahedrane, computed at the cage center (at PW91/IGLOIII); total NICS(0) = -47.5 ppm (including core orbital contributions), $\text{NICS}(0)_{\text{Walsh}} = +19.5$ ppm (includes contributions from the Walsh-type MO's 9, 10, 11, 12, 13, 14).....	81
FIGURE 5-1: In plane LMO-NICS $_{\pi\text{zz}}$ grid of C_6H_6 and C_6F_6 (NICS data computed at the PW91/IGLOIII level) (a) LMO-NICS $_{\pi\text{zz}}$ grid of benzene (b) “Ring” LMO-NICS $_{\pi\text{zz}}$ grid of C_6F_6 (c) “F” IGLO-LMO-NICS $_{\pi\text{zz}}$ grid of C_6F_6	94
FIGURE 5-2: ECRE vs. ring-LMO NICS(0) $_{\pi\text{zz}}$ values for heterocyclic six membered rings $\text{C}_5\text{X}_5\text{Y}$ (X= H, F; Y = BH^- , CH, N, NH^+ , O^+). All ECRE data were computed with the BLW method at the B3LYP/6-31G* level, all NICS(0) $_{\pi\text{zz}}$ values were computed at the PW91/IGLOIII level	98
FIGURE 6-1: Geometries of C_{2h} C_4F_4 (a-b), D_{2h} C_4F_4 (c), and cyclobutadiene (d), computed at B3LYP/6-311+G** and Mk-MRCCSD/cc-PVTZ (in italics)	108
FIGURE 6-2: Homodesmotic evaluations of the vicinal FCCF repulsion in fluorinated cyclobutadienes (B3LYP/6-311+G** + ZPE data)	112
FIGURE 6-3: NICS $_{\text{zz}}$ data for the π MO's of C_4F_4 (C_{2h} and D_{2h}) and cyclobutadiene (CBD) and their total NICS(0) $_{\pi\text{zz}}$ values. All canonical molecular orbital (CMO) NICS data were computed at the PW91/IGLOIII level.....	115
FIGURE 6-4: NICS $_{\pi\text{zz}}$ grid of antiaromatic C_{2h} C_4F_4 (at PW91/IGLOIII).....	115
FIGURE 6-5: Planarization energies for non-planar $(\text{CF})_n^q$ species (at B3LYP/6-311+G*) with planar hydrocarbon analogs	117

FIGURE 7-1: Heats of hydrogenation for the diazapentacenes 5-7 and pentacene 8 reduced to the dihydroazaacenes 5(a-c)-H₂-7-H₂ and dihydropentacenes 8(a-c)-H₂ (all data are computed at the B3LYP/6-311+G** level including ZPE correction).....	124
FIGURE 7-2: Heats of hydrogenation for the smaller azaacenes 1-4 reduced to dihydroazaacenes 1-H₂-4(a-b)-H₂ (all data are computed at the B3LYP/6-311+G** level including ZPE correction).....	125
FIGURE 7-3: Heats of hydrogenation for the smaller acenes reduced to dihydroacenes (all data are computed at the B3LYP/6-311+G** level including ZPE correction).....	126
FIGURE 7-4: Resonance energies (RE's) per ring vs. the number of annulated rings (N = 2 to 5) for the dihydroazaacenes (2-H₂ to 5(a-c)-H₂ ; blue and green rhomboids) and diazaacenes (2 to 5(a-c) ; red triangles). The 1,4-dihydroazaacenes (2-H₂ , 3a-H₂ , 4a-H₂ and 5a-H₂) are in blue; their isomers with reduced inner rings (3b-H₂ , 4b-H₂ and 5(b-c)-H₂) are in green. All BLW data are computed at the B3LYP/6-31G* level	131
FIGURE 7-5: Extra cyclic resonance energies (ECRE's) per ring vs. the number of annulated rings (N = 2 to 5) for dihydroazaacenes (2-H₂ to 5(a-c)-H₂ , blue and green rhomboids) and diazaacenes (2 to 5(a-c) , red triangles) All BLW data are computed at the B3LYP/6-31G* level.....	134
FIGURE 7-6: LMO NICS(0) _{πzz} data (computed at the PW91/IGLOIII level) for the individual rings of 6 , 6-H₂ , 8 and planar- 8-H₂	137
FIGURE 7-7: Different PWRE values of various BLW localizations for 5b-H₂	141

CHAPTER 1

INTRODUCTION

Simple intuitive chemical concepts that relate the structures and energies of molecules are highly desirable because of their broad implications for organic chemistry. For example, the deformed structures of “strained” compounds result in energies higher than those having “normal” geometries (i.e. bond angles, torsional angles, and bond lengths that follow expectations based on simple hybridization considerations). Conversely, energetically stabilized molecules benefiting from unusually large electron delocalization are described as being “aromatic,” “conjugated,” or “hyperconjugated.” These virtual chemical properties are not directly measureable, but have profound impact on chemical thinking, e.g. on helping identify a preferred molecular conformation, a favorable or unfavorable structural motif, as well as potential reaction sites, for wide ranges of chemical problems. But the commonly used reference standards to evaluate these effects typically have serious flaws for such purposes, as their choice often is based on historical convention and tradition. Central to this dissertation are two issues: How can one obtain quantitative estimates of these highly important but not directly measurable chemical properties? And to what extent are they “transferable” from one molecule to another?

Computational chemistry has become the key approach to understanding, interpreting, and quantifying the elusive nature of many of these “non-measurable” chemical properties. This is in part due to the growing sophistication as well as versatility of *ab initio* and density functional theory (DFT) computations, which can be designed to isolate specific magnetic, energetic, and electronic manifestations, closely related to the phenomena of interest, much more

effectively than experiment. The hierarchy of refined nucleus independent chemical shifts (NICS) based indices, selectively eliminates magnetic responses not related to aromaticity, and is exemplary of this advantage. Evaluations of stabilizing (and destabilizing) energetic effects that arise from electron delocalization (or strain) also benefit from the use of sophisticated wave function analyses programs. The block-localized wave function (BLW) method offers superior theoretical reference standards that are free of undesired contaminating energetic effects. However, the energies of hydrocarbons often are governed by blends of stabilizing and destabilizing effects that are difficult to separate and examine individually. Thus, quantitative estimates of energetic consequences related to specific structural features rely on the cancellation of other energetic effects, not including the effect of interest, in the target and reference molecule.

This dissertation focuses on computational investigations concerning the simplest iconic organic molecules, i.e., cyclopropane, benzene, cyclobutadiene, cyclooctatetraene, as well as the polybenzenoid hydrocarbons. The following six chapters branch into the following themes: (1) strain in hydrocarbons, (2) σ - and π -electron delocalization (i.e. geminal, vicinal hyperconjugation, and π conjugation), and (3) substituent effects on aromaticity.

Highly strained molecules usually are unstable and not very persistent, unless other compensating stabilizing electronic effects are present. Thus, strained species like cubane and propellane, despite being high in energy, are experimentally viable. On the other hand, thermochemically stable molecules can be strained in the relative sense. For example, benzene suffers from angle strain (benzene has 120° CCC angles, but the carbons have no local D_{3h} symmetry), torsional strain (eclipsed CH's and CC's), and compression strain (non-ideal C-C and C=C bond lengths). However, these destabilizing “strain effects” are compensated by the

stabilizing σ - and π - electron delocalizations in benzene. Conformationally flexible alkanes and alkenes can adopt optimum geometries to minimize strain (or increase electron delocalization), but such alternatives are not possible for the more rigid ring and cage compounds. For example, the tub-shaped cyclooctatetraene (COT) (D_{2d}) is essentially strain-free and considered to be quite “normal” energetically ($\Delta H_f^\circ(298) = 71.1$ kcal/mol), while cubane suffers from significant angle strain and is much higher in energy ($\Delta H_f^\circ(298) = 148.7$ kcal/mol). As the structures and energies of molecules often are governed by blends of virtual chemical effects, which may work simultaneously in the same or opposite direction, the energies associated with these effects (e.g. various sources of strain, conjugation, hyperconjugation, and aromaticity) are difficult to quantify individually. The first three chapters present detailed analyses of the interplay of strain, electron delocalization, and aromaticity/antiaromaticity involved in the geometrical inversion of COT (chapter 2), the high energy of cyclobutadiene (chapter 3), and the unexpectedly low ring strain of cyclopropane (chapter 4).

Substituents also can influence the structures and energies of molecules depending on the degree of electronic structural changes they impose. Thus, benzene and perfluorobenzene have completely opposite electrostatic potentials at their ring centers (negative for benzene, but positive for perfluorobenzene), and have very different magnetic effects on the chemical shifts of molecules when applied as NMR solvents. On the other hand, perfluorocyclobutadiene displays a peculiar non-planar geometry, very different from the parent cyclobutadiene. But to what extent do such electronic and geometric structural changes affect the aromaticities of molecules? Single atom substitution in or on benzenoid rings usually have no affect on aromaticity. Conversely, *para*-substitution of nitro and amino groups on opposite sides of a phenyl ring resemble quinoidal-like structures and result in reduced aromaticity. Chapters 5 and 6 discuss the extreme

cases of perfluorination on the aromaticity and antiaromaticity of benzene and cyclobutadiene, respectively.

Fused benzenoid ring systems also can be viewed as “substituted” aromatics molecules. In particular, those involving strained (e.g. the [n]phenylenes) or antiaromatic (e.g. the dihydrodiazacenes) subunits can introduce dramatic electronic and geometric perturbations. Chapter 7 proposes a reliable treatment for measuring the aromatic stabilization energies (ASE) of the dihydrodiazacenes. We stress the conceptual distinction between ASE’s and resonance energies (RE’s). While the former is a direct measure of the extra stabilization or destabilization associated with aromaticity or antiaromaticity, the latter reflects the net energetic consequence of π conjugation. Chapter 7 also presents a detailed NICS study for the $4n$ π electron dihydrodiazapentacenes and their related $4n+2$ analogs. Evaluations of the local (magnetic responses associated with a specific ring moiety) and global magnetic aromaticities for polycyclic systems are notoriously challenging due to the presence of multiple resonance contributors and special synergistic interactions among various ring moieties.

The objective of this work is to develop a much in-depth understanding of the titled virtual chemical properties and their impact on the structures and energies of typical hydrocarbons from a 2011 standpoint.

CHAPTER 2

WHY CYCLOOCTATETRAENE IS HIGHLY STABILIZED: THE IMPORTANCE OF “TWO-FOLD” (DOUBLE) HYPERCONJUGATION[†]

[†] Judy I. Wu, Yirong Mo, and Paul von Ragué Schleyer.

To be submitted to *Chemistry – A European Journal*.

2.1 ABSTRACT

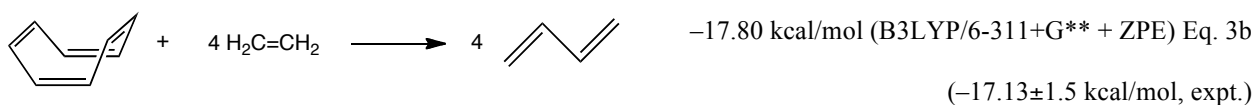
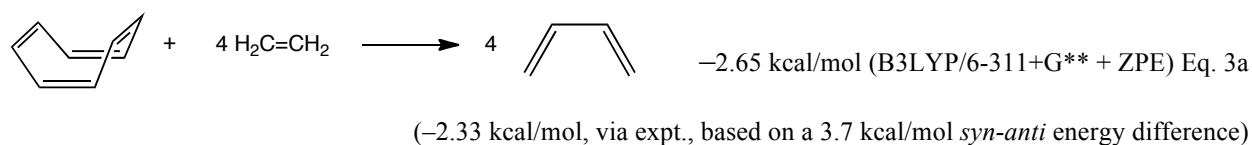
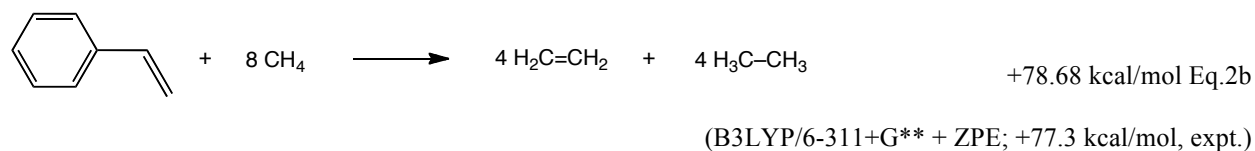
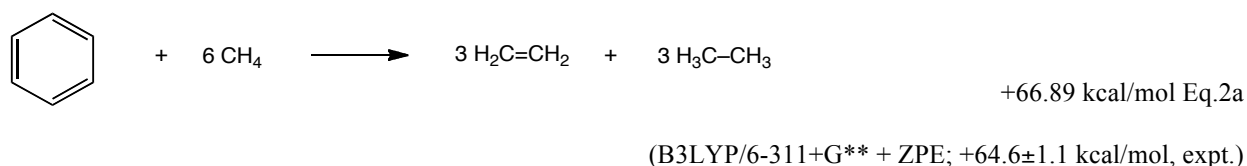
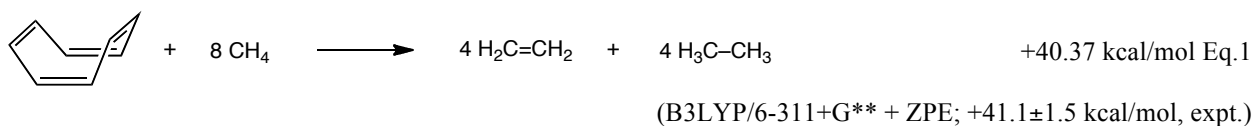
The tub-shaped D_{2d} ground state of cyclooctatetraene (COT) is highly stabilized (41.1 kcal/mol) according to its isodesmic bond separation energy. What is responsible, since D_{2d} COT is neither aromatic nor anti-aromatic and its σ skeleton is essentially strain-free? Despite its twisted π system, D_{2d} COT is far from being an unconjugated polyene model devoid of important π interactions. Along with some residual π conjugation, the large stabilization of the D_{2d} tub form is due to the eight $\text{CH} \rightarrow \pi^*$ and eight $\text{CC} \rightarrow \pi^*$ hyperconjugations (back and forth or “two-fold” across the C–C single bonds) facilitated by its warped skeleton, which compensates for the partial loss in conjugation upon ring puckering. The 12-14 kcal/mol inversion barrier of D_{2d} COT is not due to the anti-aromaticity of its planar D_{4h} transition state (this is only 3.2 kcal/mol, relative to that expected from mere conjugation without cyclic interaction). Instead, the strain of its 135° CCC angles and the eclipsing of its vicinal CC and CH bonds are responsible. Actually, the π stabilization of planar D_{4h} COT due to its four π conjugations is quite large (38.8 kcal/mol, at the BLW B3LYP/6-31G* level) and is nearly the same as that of appropriate acyclic polyene models. Hence, the large *net stabilization* due to electron delocalization, of both D_{2d} and D_{4h} COT, are nearly equal. The similar interplay of stabilization due to π conjugation and “two-fold” (double) hyperconjugation during rotation around the single bond of 1,3-butadiene serves as a simple model for the inversion of D_{2d} to D_{4h} COT. The rotational transition states of many other systems, e.g, styrene, biphenyl, and are affected similarly. Species with D_{2d} symmetry, like allene, triplet ethylene, diboryl, and the ethene dication also are stabilized by “two-fold” (double) hyperconjugation.

2.2 INTRODUCTION

Cyclooctatetraene (COT) is one of the decisive molecules in the history of chemistry. Willstätter's discovery in 1911 that its chemical properties were polyolefinic and quite unlike those of benzene¹ “rang the death knell”² on Johannes Thiele's partial valence theory of aromaticity, which predicted that all fully conjugated cyclic polyenes (annulenes) should display benzene-like aromatic behavior.³ The usual interpretation is that the highly nonplanar tub-shaped (D_{2d}) COT ground state is largely free from angle strain and is *non-aromatic*.⁴ Since the twisting of the π system *effectively precludes conjugation*; neither $4n + 2$ aromaticity nor $4n$ electron anti-aromaticity is present. Consequently, the energy of D_{2d} COT is expected to be quite normal, i.e., neither destabilized nor stabilized relative to appropriate reference models. Thus, Pauling deduced that the resonance energy of the COT ground state was only 5 kcal/mol based on heats of hydrogenation.⁵

In startling contradiction, the isodesmic bond separation energy (BSE) of the 8 π electron tub-shaped COT (D_{2d}) minimum^{4,6} of **1** is extremely large (41.1 kcal/mol, expt., eq. 1, based on ethane and ethene). This truly remarkable thermochemical stabilization is nearly 2/3 that of the BSE of the highly aromatic 6 π electron benzene (64.9 kcal/mol, expt., eq. 2a) and over half that of the directly comparable aromatic C_8H_8 COT isomer (with four conjugations), styrene (77.3 kcal/mol, expt., eq. 2b)!⁷ No satisfactory explanation has been advanced for this unexpectedly high stability of **1**. Polizer, et al.⁶ attributed the “considerable degree of stabilization” of COT “to limited π delocalization” and noted “that an ‘antiaromatic’ system need not necessarily show a net destabilization.” Clearly, systems with orthogonal π orbitals ($\varphi = 90^\circ$) do not “conjugate” in the usual sense. Hence, π – π interactions in D_{2d} COT (with $\varphi = 56^\circ$)⁸ are not favorable. Indeed, Fowler, et al.'s current density analysis demonstrated the absence of a π ring current (paratropic

or diatropic) in the COT ground state (D_{2d}) geometry.⁹ In contrast, the perfect π orbital alignments ($\varphi = 0^\circ$) in C_{2h} *anti*-butadiene and in planar C_{2v} *syn*-butadiene ($\varphi = 180^\circ$) are optimum⁸ for π conjugation, which results in 14.5 kcal/mol (*anti*, C_{2h}) and 10.8 kcal/mol (*syn*, C_{2v}) stabilization, respectively, as evaluated by their isodesmic BSE's (butadiene + 4 methane \rightarrow 2 ethylene + 2 ethane, at the B3LYP/6-311+G** level + ZPE).



However, the -2.7 kcal/mol energy of eq. 3a reveals that the stabilization of D_{2d} COT is nearly the same as that of four *fully conjugated syn*-butadienes (43.2 kcal/mol, 4×10.8), and only modestly less than that of four *anti*-butadienes (eq. 3b, -17.8 kcal/mol, also see footnote 10). But what is responsible for D_{2d} COT's enormous (ca. 40 kcal/mol) stabilization (eq. 1)?⁶ Could the strongly twisted σ -framework be involved? The CC bond lengths (C–C 1.470 Å, C=C 1.337 Å)¹¹ of D_{2d} COT also pose interpretive problems when compared, on the one hand, with the 1.535 Å C–C and the 1.331 Å C=C bond lengths in ethane and ethene, respectively, and on the other hand, with the 1.454 Å C–C and 1.338 Å C=C distances in the planar, fully π conjugated *anti*-butadiene (for comparison, the B3LYP/6-311+G** geometry of the C_{2v} conformation of *syn*-butadiene has 1.470 Å C–C and 1.338 Å C=C bond lengths). If the highly twisted D_{2d} COT framework precludes effective π conjugation, to what extent do the COT CC lengths reflect the effects of hybridization¹² rather than electron delocalization?

Electron diffraction and reliable low temperature X-ray analyses establish COT's highly nonplanar geometry (D_{2d} symmetry, $\varphi = 56^\circ$ CCCC dihedral angles) and the alternating CC bond lengths (see above).¹³⁻¹⁸ COT exhibits the olefinic chemical behavior expected from the lack of π conjugation due to its 8π electron highly twisted molecular framework.¹⁹ But what is the reason for COT's preferred tub-shaped geometry? Planar D_{4h} and D_{8h} COT have optimum π conjugation but are only transition states (see Figure 2-1).²⁰ The D_{8h} form is a typical “disjoint radical,”²¹ in which the open-shell singlet (transition state) is favored over the D_{8h} aromatic triplet state²² minimum by $8-9$ kcal/mol.²³ NMR evaluation of the dynamic tub-tub ring inversion process of COT revealed a $12-14$ kcal/mol activation barrier via the bond-alternating (D_{4h}) singlet TS's,²⁴ and a $3-4$ kcal/mol higher activation barrier for π bond shifting via the bond-equalized D_{8h} TS

(see Figure 2-1).²⁵ Kato et al.'s 12.7 ± 0.5 kcal/mol estimate of COT's D_{2d} to D_{4h} inversion barrier, based on the D_{2d} vs. D_{4h} COT electron binding energy difference, was similar.²⁶

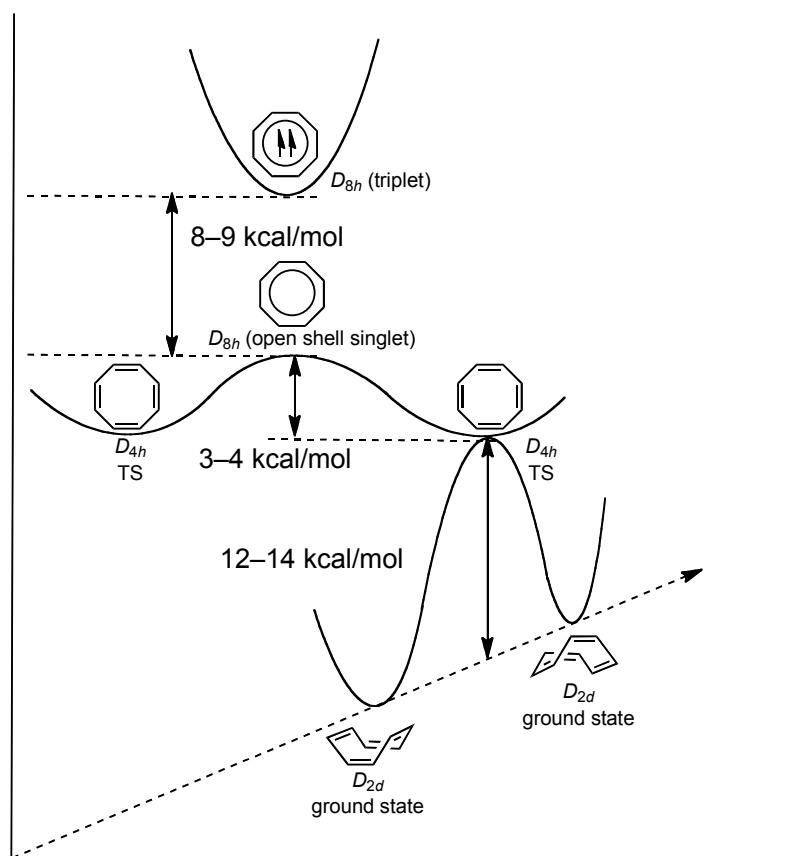


Figure 2-1. Schematic representation of the COT potential energy surface (adapted from ref. 34 with permission). Note that the singlet D_{8h} and D_{4h} TS's connect directly without an intervening intermediate and that the entire triplet PES, including the aromatic D_{8h} minimum, is higher in energy.

Nevertheless, viable planar COT derivatives have been achieved via annelation strategies or by replacing double with triple bonds.²⁷⁻³¹ Thus, 9,10-diphenylbicyclo[6.2.0]deca-pentaene, tetrakis

(bicyclo[2.1.1]hexeno)-cyclooctatetraene, and perfluoro-tetracyclobutacyclooctatetraene all have planar or near planar COT skeletons with alternating CC bond lengths. Ohmae et al. synthesized various cyclic tetrathiophenes containing dimethylsilyl, sulfur, and sulfone bridges accommodating fully planar (antiaromatic) cyclooctatetraene rings.³² Very recently, Summerscales et al. reported a digermyl COT complex (based on a 10 π electron aromatic dianion), which underwent a remarkable C=C bond cleavage and rearrangement into a tetracyclic digermane cage containing an inserted single Ge–Ge bond.³³

Compared to the parent D_{2d} minimum, the higher energies of D_{4h} and D_{8h} COT are attributed either to the effects of ring strain or to 8π -electron antiaromaticity.³⁴ The much wider 135° CCC angles in planar D_{4h} and D_{8h} COT (but not the 126.5° in tub D_{2d} COT), deviate significantly from the CCC angles in appropriate hydrocarbon models (e.g. 125.1° in the allyl radical, 124.3° in C_{2h} butadiene, and 124.7° in propene). Pierrefixe and Bickelhaupt also noted that the H's are forced to be closer together in D_{4h} than in D_{2d} COT.³⁵ Upfield ^1H chemical shifts of planar COT derivatives ($\delta = 3.6\text{--}4.6$ ppm, parent D_{2d} COT: $\delta = 5.68$ ppm)³⁶ as well as the large positive NICS values^{22b} of D_{4h} COT^{37,38} and strong paratropic ring currents,^{9, 39–41} relative to D_{2d} COT, illustrate the expected “magnetic” manifestations of its antiaromaticity.⁴² Although Breslow associated “destabilization” with his “antiaromaticity” concept,⁴³ appreciable energetic effects are *not* expected in an absolute sense for larger planar $4n$ π electron annulenes like planar COT.⁴⁴ Instead, the energies of such species only are higher when compared with their aromatic-stabilized $4n+2$ π electron counterparts.⁴⁵ Estimates of the antiaromatic destabilization energy of D_{4h} COT's based on molecular mechanics^{46,47} and various isomerization comparisons^{48,49} gave very small values (1 to 3 kcal/mol). Indene-isoindene isomerization energies of $[4n]$ annulenes deduced very insignificant antiaromatic destabilization energies generally with $n = 2\text{--}6$ (e.g., -2.9

kcal/mol for D_{4h} COT).⁴⁴ In fact, none of the $[4n]$ annulenes, except for cyclobutadiene, have appreciable destabilizing energies relative to acyclic conjugated reference molecules.⁴⁴ Breslow's 1973 Account presented no strong evidence supporting conjugative destabilization of the larger $[4n]$ π electron systems.⁵⁰ Hess and Schaad's REPE (resonance energy per π electrons) analysis found that the antiaromaticity of the $[4n]$ annulenes larger than cyclobutadiene decreased and became insignificant.⁵¹ Based on MM2, MM3, and MM4 force field computations, Allinger et al. concluded that angular bending and an increase in van der Waals energy in going from the tub to the planar form dominates COT's inversion barrier.^{46,52} They pointed out that there was no need to invoke "anti-aromatic destabilization" of the planar D_{4h} TS.

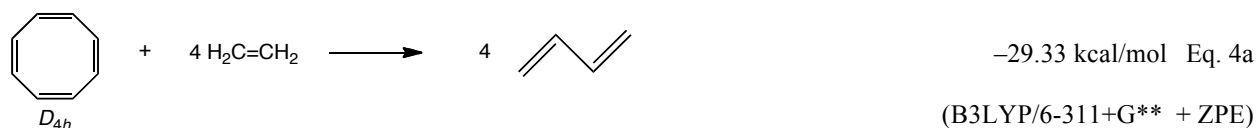
Traditionally, the energies of isodesmic and homodesmotic equations⁵³ have been used to evaluate the effects that stabilize (e.g., conjugation) or destabilize (e.g., strain and antiaromaticity) D_{4h} COT. But such evaluations depend critically on the choice of reference molecules and on the objective. In particular, resonance energies (RE) and aromatic stabilization energies (ASE) are not the same conceptually. RE's do not measure the energies corresponding to aromaticity/antiaromaticity directly. RE's measure the total stabilization due to π conjugation of a molecule relative to *unconjugated* references, whereas ASE's measure the "extra" cyclic π stabilization of fully conjugated rings. This difference, defined as the "aromatic stabilization energy" (positive ASE's), is based on the larger RE's of aromatic molecules than the RE's of their appropriate non-aromatic analogs with the same number of conjugations. The Pauling-Wheland RE definition is based on comparisons of the energy of a real molecule with that of its hypothetical most stable resonance contributor.⁵⁴ It often is not appreciated that antiaromatic molecules have *stabilizing* RE's and that their magnitude can be quite appreciable; however, their RE's are *smaller* than those of their appropriate non-aromatic analogs with the same

number of conjugations. The *difference* is defined as the “anti-aromatic destabilization energy” and can be expressed by *negative* ASE values. ASE’s thus measure the extra stabilization (or destabilization) associated with the cyclic conjugation of an aromatic (or antiaromatic) molecule by comparisons to acyclic *conjugated* polyene references with the same number and type of π conjugations. ASE’s characterize aromaticity/antiaromaticity specifically. Aromatic molecules have positive (stabilizing) ASE values. Antiaromatic molecules have negative (destabilizing) ASE’s. Non-aromatic molecules have ASE’s close to zero.

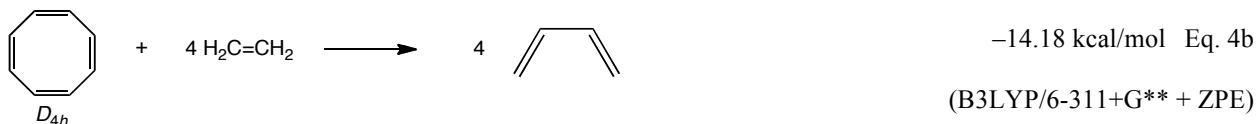
Homodesmotic equations, comparing the π energies of the cyclic conjugated species to those of acyclic conjugated polyenes, are often employed to evaluate aromatic stabilization (ASE) and antiaromatic destabilization energies (ADE). However, all reference molecules should be free from unbalanced contaminating energetic effects as well as structural mismatches.⁵³ Thus, eq. 4a (–29.3 kcal/mol) compares D_{4h} COT inappropriately to (four) *anti*-1,3-butadienes, as there only are *syn*-butadiene moieties in D_{4h} COT.⁵⁵ The eq. 4b evaluation of COT (–14.2 kcal/mol) based on *syn*-butadiene is much smaller in magnitude due to the *anti-syn* butadiene energy difference. Imbalanced differences in angle strain are additional factors that reduce the values evaluated by eq. 4a and 4b considerably. A simple strain-corrected approximation of the negative (destabilizing) ASE of D_{4h} COT evaluates eq. 4b, by employing deformed *syn*-butadiene geometries (i.e., with imposed 135° CCC bond angles); the resulting corrected ASE (eq. 4c) is only –3.79 kcal/mol (at the B3LYP/6-311+G** level, no ZPE correction).

Isodesmic bond separation energies (BSE) evaluate the net π stabilization of cyclic conjugated species relative to unconjugated reference compounds, but are marred somewhat by hybridization imbalances and other uncompensated effects.⁵³ Hence, the BSE of D_{4h} COT (+28.8 kcal/mol), relative to four ethanes and four ethylenes (eq. 5), underestimates the π conjugation

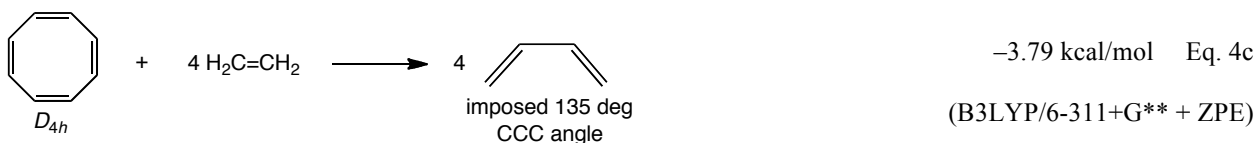
energy of D_{4h} COT, due to angle strain and eclipsing strain. On the other hand, the “strain-free” but putatively “unconjugated” D_{2d} COT exhibits a truly remarkable BSE *stabilization* (+41.1 kcal/mol, expt., eq. 1), as well as shortened C–C single bonds in D_{2d} COT (1.470 Å) compared to those of normal unconjugated hydrocarbons (e.g. 1.535 Å for ethane). Politzer et al. noted D_{2d} COT’s considerable BSE stabilization and attributed it to limited π delocalization but offered no detail explanation for this peculiar behavior⁶ (Mulliken’s view of COT⁵⁶ is discussed below).



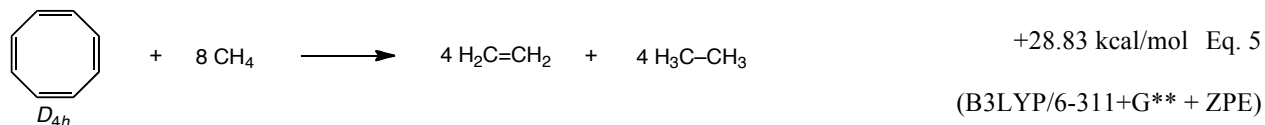
Improper ASE evaluation



Flawed ASE evaluation



Better ASE evaluation



Isodesmic RE evaluation

The single bond rotation of 1,3-butadiene provides the most basic model system for the D_{2d} to D_{4h} inversion of COT. There are four twisted butadiene moieties in D_{2d} COT and four *syn*-butadiene moieties in D_{4h} COT. Daudey et al. first proposed that hyperconjugation (two CH →

π^* and two $\text{CC} \rightarrow \pi^*$ interactions) stabilized perpendicular (*perp*-) butadiene (8.9 kcal/mol) to a similar degree as the π conjugation energy of planar *anti*-butadiene (10.4 kcal/mol), and that both led to a shortened C–C central bond.⁵⁷ In absence of π conjugation and hyperconjugation effects, the C–C central bonds of both *perp*- and *anti*- butadiene elongated to an equilibrium distance close to the C–C bond length of ethane.⁵⁷ Although George et al.⁵⁸ suggested the use of *perp*-butadiene as a reference compound for evaluating the stabilization energies of conjugated hydrocarbons, they did not consider the favorable effects of hyperconjugation. More recently, Feller et al. proposed that the CC single bonds of both *perp*-butadiene (1.4818 Å, from high level *ab initio* computations) and that of D_{2d} COT (1.4668 Å, X-ray data)¹⁶⁻¹⁸ modeled the “naked” $\text{Csp}^2\text{-Csp}^2$ single bond.⁵⁹ They noted that the COT $\text{Csp}^2\text{-Csp}^2$ single bond was slightly shorter than that of perpendicular butadiene, and commented that “some π -electron delocalization presumably occurs.” Following Daudey, et al.⁵⁷ we emphasize below that “two-fold” (double) hyperconjugation, back and forth across the single CC bond, involving both $\text{CH} \rightarrow \pi^*$ and $\text{CC} \rightarrow \pi^*$ two times stabilizes *perp*-butadiene (see Figure 2-2).

If hyperconjugation stabilizes the perpendicular butadiene, it also must stabilize the tub-shaped COT ground state! Mulliken first considered this possibility in D_{2d} COT a half-century ago (in 1959!).⁵⁶ He noted that the twisting of C–C bonds in D_{2d} COT “*destroys π -conjugation, but creates first-order hyperconjugation at both ends of the C–C bond;*” thus, “some resonance shortening is still expected.”⁵⁶ Pitzer’s even earlier work (in 1946) on the rotational barrier of styrene also noted the possible stabilization of the perpendicular styrene TS by hyperconjugation between the orthogonal vinyl and phenyl groups.⁶⁰ However, both these prescient observations seems to have eluded further attention in the analyses of COT and related systems until Daudey, et al.’s 1980 paper.⁵⁷

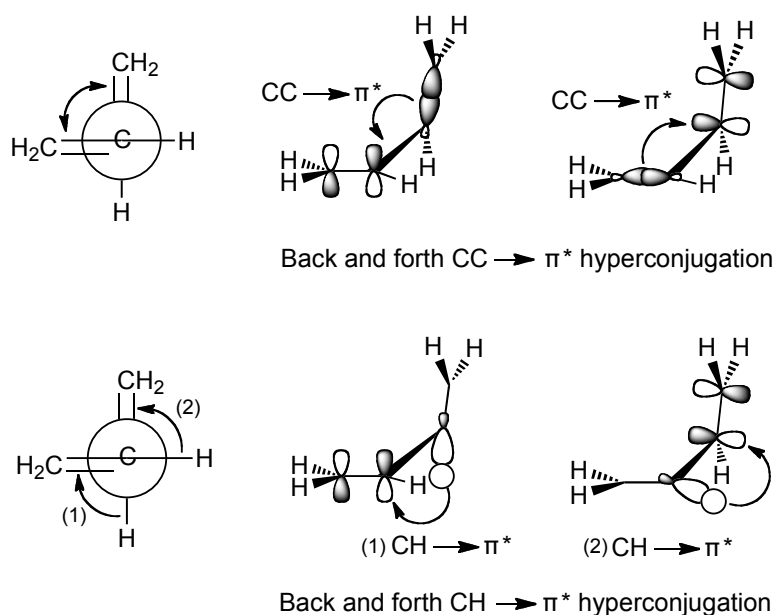


Figure 2-2. Schematic representation of “two-fold” (double hyperconjugation) in *perp*-butadiene.

Hyperconjugation and conjugation are virtual energetic properties that arise due to electron delocalization from filled bonding orbitals to adjacent empty or antibonding orbitals that may involve σ and/or π bonds in both the σ - and π molecular frameworks. While hyperconjugation and conjugation effects differ quantitatively, they are similar qualitatively. Such virtual effects, like antiaromaticity, are not measurable (or are only poorly evaluated) experimentally but can be quantified by computational methods, i.e. the block-localized wavefunction (BLW) or other valence bond methods.⁶¹⁻⁶⁴ The BLW method computes electron delocalization energies (DE), and can do so separately for the σ and the π framework of planar molecules. There is no recourse to other species; the molecule itself serves as its own reference. This overcomes the shortcomings of typical isodesmic and homodesmotic evaluations in quantifying the π conjugation or antiaromatic destabilization energy of COT.

This paper analyzes the geometric (ring strain) and electronic (i.e., hyperconjugation, conjugation, and antiaromaticity) effects involved in the 12-14 kcal/mol D_{2d} to D_{4h} inversion barrier of COT. The electron delocalization energies of D_{2d} and D_{4h} COT as well as the various model 1,3-butadiene conformers are evaluated by the BLW method by using the molecules themselves as their own references.⁶⁴ We answer the following questions: Why does COT prefer the puckered D_{2d} conformation? To what extent is hyperconjugation involved in stabilizing D_{2d} COT? Is the tub-shaped D_{2d} COT really devoid of all π -type electron delocalization stabilization? Can hyperconjugative interactions similar to those in D_{2d} COT stabilize other molecules with twisted σ -frameworks? How much is D_{4h} COT destabilized by antiaromaticity?

2.3 METHODS

All geometries were optimized with the Gaussian 03 program;⁶⁵ harmonic vibrational frequency analyses established the nature of the stationary points and provided the zero point energy corrections. Both D_{2d} and D_{4h} COT are closed shell singlets with stable wavefunctions.⁶⁶ The computed geometries of D_{2d} COT even at the HF/6-31G* level (C–C: 1.478 Å, C=C: 1.324 Å, CCC angle 127.3°, CCCC dihedral angle 54.5°) agree reasonably well with experimental X-ray diffraction data (C–C: 1.469 Å, C=C: 1.333 Å, CCCC dihedral angle 57.2°),¹⁶⁻¹⁸ as well as equilibrium structure parameters obtained by combined *ab initio* computations with femtosecond rotational coherence spectroscopy (C–C: 1.470 Å, C=C: 1.337 Å, CCC angle 126.6°).¹¹ Our HF level computation of the D_{2d} to D_{4h} inversion barrier of COT (13.9 kcal/mol with ZPE and 14.4 kcal/mol with additional thermal corrections giving the Gibbs free energy at 263 K) also is not far from Anet et al.'s 13.7 kcal/mol, by low temperature NMR measurements (263 K),²⁴ and the 12.7±0.5 kcal/mol value of Kato et al., based on the electron binding energy differences between

D_{2d} and D_{4h} COT.²⁶ MM4 computations estimated a 13.5 kcal/mol (263 K) D_{2d} to D_{4h} inversion barrier.^{46,52}

Block-localized wavefunction (BLW) computations, employing the Xiamen Valence Bond (XMVB) program⁶⁷ (implemented in GAMESS-R5),⁶⁸ evaluated the total electron delocalization energies (DE) of D_{2d} and D_{4h} COT, as well as the DE's of the series of 1,3-butadiene conformations at 30° CCCC dihedral angle (φ) intervals. Due to the methodological and basis set limitations of the XMVB program, all BLW-DE computations of non-planar systems were performed at the HF/6-31G* level, unless noted otherwise. The BLW method also can be used to evaluate the vertical and adiabatic π resonance energies (RE) of planar π conjugated molecules. Vertical BLW-DE's (and BLW-RE's) are derived from the energy difference between the strictly localized Lewis structure (Ψ^{Loc} , artificially constructed via the block-localized wavefunction method, see below) of the molecule at a particular geometry and its fully delocalized state (Ψ^{Del}), both at the completely optimized geometry of the latter. Adiabatic BLW-RE's are based on the energy difference between Ψ^{Loc} (optimized under the imposed BLW constraint) and Ψ^{Del} , both at their individual optimized geometries. In both D_{2d} and D_{4h} COT, Ψ^{Loc} was constructed by separating the basis functions and valence electrons that describe the eight C–H (two electrons each), four C–C (two electrons each), and four C=C (four electrons each; includes both σ and π electrons) bonds into 16 “blocks,” in which orbital's belonging to the same subspaces are orthogonal while those in different subspaces are non-orthogonal and are allowed to overlap. Both Ψ^{Loc} and Ψ^{Del} were optimized self-consistently.

Likewise, the BLW-DE of *syn*-butadiene is the computed energy difference between Ψ^{Del} and a strictly localized Lewis structure, Ψ^{Loc} , in which all basis functions and electrons are separated into nine “blocks” to describe the artificially localized six C–H (two electrons each),

one C–C (two electrons each), and two C=C (four electrons each; includes both σ and π electrons) bonds (BLW-DE = 28.1 kcal/mol, see Figure 2-3). This procedure “disables” all the electron delocalization (see Figure 2-3 for a schematic representation). For planar molecules, the π delocalization energy (BLW-DE $_{\pi}$) also can be evaluated separately from the σ -framework. For example, the BLW-DE $_{\pi}$ (i.e., resonance energy, BLW-RE) of *syn*-butadiene is the computed energy difference between Ψ^{Del} and a “ π localized” wavefunction, $\Psi^{\text{Loc}(\pi)}$, constructed by separating all basis functions and electrons into three “blocks” to describe the two (localized) π bonds (two π electrons in each block) and the remaining σ -framework (includes 18 σ electrons) of the molecule (BLW-DE $_{\pi}$ = RE = 8.0 kcal/mol, adiabatic, 8.8 kcal/mol, vertical, at HF/6-31G*). BLW computed DE’s are generally relatively insensitive to basis set effects,^{54, 64} e.g. the DE’s for *syn*-butadiene at HF/6-31G*, 6-31+G*, and 6-311+G** are 28.1 kcal/mol, 27.7 kcal/mol, and 32.3 kcal/mol, respectively, but the use of small to medium size basis sets are recommended to minimize complications that can arise from orbital non-orthogonality between the constructed subspaces (“blocks”).

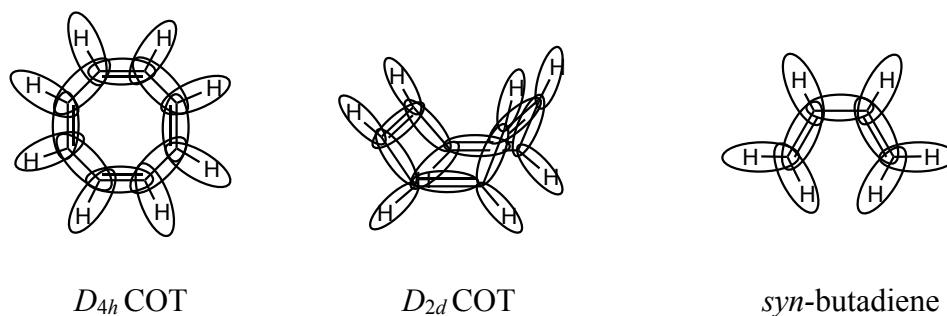


Figure 2-3. Schematic representation of the imposed BLW constraints for D_{4h} COT (16 blocks), D_{2d} COT (16 blocks), and C_{2v} *syn*-butadiene (nine blocks). The CH and CC “blocks” are circled. When this BLW scheme is imposed, both the σ (CC, CH) as well as the π (CC) bonds are fully localized.

2.4 ELECTRON DELOCALIZATION IN D_{2d} AND D_{4h} COT

The stabilization of tub-shaped COT due to its (geminal and vicinal) hyperconjugation and partial π conjugation across the twisted C–C single bonds is remarkable! The computed BLW-DE's of D_{2d} (71.6 kcal/mol) and D_{4h} (75.3 kcal/mol) COT both are surprisingly large. Note from the COT inversion barrier (Figure 2-1) that while the D_{2d} form is favored by 12-14 kcal/mol, the total delocalization energy of D_{4h} COT is greater than the D_{2d} form by 3.7 kcal/mol ($75.3 - 71.6 = 3.7$ kcal/mol). The interplay between conjugation and hyperconjugation is key to this unexpectedly small DE difference. In the D_{4h} form, there are four π conjugations, eight *cis*-in-plane HCCH vicinal hyperconjugations, and 16 *trans*-in-plane HCCC vicinal hyperconjugations. In D_{2d} COT, this is replaced by four partial π conjugations, four *cis*-in-plane HCCH vicinal hyperconjugations, eight *trans*-in-plane HCCC vicinal hyperconjugations, as well as eight $CH \rightarrow \pi^*$ and eight $CC \rightarrow \pi^*$ hyperconjugations across the twisted C–C single bonds (see Figure 2-4).

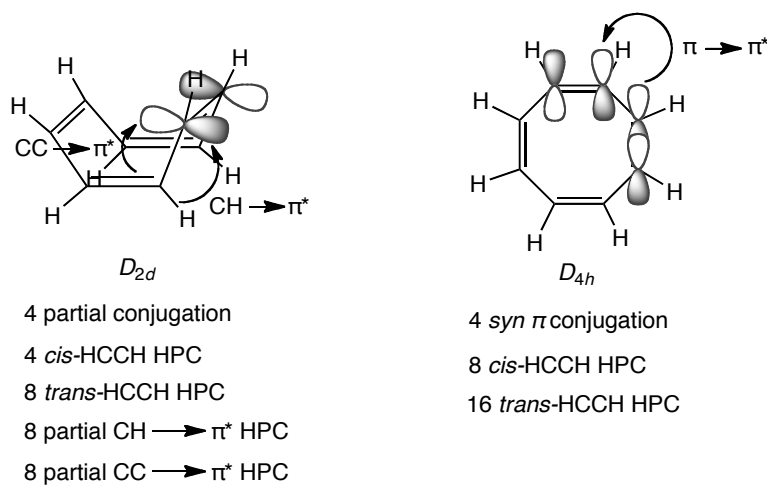


Figure 2-4. Hyperconjugation (HPC) and conjugation interactions in D_{2d} and D_{4h} COT, across the C–C single bond.

Both D_{2d} and D_{4h} COT have the same number of geminal HCC (16 in total) and CCC (8 in total) hyperconjugations. Although planarity benefits π conjugation substantially in D_{4h} COT, much larger hyperconjugation effects dominate the stabilization of D_{2d} COT and compensate for its diminished π conjugation; the twisting of four formal C–C single bonds in D_{2d} COT promote “two-fold” (double) hyperconjugation (i.e., the eight $\text{CH} \rightarrow \pi^*$ and eight $\text{CC} \rightarrow \pi^*$ hyperconjugations).

Individual hyperconjugation energies, involving interactions purely of the σ -framework (in-plane hyperconjugation), or a mixture of σ and π ($\sigma \rightarrow \pi^*$ hyperconjugation), generally are smaller compared to π conjugation, but can accumulate when many interactions are present (as in D_{2d} COT) to give quite substantial total stabilization energies (e.g. also for the various butadiene conformations, see below). Geminal hyperconjugation describes the electron delocalization interaction between C–C or C–H bonds sharing a common carbon center (see Figure 2-5a). Vicinal hyperconjugation interactions (HCCH, HCCC, or CCCC) occur between C–C and C–H bonds that are separated by a CC bond (see Figure 2-5b).

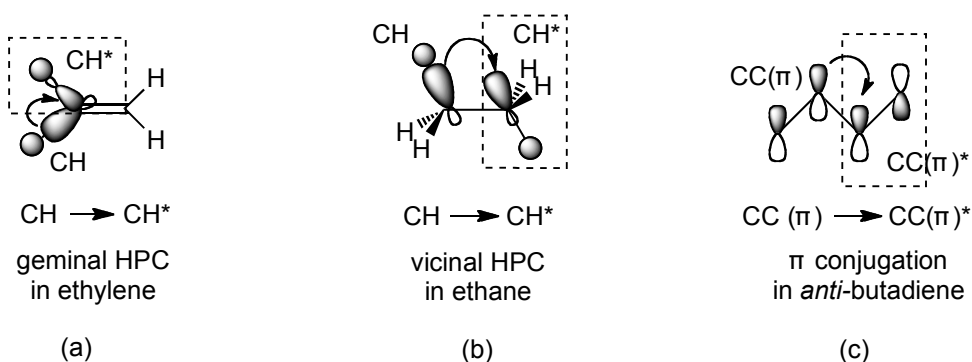


Figure 2-5. Schematic representations of geminal (HCH) and vicinal (HCCH) hyperconjugation (HPC) as well as π conjugation (CCCC) in ethylene, ethane, and *anti*-butadiene, respectively.

Thus, the π electron delocalization energy for planar D_{4h} COT (34.6 kcal/mol, vertical BLW- DE_{π}), when evaluated separately from the alkyl-type σ -framework interactions, is less than half the total BLW-DE of D_{4h} COT (75.3 kcal/mol). We stress that the origin of hyperconjugation effects (either geminal or vicinal) are qualitatively similar to π conjugation effects; both result in the energetic stabilization of molecules due to electron delocalization from filled bonding orbital's to adjacent empty or antibonding orbitals.

Substantial hyperconjugative interactions across the twisted C–C single bonds of D_{2d} COT are the underlying reason for the stabilization of its tub-shape conformation, documented by eq. 1 (relative to four ethanes and four ethylenes) and by BLW (relative to an “artificially” fully unconjugated D_{2d} COT reference). But this does not rationalize the 12-14 kcal/mol preference for the tub-shaped D_{2d} COT conformation (Figure 2-1). Instead, the difference in electron delocalization stabilization of D_{2d} (71.6 kcal/mol) and D_{4h} (75.3 kcal/mol) COT favors the D_{4h} form by 3.7 kcal/mol. Thus, other factors present in the D_{2d} or D_{4h} form must favor the D_{2d} tub shape conformation by ca. 16-18 kcal/mol.

2.5 THE D_{2D} TO D_{4H} INVERSION BARRIER OF COT

Compared to the tub-shaped D_{2d} COT, planar D_{4h} COT suffers from angle strain and CH bond eclipsing (four more in D_{4h} COT than in the D_{2d} form).³⁵ The 135° CCC angles of D_{4h} COT deviate significantly from those in unstrained reference hydrocarbons, such as *anti*-butadiene (124.3°), propene (124.7°) and the allyl radical (125.1°). As D_{2d} and D_{4h} COT have essentially the same C–C single bond lengths (e.g., D_{2d} : 1.478 Å, D_{4h} : 1.479 Å, at HF/6-31G*), the vicinal H's across the C–C single bonds in D_{4h} COT experience increased steric repulsion.³⁵ Additionally, D_{4h} COT suffers from a “buttressing effect” between the vicinal H's across the

double bonds. As noted earlier by Allinger et al.,⁵² each of the two hydrogens sharing the same double bond are forced to be closer together in the D_{4h} form (vicinal H...H distance: 2.199 Å, at HF/6-31G*) than in the twisted D_{2d} form (vicinal H...H distance: 2.328 Å, at HF/6-31G*). Since the electron delocalization stabilizations in D_{4h} and D_{2d} COT cancel out, these destabilizing geometric effects, present in the planar D_{4h} form but absent from the tub-shaped D_{2d} form, are the main contributors to COT's inversion barrier.

Simple evaluations of the degree of angle strain and buttressing effect in D_{4h} COT's, relative to D_{2d} COT (CCC angle = 127.3°, at HF/6-31G*), can be estimated by the energetic cost of deforming *syn*-butadiene from its equilibrium geometry (CCC angle 127.1°, at HF/6-31G*). Fixing both CCC angles in *syn*-butadiene to 135.0° while allowing everything else to relax, resulted in a 3.40 kcal/mol strain at the HF/6-31G* level. On this basis, the increase in angle strain (eight widened CCC bond angles) and buttressing effect in D_{4h} COT, relative to the D_{2d} form, is approximately 13.6 kcal/mol (3.4×4). Eclipsing strain in the planar D_{4h} COT, due to four additional eclipsed CH's across the C–C single bonds,³⁵ also contribute to the COT inversion barrier, but to a lesser extent. The energy increase due to additional CH bond eclipsing in the D_{4h} COT can be estimated by the rigid rotation barrier of a model ethane (3.5 kcal/mol, at HF/6-31G*), i.e., by fixing the C–C single bond length to 1.48Å, while allowing everything else to relax. At their constrained geometries, the BLW-DE's of the staggered (13.2 kcal/mol) and the eclipsed (12.4 kcal/mol) forms differ by only 0.8 kcal/mol. Thus, the remaining 2.7 kcal/mol ($3.5 - 0.8 = 2.7$ kcal/mol) approximates the energetic penalty for eclipsing three pairs of CH bonds (0.9 kcal/mol each). On this basis, planar D_{4h} COT suffers ca. 3.6 kcal/mol of eclipsing strain ($0.9 \times 4 = 3.6$ kcal/mol) relative to the D_{2d} form.

Hence, the 12-14 kcal/mol D_{2d} to D_{4h} COT inversion barrier depends on a combination of electronic (π conjugation vs. hyperconjugation, favor the D_{4h} form by 3.7 kcal/mol) and geometric effects (CH bond eclipsing, angle strain, and buttressing effects in the D_{4h} form favor the D_{2d} form by 17.2 kcal/mol), but geometric strain in the D_{4h} form dominates ($17.2 - 3.7 = 13.5$ kcal/mol). We agree with Allinger et al. that there is no need to invoke “anti-aromatic destabilization” of the planar D_{4h} to account for the COT inversion barrier.^{46, 52} Instead, D_{2d} and D_{4h} COT both have significant electron delocalization energies that are nearly equal in magnitude. The *negative* ASE (i.e. ADE) of D_{4h} COT, already accounted for by its computed total BLW-DE does not contribute additionally to COT’s inversion barrier, but in fact, reduces the π conjugation energy of D_{4h} COT only minimally (see below).

2.6 ANTIAROMATICITY IN D_{4h} COT

Antiaromatic destabilization energies (ADE, or *negative* ASE) and aromatic stabilization energies (ASE) are relative quantities whose estimation requires comparisons with models. Thus, the π resonance energies (RE) of cyclic conjugated aromatic or antiaromatic compounds are evaluated typically using the REs of non-aromatic acyclic reference compounds. However, equations employed for such purposes often are flawed by various uncompensated “hidden” contaminations, which can affect the energy strongly, but were not considered. In particular, the inseparability of a plethora of co-existing σ effects from the desired π ASE quantification, is especially challenging. In eq. 4b, the -14.2 kcal/mol COT *negative* ASE estimate arises from a combination of the COT antiaromaticity, angle strain, steric repulsion between the “bay hydrogens” in the *syn*-butadiene reference (four times), and different numbers of eclipsed CH bonds in COT relative to the reference compound.

Block localized wavefunction (BLW) computations provide superior ASE analyses, as only the π RE's of the target molecule and of the reference molecule are considered. Thus, no contaminating σ effects are involved. For example, the ASE of benzene, which has three formal π conjugations, can be evaluated by comparing its adiabatic π BLW-RE (55.1 kcal/mol) to the sum of three *syn*-butadiene π RE's (8.0 kcal/mol each). The resulting ASE (31.1 kcal/mol, see Table 2-1) is close to the best estimate (28.8 kcal/mol), based on experimental data and 1,3-cyclohexadiene–benzene comparisons.⁶⁹ Employing *syn*- rather than *anti*-butadiene as the reference eliminates the need for *syn/anti* corrections.

Table 2-1. Computed BLW-RE's and ASE's of benzene and cyclooctatetraene at HF/6-31G* and B3LYP/6-31G*. The ASE's are derived by the BLW-RE's of COT (and benzene) minus four (and three) times the computed BLW-RE of *syn*-butadiene. Positive ASE's indicate aromaticity; negative ASE's indicate antiaromaticity.

	BLW-DE $_{\pi}$ (RE)		ASE	
	HF/6-31G*	B3LYP/6-31G*	HF/6-31G*	B3LYP/6-31G*
<i>Syn</i> -butadiene	8.0	10.5	–	–
COT (D_{4h})	30.2	38.8	–1.8	–3.2
Benzene	55.1	61.4	+31.1	+29.9

Although D_{4h} COT is stabilized substantially by its four π conjugations (the adiabatic π BLW-RE is 30.2 kcal/mol), this is much less than benzene and is actually 1.8 kcal/mol *less* than the π BLW-RE sum of four *syn*-butadienes (see Table 2-1). On this basis, the *negative* ASE (antiaromaticity) of D_{4h} COT is only –1.8 kcal/mol. Computations of the benzene ASE and the

negative COT ASE at the B3LYP/6-31G* DFT level agree with the HF results (see Table 2-1). This refutes the traditional view that COT adopts the tub-shaped conformation to avoid 8 π electron antiaromaticity in the planar D_{4h} form. On this basis, the *negative* ASE of D_{8h} COT is at most -3 to -6 kcal/mol, based on the 3-4 kcal/mol energy difference between D_{4h} and D_{8h} COT (see Figure 2-1).

In general, antiaromatic destabilization of $4n$ π electron annulenes is not appreciable. The cyclobutadiene (CBD) *negative* BLW-ASE (-9.2 kcal/mol, CBD BLW-RE: 6.8 kcal/mol, at HF/6-31G*) is much smaller than that proposed by some authors.⁷⁰ Our paper in preparation addresses this issue in detail and concludes that the high thermochemical instability of CBD is not due to overwhelming antiaromatic destabilization, but due to an exceptionally highly strained σ -framework.⁷¹

2.7 1,3-BUTADIENE ROTATION

The C–C single bond rotation of 1,3-butadiene is the simplest model involving a similar conjugation/hyperconjugation interplay as in the D_{2d} to D_{4h} COT conversion (see Figure 2-6). *Syn*-butadiene ($\varphi = 0^\circ$) has one *syn*- π conjugation and four in-plane vicinal hyperconjugations (two *anti*-HCCC, one *syn*-HCCH, and one *syn*-CCCC) across the C–C single bond. *Trans*-butadiene ($\varphi = 180^\circ$) has one *anti*- π conjugation and four in-plane vicinal hyperconjugations (two *syn*-HCCC, one *anti*-HCCH, and one *anti*-CCCC) across the C–C single bond. The in-plane π conjugation and vicinal hyperconjugations across the C–C single bond in the C_{2v} and C_{2h} conformations ($\varphi = 0^\circ$ and 180°), are lost in *perp*-butadiene ($\varphi = 90^\circ$), but are replaced by two sets of stabilizing $\text{CH} \rightarrow \pi^*$ and $\text{CC} \rightarrow \pi^*$ hyperconjugations (see Figure 2-6). Indeed, the computed BLW-DE of *perp*-butadiene (24.5 kcal/mol) is only moderately lower than the BLW-

DE's of *syn*- (28.1 kcal/mol) and of *anti*- (29.4 kcal/mol) butadiene (see Table 2-2). Various blends of conjugative and hyperconjugative interactions contribute to the stabilization energies of the intermediate butadiene conformations ($0^\circ < \varphi < 180^\circ$). The local *gauche*-butadiene minimum ($\varphi = 33^\circ$) benefits from this interplay; it enjoys both partial π conjugation and “two-fold” (double) hyperconjugation. The C_{2v} *syn*-butadiene conformer, albeit fully π conjugated, is not a minimum but a transition state separating the pairs of chiral C_2 *gauche* conformers as it suffers from the “bay” H...H steric repulsion.

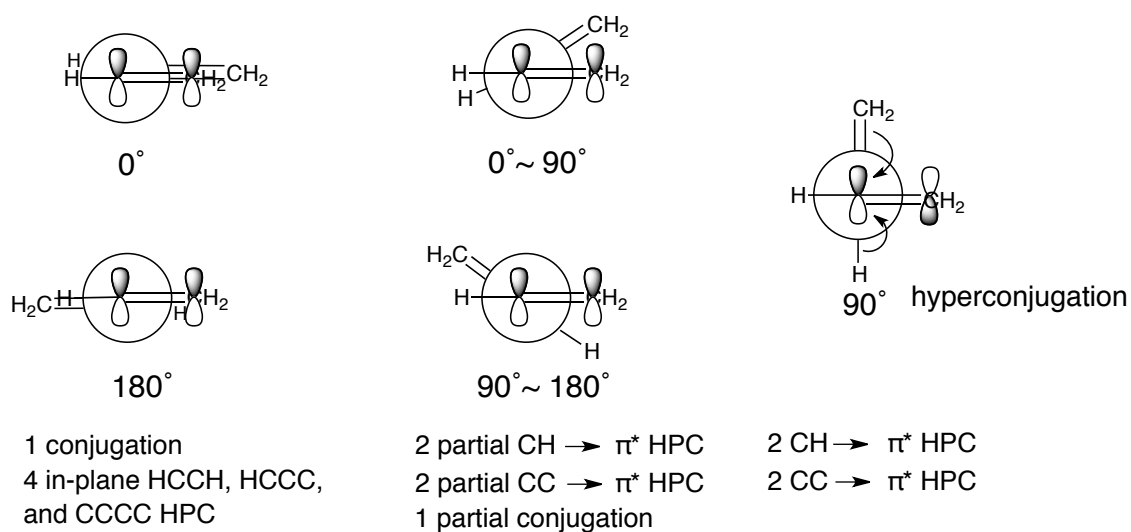


Figure 2-6. Various 1,3-butadiene conformations and the numbers of conjugation and hyperconjugations (HPC) involved.

Hence, the asymmetric rotational potential energy surface of butadiene is the result of counteracting steric and electron delocalization (π conjugation and hyperconjugation) effects. Note that the computed *perp/trans* butadiene BLW-DE difference (4.9 kcal/mol, Figure 2-7, dashed line) mirrors the *perp/trans* butadiene total energy variation (5.6 kcal/mol, Figure 2-7, solid line) generally, but the *syn/anti* butadiene BLW-DE difference (1.3 kcal/mol, Figure 2-7,

dashed line) is less than half the computed *perp/anti* butadiene energy (3.8 kcal/mol, Figure 2-7, solid line). The higher total energy of *syn*-butadiene (as well as that for the intermediate $0^\circ < \varphi < 30^\circ$ conformations) evidently is due to a composite of several effects including steric repulsion between the fully eclipsed vicinal pairs of C=C and CH bonds. But the computed DE's (Figure 2-7, dashed line) do not capture these steric effects fully.

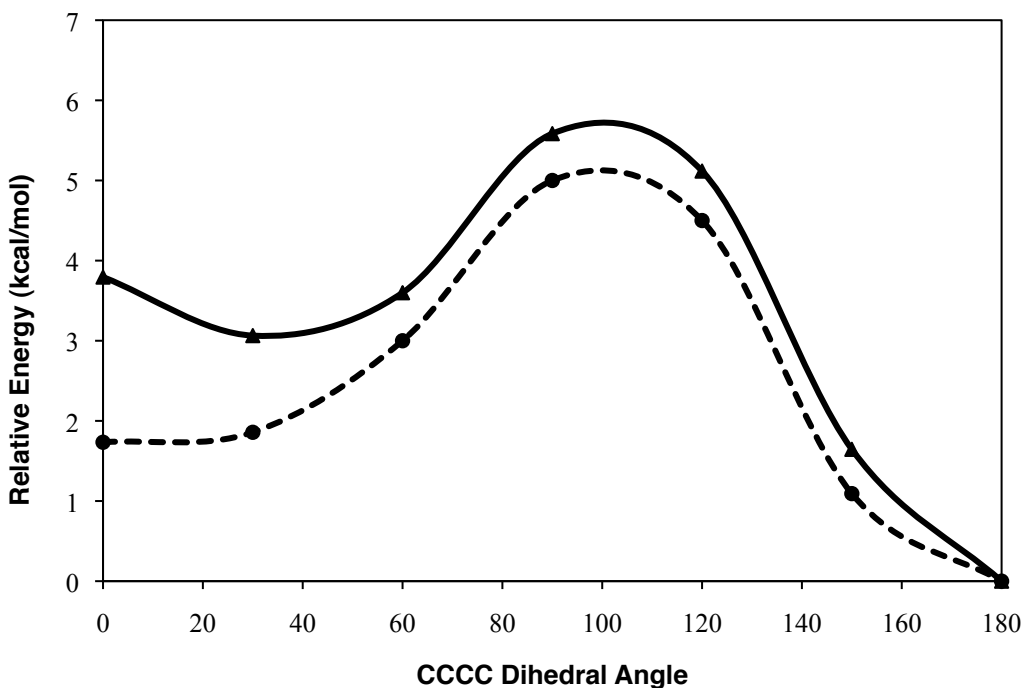


Figure 2-7. Computed (HF/6-31G*) BLW-DEs (dashed line) and total energies (solid line) of various butadiene conformers at 30° CCCC dihedral angle intervals relative to *anti*-1,3-butadiene. Note the rather close correspondence except at 0° and 30° (due to steric effects).

For the same reason, homodesmotic equations employing *syn*-butadiene reference compounds for evaluating ASE's are affected by additional σ contaminations, which are absent from the BLW approaches. The vertical BLW-DE $_{\pi}$'s (i.e., π conjugation), and the $\text{CH} \rightarrow \pi^*/\text{CC} \rightarrow \pi^*$

hyperconjugation energies for planar and *perp*-butadiene, also can be evaluated separately from the σ framework, and are 8.8 kcal/mol, 8.9 kcal/mol, and 10.7 kcal/mol for *syn*-, *perp*-, and *anti*-butadiene, respectively (see Table 2-4). Note that the π conjugation energies of the planar butadienes are less than half that of their total BLW-DE's, as geminal and vicinal hyperconjugation energies involving σ framework interactions dominate.

Table 2-2. BLW computed (HF/6-31G*) total electron delocalization energies (DE's) for various butadiene conformers (cf., Fig. 2-7).

φ (CCCC)	P.G.	DE (kcal/mol)
(<i>syn</i> -) 0°	C_{2v}	28.1
30°	C_2	27.8
60°	C_2	26.6
(<i>perp</i> -) 90°	C_2	24.5
120°	C_2	25.0
150°	C_2	28.3
(<i>anti</i> -) 180°	C_{2h}	29.4

Since both D_{2d} COT and *perp*-butadiene benefit energetically from substantial $\text{CH} \rightarrow \pi^*$, $\text{CC} \rightarrow \pi^*$ hyperconjugation arising from their non-planarity, the shortening of the central C–C bond from the Csp^3-Csp^3 1.53 Å for ethane (to 1.478 Å for COT and 1.489 Å for *perp*-butadiene at HF/6-31G*) do not represent “pure” Csp^2-Csp^2 bond lengths. The fully optimized geometry of the completely localized (Ψ^{Loc} , i.e., no electron delocalization) D_{2d} COT at HF/6-31G* displays much longer Csp^2-Csp^2 single bonds (1.519 Å, localized) than at the delocalized geometry (1.478 Å); the C=C double bond lengths vary much less (1.330 Å, localized; 1.324 Å, delocalized). Likewise, the computed “hyperconjugation free” *perp*-butadiene, evaluated by

relaxing the geometry under the imposed BLW restrictions (“disabled” π interactions between the orthogonal double bonds), reveals longer Csp^2-Csp^2 single bond distances (1.533 Å, HF/6-31G*), close to ethane’s 1.528 Å Csp^3-Csp^3 (HF/6-31G*)! In the absence of π conjugation (i.e. computed under BLW constraints at B3LYP/6-311+G**), the optimized geometries of D_{4h} COT, benzene, *syn*-butadiene, and *anti*-butadiene also display ethane and ethylene-like C–C single (ethane: 1.531 Å) and C=C double (ethylene: 1.329 Å) bond lengths despite the sp^2 hybridization of their skeletal carbon atoms. The C–H bond lengths also display very subtle changes due to the BLW treatment (see Table 2-3).

Table 2-3. B3LYP/6-311+G** geometries for D_{4h} COT, benzene, *syn*-butadiene, *anti*-butadiene, and diacetylene with and without π conjugation (i.e. under BLW constraints, in italics in parenthesis). Geometries for ethane and ethylene, computed at the same level, are listed for comparison.

	C–C	C=C	C–H
D_{4h} COT	1.476 Å (1.532 Å)	1.343 Å (1.324 Å)	1.087 Å (1.088 Å)
Benzene	1.395 Å (1.533 Å)	1.395 Å (1.325 Å)	1.085 Å (1.085 Å)
<i>Syn</i> -butadiene	1.470 Å (1.538 Å)	1.338 Å (1.326 Å)	1.083-1.087 Å (1.085-1.087 Å)
<i>Anti</i> -butadiene	1.456 Å (1.526 Å)	1.338 Å (1.325 Å)	1.084-1.089 Å (1.085-1.089 Å)
Diacetylene	1.365 Å (1.465 Å)	C≡C: 1.207 Å (C=C: 1.194 Å)	1.063 Å 1.066 Å
Ethane	staggered: 1.531 Å eclipsed: 1.545 Å	—	1.094 Å 1.093 Å

Ethylene	–	1.329 Å	1.085 Å
----------	---	---------	---------

Note that the ethane 1.53 Å Csp^3-Csp^3 bond length (which reflects a balance between lengthening of the CH bonds due to Pauli repulsion and shortening due to three vicinal HCCH hyperconjugations)⁶² does *not* represent the “pure” Csp^3-Csp^3 bond length. Without hyperconjugation (i.e., via BLW constraints), the ethane Csp^3-Csp^3 bond lengthens from 1.528 Å to 1.565 Å (at HF/6-31G*). Thus, Dewar’s early proposal¹² that hybridization contributes to the shortening of C–C bonds, for Csp^3-Csp^3 (1.531 Å, expt., for the central C–C single bonds of butane), Csp^2-Csp^2 (1.476 Å, expt., for 1,3-butadiene), and $Csp-Csp$ (1.378 Å, expt., for diacetylene) hybridized carbons, just as they do for C–H bonds, with sp^3 (1.091 Å, expt., in ethane), sp^2 (1.086 Å, expt., in ethylene), and sp (1.063 Å, expt., in acetylene) hybridized carbons, appears to be only partially valid (experimental bond distances taken from ref. 72). Notably, the percent reduction of the CH bond distances with respect to changes in their hybridization, 0.4% (ethylene vs. ethane) and 2.6% (acetylene vs. ethane), are much less compared to the percent reduction of the central C–C bond lengths of butane, butadiene, and acetylene relative to their carbon hybridizations, 3.5% (butadiene vs. butane) and 10.0% (acetylene vs. butane). When π conjugation (one in butadiene and two in acetylene) is disabled via BLW constraints, the central C–C bond distances elongate from 1.456 Å to 1.526 Å for butadiene and 1.365 Å to 1.465 Å for diacetylene (at B3LYP/6-311+G**); the “hyperconjugation-free” central C–C distances still are shorter compared to that of butane (1.531 Å, computed at the same B3LYP/6-311+G**) due to hybridization differences. Hence, the lengths of typical C–C single bonds (either Csp^3-Csp^3 , Csp^2-Csp^2 , $Csp-Csp$, Csp^3-Csp^2 , Csp^3-Csp , or Csp^3-Csp^2) are influenced by blends of conjugation/hyperconjugation effects,

hybridization changes, as well as mixtures of various virtual chemical effects (e.g., steric repulsion, geminal interactions, strain).⁷³

2.8 OTHER MOLECULES WITH “TWO-FOLD” (DOUBLE) HYPERCONJUGATION

Besides COT, the D_{2d} minima of allene (Figure 2-8c), triplet ethylene (C_2H_4 , Figure 2-8d), the ethylene dication ($C_2H_4^{2+}$, Figure 2-8d), diboryl (B_2H_4 , Figure 2-8d), as well as many twisted conjugated molecules and polyenes with non-planar equilibrium structures, e.g. biphenyl (D_2 , 44.4° torsional angle, Figure 2-8a), styrene (C_1 , 27.2° torsional angle, Figure 2-8b), and many non-planar Möbius as well as the higher Hückel annulenes, also benefit from “two-fold” (double) hyperconjugative stabilization. Triplet ethylene has a D_{2d} ground state 16.7 kcal/mol lower in energy than the D_{2h} rotation transition state (TS)⁷⁴ (the open-shell singlet D_{2d} TS is 1-2 kcal/mol lower in energy than triplet D_{2d} ethylene).⁷⁵ Likewise, the energy of the D_{2d} minima of the ethylene dication ($C_2H_4^{2+}$) and diboryl (B_2H_4) are 28.1 kcal/mol⁷⁶ and 10.9⁷⁷ kcal/mol lower than their D_{2h} TS's. The oversight of “two-fold” (double) hyperconjugation in molecules has serious consequences in interpreting the structures and energies of molecules.

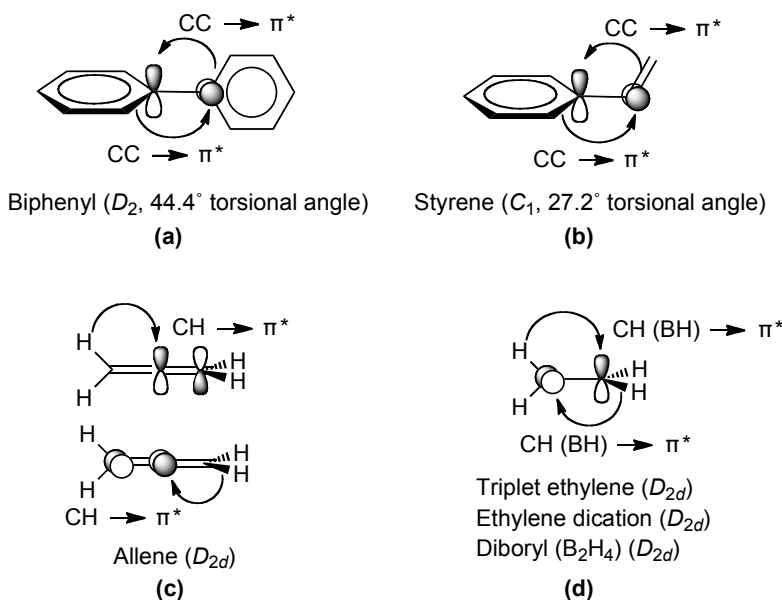


Figure 2-8. Schematic representations of “two-fold” (double) hyperconjugation in biphenyl (D_2), styrene (C_1), allene (D_{2d}), triplet ethylene (D_{2d}), ethylene dication (D_{2d}), diboryl (D_{2d}).

Thus, the conventional view that the CC π bond energy of ethylene,⁷⁸ evaluated by its 65.8 kcal/mol rotational barrier⁷⁴ (but this neglects “two-fold” (double) hyperconjugation), is much weaker than the CC σ bond energy certainly is untrue. Vertical BLW (UHF/6-31G* computations reveal that the D_{2d} triplet ethylene ground state is stabilized by “two-fold” (double) hyperconjugation by 14.0 kcal/mol. On this basis, the actual π bond energy of ethylene is much higher (79.8 kcal/mol, 65.8 + 14.0 = 79.8). If the C=C energy of ethylene is considered to be 139.1 kcal/mol,⁷⁹ this means that the π bond of ethylene is stronger than its single bond (139.1 – 79.8 = 59.3 kcal/mol)! Compared to the C–C single bond energy of ethane (86.6 kcal/mol), the C–C single bond of ethylene (compressed from ethane’s 1.531 Å length to ethylene’s 1.329 Å distance) is weakened by compression energy by 27.3 kcal/mol (86.6 – 59.3 = 27.3). This is close to Batsanov et al.’s estimate of the C–C σ -bond compression of ethylene (23.9 kcal/mol) based on the mechanical compressibility of diamond,⁷⁸ and is not far from the computed energetic penalty of compressing the 1.541 Å C–C bond length of triplet D_{2h} ethylene (TS) to a 1.329 Å distance (20.3 kcal/mol, at B3LYP/6-311+G**).

The allyl radical exemplifies the many cases where rotational barriers give misleading estimates of stabilization energies. Since, its perpendicular C_s rotational transition structure is 15.7±1.0 kcal/mol⁸⁰ higher in energy than the planar C_{2v} minimum, Korth et al. concluded that the π delocalization energy of the allyl radical should be approximately 14-14.5 kcal/mol (after correction for an assumed ca. 1 kcal/mol destabilization due to vicinal H eclipsing in the planar C_{2v} form).⁸⁰ But the partially compensating effect of hyperconjugation, which stabilizes the perpendicular conformation of the C_s rotational TS, was overlooked. Vertical BLW

computations at UHF/6-31G* find that the planar C_{2v} minimum is stabilized by 20.4 kcal/mol due to the conjugation of the radical with the double bond ($\pi_{\text{rad}} \rightarrow \pi^*$ and $\pi \rightarrow \pi_{\text{rad}}^*$, see Figure 2-9), and that the perpendicular C_s TS conformation is stabilized by 6.8 kcal/mol due to hyperconjugation of the double bond with the in-plane CH σ^* orbitals ($\pi \rightarrow \text{CH}^*$ and $\text{CH} \rightarrow \pi^*$, see Figure 2-9). This stabilization of the rotational barrier to allyl radical rotation depends on the *difference* between the stabilization of the planar C_{2v} ground state by conjugation and of the perpendicular C_s TS by its hyperconjugative interactions. Since other effects, like CH eclipsing, contribute minimally, the vertical BLW UHF/6-31G* estimate of the allyl radical rotational barrier ($20.4 - 6.8 = 13.6$ kcal/mol, also see Table 2-4) agrees satisfactorily with experiment.⁸⁰

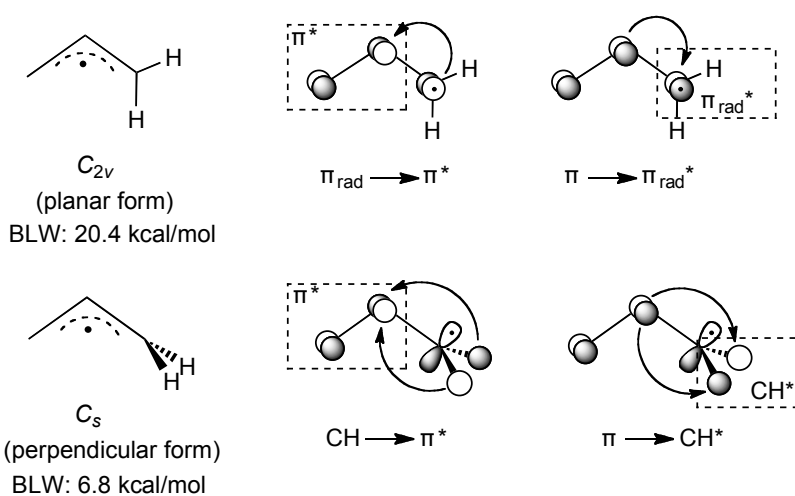


Figure 2-9. $\pi_{\text{rad}} \rightarrow \pi^*$ ($\pi \rightarrow \pi_{\text{rad}}^*$) conjugation and $\text{CH} \rightarrow \pi^*$ ($\pi \rightarrow \text{CH}^*$) hyperconjugation in the planar (C_{2v}) and perpendicular (C_s) conformations of the allyl radical; the planar C_{2v} form is stabilized by conjugation between the radical and double bond by 20.4 kcal/mol, the perpendicular C_s form is stabilized to a lesser extent by hyperconjugation between the CH's and double bond by 6.8 kcal/mol. The vertical BLW delocalization energies were computed at the UHF/6-31G* level.

Rotational barriers do not provide satisfactory estimates of conjugation and hyperconjugation interaction energies in planar molecules, since the corresponding transition structures also are stabilized. The non-planar equilibrium geometries of biphenyl and styrene are illustrative. In biphenyl, the ca. $44.4 \pm 1.4^\circ$ ⁸¹ dihedral angle between the two benzene rings of the D_2 biphenyl minimum energy conformation results in partially developed “two-fold” (double) $CC \rightarrow \pi^*$ hyperconjugation. The stabilizing effect of $CC \rightarrow \pi^*$ hyperconjugation is maximized in the perpendicular (D_{2d}) transition state conformation and reduces the energy of the D_{2d} biphenyl rotation barrier. Indeed, the $D_2 \rightarrow D_{2d}$ (1.4 kcal/mol, expt.) and the $D_2 \rightarrow D_{2h}$ barriers (1.6 kcal/mol, expt.)⁸²⁻⁸⁴ are nearly the same. According to the classical explanation, planar D_{2h} biphenyl is fully conjugated but it suffers from steric repulsion between the two sets of “bay” hydrogens and thus is only a rotation TS (the more complex “H-H bonding” interpretation also results in a greater net energy).⁸⁵ Vertical BLW computations (at HF/6-31G*) show that stabilizing interactions lower the energies of both biphenyl rotation transition states, the planar D_{2h} TS by 8.8 kcal/mol, due to conjugation, and the perpendicular D_{2d} TS by 7.5 kcal/mol, due to “two-fold” (double) hyperconjugation (see Table 2-4). It is important to note that CC σ bonds, e.g., of the phenyl rings in perpendicular biphenyl, are effective hyperconjugation donors. This is true generally, as Mulliken⁵⁴ and Pitzer⁵⁵ recognized long ago.

Styrene is a further example. Its ground state only is twisted slightly, and the tiny planarization energy (less than 0.3 kcal/mol) is negligible.^{86a} Despite its ca. 8 kcal/mol conjugation energy (vertical BLW at HF/6-31G*, see Table 2-4), determinations of the rotation barrier via the perpendicular C_s TS only are in the 1.8 to 3.3 kcal/mol range.⁸⁶ Pitzer et al. noted in 1946 that hyperconjugation between the perpendicular vinyl group and the phenyl ring should

stabilize the perpendicular styrene TS.⁶⁰ Our BLW computations confirm Pitzer’s suggestion by quantifying the important “two-fold” (double) hyperconjugation in the *perp*-styrene TS; the computed interaction energies between the vinyl and phenyl ring in styrene are 8.0 kcal/mol, in the planar form, and 7.8 kcal/mol, in the perpendicular form (see Table 2-4). At the same HF/6-31G* BLW level, the hyperconjugative interaction between the two perpendicular double bonds in *perp*-butadiene is 8.9 kcal/mol (Table 2-4). Although molecular planarity encourages π conjugation, the twisting of formal C–C single bonds in non-planar geometries promotes “two-fold” (double) hyperconjugation.

Table 2-4. π Conjugation and “two-fold” double hyperconjugative (HPC) interactions (in kcal/mol) in the planar and perpendicular forms of biphenyl, styrene, butadiene, as well as radical stabilization in the planar (C_{2v}) and perpendicular (C_s) forms of allyl radical. All vertical BLW computations are at the HF/6-31G* level//HF/6-31G*.

	Perpendicular	Planar
Butadiene	8.94 ^a	8.83 (<i>syn</i>) ^a / 10.17 (<i>anti</i>) ^a
Styrene	7.83 ^b	7.98 ^b
Biphenyl	7.52 ^c	8.83 ^c
Allyl radical	6.82 ^d	20.39 ^d

Computed BLW π conjugation/hyperconjugation between ^atwo double bonds, ^bthe vinyl and phenyl ring, ^cand two phenyl rings, in butadiene, styrene, and biphenyl. ^dThe radical stabilizations of planar and perpendicular allyl radical are computed by blocking one double bond.

2.9 CONCLUSIONS

“Two-fold” (double) hyperconjugative interactions across the twisted C–C bonds of D_{2d} COT stabilize its tub-shape conformation considerably and compensate for the reduction in π

conjugation. The surprisingly large computed BLW total delocalization energies of both D_{2d} (DE = 71.6 kcal/mol) and D_{4h} (DE = 75.3 kcal/mol) COT are nearly equal. While the planar D_{4h} form is stabilized considerably by π -conjugation (despite its 4 π electron character), tub-shaped D_{2d} COT is stabilized to nearly the same extent by “two-fold” (double) hyperconjugation. As a consequence of the shortening due to various hyperconjugative interactions, the lengths of the C–C single bonds of D_{2d} COT and of *perp*-butadiene do *not* represent those of “pure” (i.e., unconjugated) Csp^2 – Csp^2 bonds. Likewise, D_{2d} COT and *perp*-butadiene certainly are not suitable models⁵⁴ for estimating the π RE’s of planar π conjugated hydrocarbons. The tub-shape conformational preference of COT is *not* due to avoided antiaromaticity in the planar D_{4h} form, the strained σ -framework of D_{4h} COT is responsible instead. Our *ab initio* valence bond BLW study confirms that the 12-14 kcal/mol inversion barrier of cyclooctatetraene is dominated by destabilizing angle strain and steric eclipsing between the vicinal CH’s in the D_{4h} form.^{35,46} Planar D_{4h} COT, like comparable acyclic polyene models, is *stabilized* by its π conjugation (antiaromaticity is a minor effect).

The understanding of molecular structure and energy still is overly “ π -focused,” even though electron delocalization effects involving σ -frameworks can be equally important. We demonstrate this here for COT, biphenyl, as well as many other non-planar but hyperconjugative-stabilized species. We stress that the differences between hyperconjugation and conjugation effects are only quantitative rather than qualitative. In effect, both are virtual chemical properties that describe the energetic stabilization of molecules due to electron delocalization from filled orbitals to unfilled antibonding orbitals. The only notable differences between hyperconjugation and conjugation are the magnitude of stabilization they produce and the symmetry of the orbitals involved. π conjugation effects involve interactions purely of the π -

framework and generally offer greater energetic stabilization per interaction. Geminal and vicinal hyperconjugation effects involving purely of the σ - framework, or both the σ - and π -framework of molecules have less energetic impact, per interaction, but their large number of interactions present in molecules can accumulate to quite substantial stabilizing effects. Furthermore, our BLW investigation of the effect of π conjugation on the geometries of typical planar conjugated hydrocarbons (e.g. D_{4h} COT, benzene, and butadiene) demonstrates convincingly that electron delocalization effects, hybridization changes,¹² as well as blends of various virtual chemical effects (e.g., steric repulsion, geminal interactions, strain) govern the lengths of typical C–C, C=C, and C–H bonds cooperatively.

2.10 REFERENCES

1. a) Willstätter, R.; Waser, E. *Chem. Ber.* **1911**, *44*, 3423-3445; b) Willstätter, R.; Heidelberger, M. *Chem. Ber.* **1913**, *46*, 517-527. The difficulty of characterizing liquid compounds well (e.g., through b.p.'s, refractive index, and density) and the possibility of polycyclic isomer formation raised doubts about Willstätter's results (see Baker, W. *J. Chem. Soc.* **1945**, 258-267) until his synthesis was repeated and verified by Cope in 1948 (Cope, A. C.; Overberger, C. G. *J. Am. Chem. Soc.* **1948**, *70*, 1433-1437). As the determination of the D_{2d} structure of COT lay in the future (see below), Willstätter assumed COT to have a planar structure and rationalized its unexpected olefinic (rather than aromatic) behavior by an imaginative (but now amusingly quaint) explanation. He invoked the "centric" benzene model of Claus (Claus, A. *Theoretische Betrachtungen und deren Anwendungen zur Systematik der Organischen Chemie*; Freidburg, Germany, **1867**, p 207), Armstrong (Armstrong, H. E., *J. Chem. Soc.*, **1887**, *51*, 258-268) and Baeyer (Baeyer, A., *Ann. Chem.*, **1887**, *245*, 103-190; **1888**, *251*, 257-311), which assumed that the six "extra" valences of benzene extended from each of the carbons towards the ring center where they were "saturated" by their centric interactions. The 1/3 larger radius of the planar 8-membered COT ring diminished the possibility of centric "saturation" compared to that of the six-membered benzene ring. According to Willstätter, this difference was responsible for the olefinic behavior of the double bonds of COT.
2. Balaban, A. T. *Pure Appl. Chem.* **1980**, *52*, 1409-1429.
3. Thiel, J., *Ann. Chem.* **1899**, *306*, 87-142
4. Stevenson, G. R. *J. Chem. Ed.* **1972**, *49*, 781-782.
5. Pauling, L. *The Nature of the Chemical Bond*, 3rd ed., Cornell University Press, **1960**, p. 196

6. Politzer, P.; Murray, J. S.; Seminario, J. M. *Int. J. Quant. Chem.* **1994**, *50*, 273-277.
7. Prosen, E. J.; Johnson, W. H.; Rossini, F. D. *J. Am. Chem. Soc.* **1947**, *69*, 2068-2069.
8. Bachrach, S. M.; Liu, M. *J. Am. Chem. Soc.* **1991**, *113*, 7929-7937.
9. Havenith, R. W. A.; Fowler, P. W.; Jenneskens, L. W. *Org. Lett.* **2006**, *8*, 1255-1258.
10. Benson's analysis also gives essentially the same result (−16.89 kcal/mol) based of the expt. ΔH_f^{298} of COT (71.13 kcal/mol) and the 6.78 kcal/mol C_d-(C_d)(H) group increment. (see also, Cohen, N.; Benson, S. W. *Chem. Rev.* **1993**, *93*, 2419-2438.)
11. Dominique, S. K.; Lobsiger, S.; Frey, H. M.; Leutwyler, S. Stanton, J. F. *J. Phys. Chem. A* **2008**, *112*, 9134–9143.
12. Dewar M. J. S.; Schmeising A. N. *Tetrahedron* **1956**, *5*, 166-178.
13. Cope, A. C.; Overberger, C. G. *J. Am. Chem. Soc.* **1948**, *70*, 1433-1437.
14. Traetteberg, M. *Acta. Chem. Scand.* **1966**, *20*, 1724-1726.
15. Bastiansen, O.; Hedberg, L.; Hedberg, K. *J. Chem. Phys.* **1957**, *27*, 1311-1317.
16. Claus, K. H.; Krüger, C. *Acta. Crystallogr.* **1988**, *C44*, 1632-1634.
17. Bordner, J.; Parker, R. G.; Stanford, R. H. *Acta. Crystallogr. Sect. B* **1972**, *28*, 1069-1074.
18. Kaufman, H. S.; Fankuchen, I.; Mark, H. *Nature* **1948**, *161*, 165.
19. a) Snyder, J. P. *Nonbenzenoid Aromatics*; Vol. 1, Academic Press, New York, **1969**, p 29; b) Fray, G. I.; Saxton, R. G. *The Chemistry of Cyclo-octatetraene and its Derivatives*; Cambridge University Press, Cambridge, **1978**; c) Raphael R. A. Cyclooctatetraene. In *Nonbenzenoid Aromatic Compounds*; Interscience Publishers, Inc., New York, **1959**, p 465.
20. Hrovat, D. A.; Borden, W. T. *J. Am. Chem. Soc.* **1992**, *114*, 5879-5881.
21. Borden, W. T.; Davidson, E. R. *J. Am. Chem. Soc.* **1977**, *99*, 4587-4594.

22. a) Baird, N. C. *J. Am. Chem. Soc.* **1972**, *94*, 4941-4948; b) Gogonea, V.; Schleyer, P. v. R.; Schreiner, P. R. *Angew. Chem. Int. Ed.* **1998**, *37*, 1945-1948.
23. Wenthold, P. G.; Hrovat, D. A.; Borden, W. T.; Lineberger, W. C. *Science* **1996**, *272*, 1456-1459.
24. a) Anet, F. A. L. *J. Am. Chem. Soc.* **1962**, *84*, 671-672; b) Anet, F. A. L.; Bourn, A. J. R.; Lin, Y. S. *J. Am. Chem. Soc.* **1964**, *86*, 3576-3577.
25. Oth, J. F. M. *Pure Appl. Chem.* **1971**, *25*, 573-622.
26. Kato, S.; Lee, H. S.; Gareyev, R.; Wenthold, P. G.; Lineberger, W. C.; DePuy, C. H.; Bierbaum, V. M. *J. Am. Chem. Soc.* **1997**, *119*, 7863-7864.
27. Kabuto, C.; Oda, M. *Tetrahedron Lett.* **1980**, *21*, 103-106.
28. Einstein, F. W. B.; Willis, A. C. *J. Chem. Soc. Chem. Commun.* **1981**, 526-528.
29. Huang, N. J.; Sonheimer, F. *Acc. Chem. Res.* **1982**, *15*, 96-102.
30. Dürr, H.; Klauck, G.; Peters, K.; Schnering, H. G. *Angew. Chem. Int. Ed. Engl.* **1983**, *22*, 332-333.
31. Matsumura, A.; Komatsu, K. *J. Am. Chem. Soc.* **2001**, *123*, 1768-1769.
32. Ohmae, T.; Nishinaga, T.; Wu, M.; Iyoda, M. *J. Am. Chem. Soc.* **2010**, *132*, 1066-1074.
33. Summerscales, O. T.; Jiménez-Halla J. O.; Merino, G.; Power, P. P. *J. Am. Chem. Soc.* **2011**, *133*, 180-183.
34. Klärner, F. G. *Angew. Chem. Int. Ed.* **2001**, *40*, 3977-3981.
35. Pierrefixe, S. C. A. H.; Bickelhaupt, F. M. *J. Phys. Chem. A* **2008**, *112*, 12816-12822.
36. a) Nishinaga, T.; Ohmae, T.; Iyoda, M. *Symmetry* **2010**, *2(1)*, 76-97; b) Kieswetter, M. K.; Reiter, R. C.; Stevenson, C. D. *J. Am. Chem. Soc.* **2005**, *127*, 1118-1119; c) Willner, I.; Rabinovitz, M. *J. Org. Chem.* **1980**, *45*, 1628-1633.

37. Schleyer, P. v. R.; Maerker, C.; Dransfeld, A.; Jiao, H.; Hommes, N. J. R. v. E. *J. Am. Chem. Soc.* **1996**, *118*, 6317-6318.
38. Karadakov, P. B. *J. Phys. Chem. A* **2008**, *112*, 12707-12713.
39. Fowler, P. W.; Bean, D. E.; Seed, M. *J. Phys. Chem. A* **2010**, *114*, 10742-10749.
40. Fowler, P. W.; Havenith, R. W. A.; Jenneskens, L. W.; Soncini, A.; Steiner, E. *Angew. Chem. Int. Ed.* **2002**, *41*, 1558-1560.
41. a) Steiner, E.; Socini, A.; Fowler, P. W. *J. Phys. Chem.* **2006**, *110*, 12882-12886; b) Monaco, G.; Zanasi, R.; Pelloni, S.; Lazzeretti, P. *J. Chem. Theory Comput.* **2010**, *6*, 3343-3351.
42. Corminboeuf, C.; Heine, T.; Weber, J. *Phys. Chem. Chem. Phys.* **2003**, *5*, 246-251.
43. Breslow, R. *Chem. Eng. News* **1965**, *43*, 90-99.
44. Wannere, C. S.; Moran, D.; Allinger, N. L.; Hess Jr., B. A.; Schaad, L. J.; Schleyer, P. v. R. *Org. Lett.* **2003**, *17*, 2983-2986.
45. Breslow, R. *Pure Appl. Chem.* **1971**, *28*, 111-130.
46. Allinger, N. L.; Sprague, J. T.; Finder, C. J. *Tetrahedron* **1973**, *29*, 2519-2523.
47. Roth, W. R.; Lennartz, H. W.; Vogel, E.; Leiendecker, M.; Oda, M. *Chem. Ber* **1986**, *119*, 837-843.
48. Schleyer, P. v. R.; Pühlhofer, F. *Org. Lett.* **2002**, *4*, 2873-2876.
49. Wiberg, K. B. *Chem. Rev.* **2001**, *101*, 1317-1331.
50. Breslow, R. *Acc. Chem. Res.* **1973**, *6*, 393-398.
51. Schaad, L. J.; Hess Jr. B. A. *Chem. Rev.* **2001**, *101*, 1465-1476.
52. Nevins, N.; Lii, J. H.; Allinger, N. L. *J. Comput. Chem.* **1996**, *17*, 695-729.
53. Wheeler, S. E.; Houk, K. N.; Schleyer, P. v. R.; Allen, W. D. *J. Am. Chem. Soc.* **2009**, *131*, 2547-2560.

54. Mo, Y.; Hiberty, P. C.; Schleyer, P. v. R. *Theor. Chem. Acc.* **2010**, *127*, 27-38.
55. Glukhovtsev, M. N.; Bach, R. D.; Laiter, S. *J. Mol. Struc. (Theochem)* **1997**, *417*, 123-129.
56. Mulliken, R. S. *Tetrahedron* **1959**, *6*, 68-87.
57. Daudey, J. P.; Trinquier, G.; Barthelat, J. C.; Malrieu, J. P. *Tetrahedron* **1980**, *36*, 3399-3401.
58. George, P.; Trachtman, M. C.; Bock, W.; Brett, A. M. *Tetrahedron* **1976**, *32*, 1357-1362.
59. Feller, D.; Craig, N. C.; Matlin, A. R. *J. Phys. Chem. A*, **2008**, *112*, 2131-2133.
60. Pitzer, K. S.; Guttman, L.; Westrum, E. F. Jr. *J. Am. Chem. Soc.* **1946**, *68*, 2209-2212.
 “Another complication [regarding the rotational barrier of styrene] is the hyperconjugation or second order conjugation still present when the vinyl group is perpendicular to the phenyl group. This might be of a magnitude similar to that in propylene or around 2 kcal per mole”.
61. Mo, Y.; Schleyer, P. v. R. *Chem. Eur. J.* **2006**, *12*, 2009-2020.
62. Mo, Y.; Gao, J. *Acc. Chem. Res.* **2007**, *40*, 113-119.
63. Wu, W.; Ma, B.; Wu, J. I.; Schleyer, P. v. R.; Mo, Y. *Chem. Eur. J.* **2009**, *15*, 9730-9736.
64. a) Mo, Y.; Peyerimhoff, S. D. *J. Chem. Phys.* **1998**, *109*, 1687-1697; b) Mo, Y.; Zhang, Y.; Gao, J. *J. Am. Chem. Soc.* **1999**, *121*, 5737-5742; c) Mo, Y.; Subramanian, G.; Ferguson, D. M.; Gao, J. *ibid* **2002**, *124*, 4832-4837; d) Mo, Y.; Wu, W.; Song, L.; Lin, M.; Zhang, Q.; Gao, J. *Angew. Chem.* **2004**, *116*, 2020-2024; *Angew. Chem. Int. Ed.* **2004**, *43*, 1986-1990; e) Mo, Y. *J. Chem. Phys.* **2003**, *119*, 1300-1306; f) Mo, Y.; Song, L.; Wu, W.; Zhang, Q. *J. Am. Chem. Soc.* **2004**, *126*, 3974-3982; g) Mo, Y. *J. Org. Chem.* **2004**, *69*, 5563-5567; h) Mo, Y.; Song, L.; Lin, Y. *J. Phys. Chem. A* **2007**, *111*, 8291-8301.
65. Gaussian 03, Revision C.02, M. J. Frisch, G. W. Trucks, H. B. Schlegel, G. E. Scuseria, M. A. Robb, J. R. Cheeseman, J. A. Montgomery, Jr., T. Vreven, K. N. Kudin, J. C. Burant, J.

- M. Millam, S. S. Iyengar, J. Tomasi, V. Barone, B. Mennucci, M. Cossi, G. Scalmani, N. Rega, G. A. Petersson, H. Nakatsuji, M. Hada, M. Ehara, K. Toyota, R. Fukuda, J. Hasegawa, M. Ishida, T. Nakajima, Y. Honda, O. Kitao, H. Nakai, M. Klene, X. Li, J. E. Knox, H. P. Hratchian, J. B. Cross, C. Adamo, J. Jaramillo, R. Gomperts, R. E. Stratmann, O. Yazyev, A. J. Austin, R. Cammi, C. Pomelli, J. W. Ochterski, P. Y. Ayala, K. Morokuma, G. A. Voth, P. Salvador, J. J. Dannenberg, V. G. Zakrzewski, S. Dapprich, A. D. Daniels, M. C. Strain, O. Farkas, D. K. Malick, A. D. Rabuck, K. Raghavachari, J. B. Foresman, J. V. Ortiz, Q. Cui, A. G. Baboul, S. Clifford, J. Cioslowski, B. B. Stefanov, G. Liu, A. Liashenko, P. Piskorz, I. Komaromi, R. L. Martin, D. J. Fox, T. Keith, M. A. Al-Laham, C. Y. Peng, A. Nanayakkara, M. Challacombe, P. M. W. Gill, B. Johnson, W. Chen, M. W. Wong, C. Gonzalez, and J. A. Pople, Gaussian, Inc., Wallingford CT, 2004.
66. Andrés, J. L.; Castano O.; Morreale, A.; Palmerio, R.; Gomperts, R. *J. Chem. Phys.* **1998**, *108*, 203-207.
67. Song, L.; Wu, W.; Mo, Y.; Zhang, Q. XMVB: Ab initio Non-orthogonal Valence Bond Program, Xiamen University, Xiamen 361005, China, 2003.
68. Gamess (Version R5): Schmidt, M. W.; Baldridge, K. K.; Boatz, J. A.; Elbert, S. T.; Gordon, M. S.; Jensen, J. H.; Koseki, S.; Matsunaga, N.; Nguyen, K. A.; Su, S. J.; Windus, T. L.; Dupuis, M.; Montgomery, J. A. *J. Comput. Chem.* **1993**, *14*, 1347-1363.
69. Cyrancki, M. K., *Chem. Rev.*, **2005**, *105*, 3773-3811.
70. a) Glukhovtsev, M. N.; Bach, R. D.; Laiter, S., *J. Mol. Struct. (Theochem)* **1997**, *417*, 123-129; b) Deniz, A. A.; Peters, K. S.; Snyder, G. J., *Science* **1999**, *286*, 1119-1122; c) Kovacevic, B.; Baric, D.; Maksic, Z. B.; Müller, T., *J. Phys. Chem. A* **2004**, *108*, 9126-9133;

- d) Fattahi, A.; Lis, L.; Tian, Z.; Kass, S. R., *Angew. Chem. Int. Ed.* **2006**, *45*, 4984-4988; e) see also, Bally, T., *Angew. Chem. Int. Ed.* **2006**, *45*, 6616-6619.
71. Mo, Y.; Wu, W.; Zhang Q. *J. Phys. Chem.* **1994**, *98*, 10048-10053.
72. Experimental C–H and C–C bond distances taken from <http://cccbdb.nist.gov/>.
73. Mo, Y. *Org. Lett.* **2006**, *8*, 535-538.
74. M. T. Nguyen, M. H. Matus, W. A. Lester, Jr., D. A. Dixon *J. Phys. Chem. A* **2008**, *112*, 2082-2087. For experimental data (65.9 ± 0.9 kcal/mol), see also: a) Doering, W. v. E.; Roth, W. R.; Bauer, F.; Breuckmann, R.; Ebbrecht, T.; Herbold, M.; Schmidt, R.; Lennartz, H. W.; Lenoir, D.; Boese, R. *Chem. Ber.* **1989**, *122*, 1263-1266; b) Douglas, J. E.; Rabinovitch, B. S.; Looney, F. S. *J. Chem. Phys.* **1955**, *23*, 315-323.
75. a) Kollmar, H.; Staemmler, V. *Theoret. Chim. Acta.* **1978**, *48*, 223-239; b) Buenker, R. J.; Peyerimhoff, S. D. *Chem. Phys.* **1976**, *9*, 75-89.
76. K. Lammerstma, M. Barzaghi, G. A. Olah, J. A. Pople, A. J. Kos, P. v. R. Schleyer *J. Am. Chem. Soc.* **1983**, *105*, 5252-5257.
77. M. A. Vincent, H. F. Schaefer III *J. Am. Chem. Soc.* **1981**, *103*, 5677-5680.
78. Batsanov, S. S.; Kozhevina, L. I. *Russian Journal of General Chemistry* **2004**, *74*, 314-315.
79. Exner, K.; Schleyer, P. v. R. *J. Phys. Chem. A* **2001**, *105*, 3407-3416.
80. Korth, H. G.; Trill, H.; Sustmann, R. *J. Am. Chem. Soc.* **1981**, *103*, 4483-4489.
81. Bastiansen, O. *Acta. Chem. Scand.* **1949**, *3*, 408-414.
82. Tsuzuki, S.; Uchimaru, T.; Matsumura, K.; Mikami, M.; Tanabe, K. *J. Chem. Phys.* **1999**, *110*, 2858-2861.
83. Almenningen, A.; Bastiansen, O.; Fernholt, L.; Cyvin, B. N.; Cyvin, S. J.; Samdal, S. J. *Mol. Struct.* **1985**, *128*, 59-76; Bastiansen, O.; Samdal, S. *J. Mol. Struct.* **1985**, *128*, 115-125.

84. Johansson, M. P.; Olsen, J. *J. Chem. Theory Comput.* **2008**, *4*, 1460-1471.

85. Matta, C. F.; Trujillo, J. H.; Tang, TH; Bader, R. F. W. *Chem. Eur. J.* **2003**, *9*, 1940-1951.

Based on QTAIM computations, the bay H's of biphenyl are supposed to attract, due to the presence of a bond critical point indicative of "H-H bonding." See also, support for classical viewpoint: Poater, J.; Visser, R.; Sola, M.; Bickelhaupt, F. M. *J. Org. Chem.* **2007**, *72*, 1134-1142.

86. a) Choi, C. H.; Miklos, K. *J. Phys. Chem. A*, **1997**, *101*, 3823-3831; b) Carreira, L. A.; Towns, T. G. *J. Chem. Phys.* **1975**, *63*, 5283-5286; c) Hollas, J. M.; Musa, H.; Ridley, T.; Turner, P. H.; Weisenberger, K. H.; Fawcett, V. *J. Mol. Spectrosc.* **1982**, *94*, 437-455; d) Caminati, W.; Vogelsanger, B.; Bauder, A. *J. Mol. Spectrosc.* **1988**, *128*, 384-398; e) Tsuzuki, S., Tanabe, K.; Osawa, E. *J. Phys. Chem.*, **1990**, *94*, 6175-6179.

CHAPTER 3

IS CYCLOBUTADIENE REALLY DESTABILIZED BY ANTIAROMATIVITY? AN ALTERNATIVE EXPLANATION BASED ON SIMPLE STRAIN CONSIDERATIONS[†]

[†] Judy I. Wu, Yirong Mo, Francesco A. Evangelista, and Paul von Ragué Schleyer.

To be submitted.

3.1 ABSTRACT

The exceptionally high energy of cyclobutadiene (CBD) is not due to “anti-aromatic π destabilization.” Instead, the *unique* combination of unfavorable structural features of the D_{2h} CBD σ skeleton is responsible. These features are the strain of the four highly distorted (90°) C-C bond angles, the Pauli repulsion of the parallel CC bonds (one pair at a remarkably small, 1.35 Å, separation), and the short, cross-ring 1,3-CC repulsive nonbonded interactions. No other four-membered hydrocarbon ring (e.g., cyclobutene and cyclobutane) possesses all these features, and can model the CBD strain properly. Block-localized wavefunction analyses reveal only modest antiaromatic destabilization (16.5 kcal/mol, relative to two butadienes) but substantial ring strain (ca. 60 kcal/mol) for CBD. CBD as well as the larger planar $4n \pi$ annulenes are net stabilized by π conjugation.

3.2 INTRODUCTION

The peculiar instability of cyclobutadiene (CBD) has never been explained satisfactorily. Like cyclooctatetraene, CBD was first assumed to resemble benzene, but numerous early synthetic attempts failed.¹⁻³ In contrast to their aromatic $4n + 2 \pi$ electron analogs, the cyclic conjugated $4n \pi$ electron hydrocarbons were originally designated as being “non-aromatic” or “pseudo aromatic” and were expected to have polyene character. Breslow first coined the term “antiaromaticity” (in 1956) to describe the family of $4n \pi$ electron species related to the cyclopropenyl anion, CBD, the cyclopentadienyl cation, etc., that displayed highly thermochemical instability and pronounced bond length alternation.^{4, 5} However, none of the larger $4n \pi$ electron annulenes, beginning with cyclooctatetraene show significant energetic destabilization in their bond-alternating ground states or even in their bond-equalized transition

states.⁵⁻⁸ If the “anti-aromaticity” of such systems are not destabilizing, why should antiaromaticity destabilized CBD?

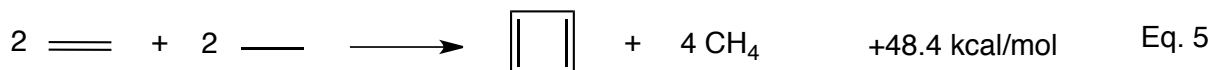
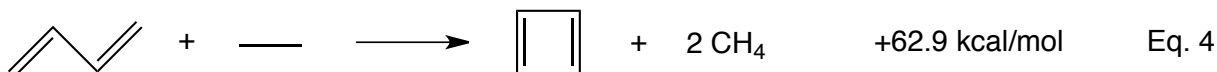
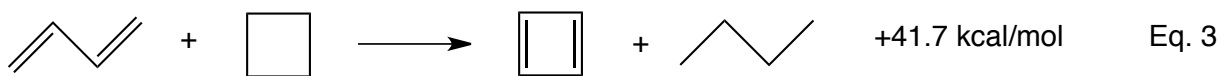
There is not doubt that CBD is highly instable thermochemically, relative to “regular” acyclic non-aromatic olefins. Even simple evaluations by comparing the heat of formation of CBD (102.4 ± 3.8 kcal/mol, expt. value from Fattahi et al.)⁹ to four times the conjugated =CH–Benson increment (6.78 kcal/mol each)¹⁰ reveal a high destabilization energy (ca. 70 to 80 kcal/mol). In effect, this approach is equivalent to eq. 1 (77.5 kcal/mol, evaluated based on a 104.6 kcal/mol computed heat of formation for CBD via the focal point analysis¹¹ (this work), also employed for equations 2 to 5), which compares the energy of CBD to two butadienes. But what part of the large destabilization energy of CBD is due to antiaromaticity and which part due to strain in the σ -framework? As such estimates are far greater than the conventional strain energy of other four membered ring hydrocarbons, e.g., cyclobutane (26.8) and cyclobutene (29.8 kcal/mol), the “extra effect” (ca. 45 kcal/mol, as given by eq. 1) is almost universally attributed to the putative $4n \pi$ electron anti-aromatic destabilization.^{9, 12-16} This assumes that the strain energies of cyclobutane/cyclobutene/cyclobutadiene increase linearly, and thus the strain energy of CBD is expected to be ca. 33 kcal/mol.^{9, 12-16}



Alternatively, the assumed “strain-balanced” equation 2 gives a slightly lower estimate for the antiaromatic destabilization energy of CBD (36.5 kcal/mol).^{9, 12-16} While “*there is no*

reason why the strain energy of CBD (CBE and CBA) needs to be additive,”¹⁷ equation 2 does not follow the definition of “antiaromaticity,” which requires the use of acyclic conjugated reference standards, and suffers from other inherent problems. Basically, CBA (with more deformable *Csp3* centers) is a totally inadequate model for the skeletal strain of cyclobutadiene (with less easily bent *Csp2* centers). Cyclobutene suffers from the same problems, and its stabilization by hyperconjugation, which also is not considered in equation 2, where four such interactions (worth 5.5 kcal/mol each) favor the left side by a total of 22 kcal/mol! Nevertheless, the strain increase along the cyclobutane, cyclobutene, and CBD series should be greater than a mere linear progression. Fattahi et al. assumed the upper bound for the ring strain of CBD based on the ring strain of 3,4-bismethylenecyclobutene (38.4 kcal/mol), since the latter has four *Csp2* centers but is not expected to be antiaromatic.⁹ But without recourse to cyclic compounds, how can the strain energy of CBD be estimated?

While both σ - and π - effects contribute to the high energy of CBD, typical homodesmotic and isodesmic equations that compare the energy of cyclobutadiene to selected reference compounds poorly distinguish these effects.



Equation 3 (41.7 kcal/mol) compares CBD with butadiene, but cyclobutane poorly compensates for the expectedly much higher ring strain of CBD. Equation 4 (62.9 kcal/mol) does the same without any compensation for the CBD ring strain. The bond separation equation (48.4 kcal/mol, eq. 5) measures a composite of strain in the σ -framework and the net π stabilization of CBD relative to unconjugated references (i.e. ethane and ethylene). But there are no unambiguous ways to dissect the σ - and π - effects of CBD! It also is important to realize that both strain and antiaromaticity are relative energetic effects, and thus their evaluations depend on the reference compounds selected for comparison. Antiaromaticity, by definition, only is manifest by comparison to acyclic conjugated reference standards.¹⁸ On the other hand, resonance energies (RE) are the net stabilization that arises from π conjugation, and thus are inherent to each molecule. Thus, the inherent destabilization energy of CBD actually is only 48.4 kcal/mol (as evaluated by eq. 5).

Nevertheless, there are good reasons to question the validity of such equations and to doubt the conventional interpretation. Although CBD has often been called the antiaromatic prototype and its energetic destabilization is assumed to characterize the whole class of $4n$ π electron compounds generally, its structural features are actually quite unlike the rest of the $4n$ annulenes and very different from any of the four membered ring compounds (i.e. cyclobutene and cyclobutane) typically used to model its strain energy (but in practice do so poorly, as discussed below). Apart from π -antiaromaticity, the σ -framework of CBD suffers from four highly distorted \angle CCC bond angles (90°) (angle strain) and eclipsed CH bonds around the ring (torsional strain). But neither cyclobutane (the D_{2d} minimum has \angle CCC = 88.6°) nor cyclobutene (94° C=C–C and 86° C–C–C bonds angles) have 90° \angle CCC bond angles. In addition, both the C–C single and C=C double bonds of D_{2h} CBD are exactly parallel and are

elongated. Politzer pointed out that the long CC single bond length of CBD (ca. 1.58 Å, much longer than that of butadiene) points to repulsive effects between the parallel π bonds (Pauli repulsion).¹⁹ No 4n annulene or four membered ring compounds exhibit all of these unfavorable features.

The widely accepted textbook proposition that the delocalization of the 4π electrons of CBD results in significant antiaromatic destabilization requires serious revision. Block-localized wavefunction (BLW) analysis of CBD and of butadiene (Table 3-1) indicates that the adiabatic Pauling-Wheland resonance energies of both are *nearly the same* (ca. 10 kcal/mol).¹⁸ When this is considered, π effects should contribute marginally to the endothermicity of Eq. 4. Hence, ring strain alone could be completely responsible for the 60 kcal/mol endothermicity, without considering the putative antiaromaticity of CBD!^{18,20} This estimate is almost twice the literature estimate of the strain energy of CBD (33 kcal/mol) based on comparisons to cyclobutane and cyclobutene. But if this is true, why is the ring strain of CBD so much higher than cyclobutene and cyclobutane? How do other types of strain (angle strain, torsional strain, and Pauli repulsion between the abnormally close double bonds) contribute? Our paper presents a detailed analysis of the interplay of π - and σ -effects that contribute to the high energy of CBD based on the BLW method.

3.3 EVIDENCE FOR HIGH RING STRAIN IN THE SIGMA-FRAMEWORK OF CBD

Our evaluation of the CBD strain energy based on numerous model computations consistently lead to the conclusion, that the thermochemical instability of CBD is dominated by a highly strained σ -framework. Triplet (D_{4h}) cyclobutadiene (12.9 kcal/mol higher in energy than the closed shell singlet D_{2h} CBD, at Mk-MRCCSD(T)/cc-PVQZ) exhibits many of the unique

geometric features of the singlet D_{2h} CBD but is confirmed by all criteria to be aromatic,^{21, 22} and thus is a superior model for the skeletal strain of singlet D_{2h} CBD. Like singlet D_{2h} CBD, triplet cyclobutadiene has all 90° \angle CCC bond angles and fully eclipsed CH bonds around the ring.



Thus, if the triplet states of both CBD and butadiene are compared, the endothermicity of equation 6 serves as a lower bound for the strain energy of singlet D_{2h} CBD. The resulting 49.7 kcal/mol (based on eq. 6) is much larger than literature estimates of the strain energy of CBD (ca. 33 kcal/mol) based on the conventional strain energies of cyclobutane and cyclobutene.

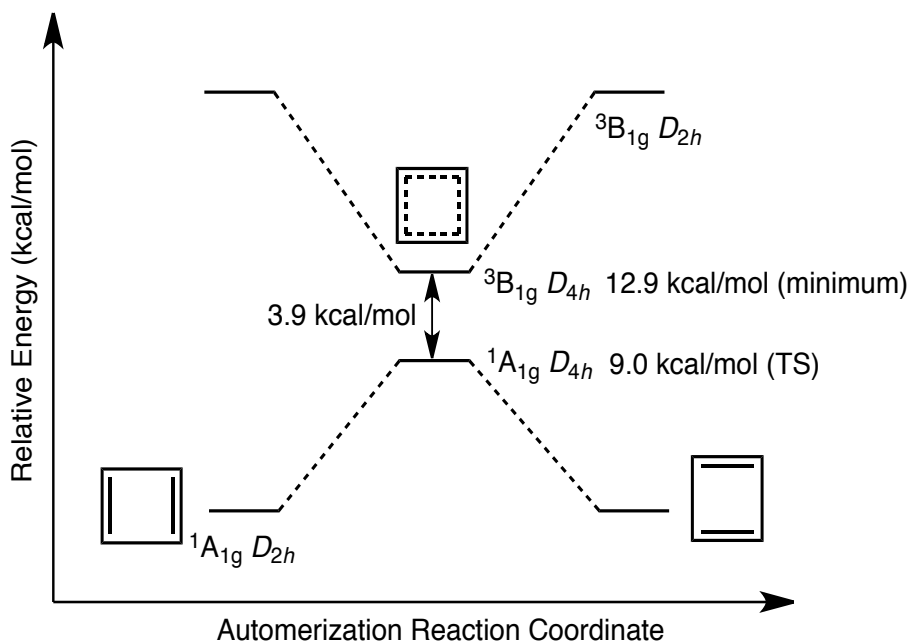


Figure 3-1. Potential energy surface for CBD (computed at Mk-MRCCSD(T)/cc-PVQZ).

The D_{4h} open-shell singlet transition state for the low-barrier degenerate CBD isomerization of the singlet D_{2h} forms has the same MO occupancy as the triplet, but is 3.9 kcal/mol lower in energy than the triplet (see Figure 3-1, potential energy surface of CBD computed at M_k-MRCCSD(T)/cc-PVQZ).²³ Like D_{8h} COT,²⁴ CBD is a typical “disjoint radical,”²⁵ in which dynamic spin polarization favors the open-shell singlet transition state over the D_{4h} aromatic triplet state minimum.

Crude estimates of the angle strain of D_{2h} CBD by deforming a model methyl radical also predict large skeletal strain for CBD. Fixing one of the HCH bonds angles of methyl radical ($\angle\text{CCC} = 120^\circ$) to 90° to simulate the CBD angle strain raises the energy by 12.8 kcal/mol (at B3LYP/PVTZ). When taken four times, this approximates a 51.2 kcal/mol angle strain for CBD ($12.8 \times 4 = 51.2$ kcal/mol, see Figure 3-2).

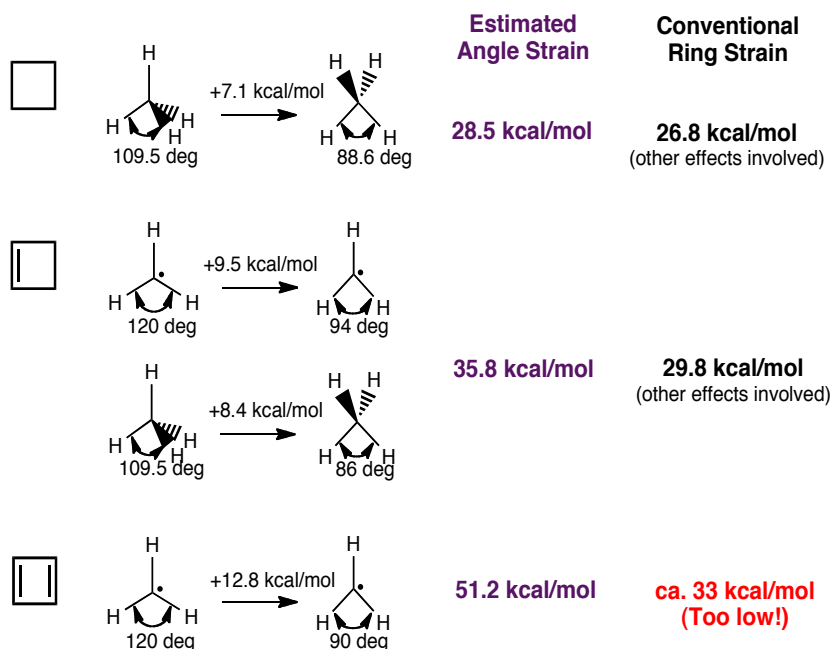


Figure 3-2. Crude angle strain estimates for cyclobutane, cyclobutene, and cyclobutadiene via deformed methane and methyl radicals (at B3LYP/PVTZ). While the simulated angles strains for

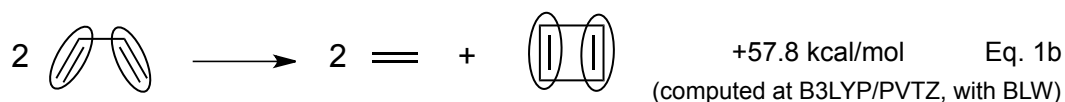
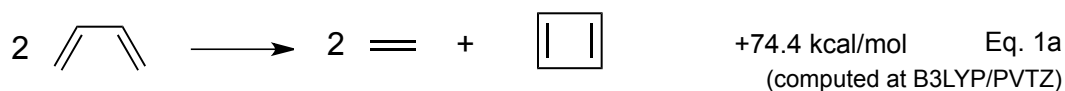
cyclobutane and cyclobutene roughly agree with their conventional strain energies, the estimated angle strain for cyclobutadiene is much higher than expected based on simple considerations of the strain energies of cyclobutane and cyclobutene.

On the other hand, when a 94° CCC angle is imposed in methyl radical to model the $Csp2Csp2Csp2$ angle deformation in cyclobutene, the energetic penalty is only 9.5 kcal/mol at the same level (see Figure 3-2). This difference, corresponding to a decrease in angle of “only” 4° , emphasizes the inadequacy of cyclobutene as a model for the strain in CBD. Hence, the total angle strain of cyclobutene is reduced appreciably by the widening of the $C=C-C$ angles to 94° ; this is only partially compensated by the commensurate decrease in its $C-C-C$ bond angles (86°). Cyclobutane is an even less satisfactory model for the strain energy of CBD. Fixing one of the HCH bond angles of methane ($\angle CCC = 109.5^\circ$) to 88.5° to simulate the angle strain of cyclobutane raises the energy by only 7.1 kcal/mol. When taken, four times ($7.1 \times 4 = 28.5$ kcal/mol, see Figure 3-2), the deformed methane model approximates the conventional strain energy of cyclobutane roughly (26.8 kcal/mol).

3.4 BLOCK-LOCALIZED WAVEFUNCTION ANALYSES

By combining the BLW method²⁶ with conventional homodesmotic equations, both the ring strain energy and antiaromatic destabilization energy of CBD can be evaluated independently without any unnecessary assumptions. In eq. 1, the total destabilization energy of CBD (77.5 kcal/mol, expt.) is evaluated by comparison to two butadienes. Employing *syn*-butadiene instead (as eq. 1a, computed at B3LYP/PVTZ) corrects for the *syn-anti* mismatch in eq. 1, since CBD has two *syn*- type conjugations. In eq. 1b, the π interactions of CBD and butadiene are “disabled”

by the BLW treatment (B3LYP/PVTZ). Thus, eq. 1b evaluates only the sigma framework of CBD to that of two *syn*-butadienes. On this basis, the sigma system of CBD is strained by 57.8 kcal/mol; this is $\frac{3}{4}$ of the total destabilization energy of CBD (see Table 3-1)!



The antiaromatic destabilization energy of CBD (−16.6 kcal/mol) also can be estimated directly based on the BLW-RE difference between CBD (10.1 kcal/mol) and two times that of *syn*-butadiene (13.3 kcal/mol) (both have two *cis*-type conjugations),¹⁸ and is much lower than previous estimates.^{9, 12-16} Note that the π resonance energy of CBD is *net stabilizing* and only relatively antiaromatic destabilized when compared to appropriate model references with the same number of conjugations.¹⁸ Even so, CBD is only modestly destabilized by antiaromaticity. In contrast to literature estimates, which reveal a rather high antiaromatic destabilization energy (but lower ring strain) for CBD, antiaromaticity contributes to only $\frac{1}{4}$ of the ca. 80 kcal/mol destabilization energy of CBD (evaluated by eq. 1, as well as the Benson scheme). Instead, angle strain is dominant.

3.5 DISCUSSIONS

But why should the ring strain of CBD be so much higher than cyclobutene and cyclobutane? As we have pointed out recently, the energy of two parallel H₂ molecules, brought together in

rectangular D_{2h} symmetry in order to model Pauli repulsion,¹⁹ increases dramatically as their separation decreases.¹⁸ When the distance is shortened to the 1.572 Å and 1.349 Å C–C separations in CBD, the CCSD(T)/6-311++G** repulsion energies are 25.6 and 50.6 kcal/mol,¹⁸ respectively. NBO steric analyses²⁷ of the steric repulsion between the π bonds of CBD give similar values (29.1 kcal/mol, at B3LYP/6-311+G**). Indeed, our estimate of the CBD ring strain is ca. 30 kcal/mol greater than that expected based on a mere linear extrapolation of the conventional strain energies vs. carbon hybridization changes of cyclobutane, cyclobutene, and cyclobutadiene. Consequently, neither cyclobutane alone (as in eq. 3), nor even a combination of cyclobutane and cyclobutene (as in eq. 2) can correct for the much larger angle strain in CBD.

Our evaluations of the ring strain (ca. 60 kcal/mol, destabilizing), resonance energy (10.1 kcal/mol, stabilizing), and antiaromaticity (16.5 kcal/mol, destabilizing) of CBD also conform to estimates based on conventional homodesmotic and isodesmic equations, when corrections for imbalanced energetic effects are made. As the resonance energy of CBD and butadiene differ by only 3.2 kcal/mol, π effects almost do not contribute to the endothermicity of eq. 3 (41.7 kcal/mol) and eq. 4 (62.9 kcal/mol). In effect, eq. 3, when corrected for the 3.2 kcal/mol π energy difference of butadiene and CBD, a 3.7 kcal/mol *syn-anti* butadiene energy difference, and two protobranchings in cyclobutane ($2.8 \times 2 = 5.6$ kcal/mol) ($41.7 - 3.2 - 3.7 - 5.6 = 29.2$ kcal/mol), estimates the ca. 33 kcal/mol ring strain difference between cyclobutane (26.8 kcal/mol) and CBD (ca. 60 kcal/mol). When corrected for the 3.2 kcal/mol π energy difference and a 3.7 kcal/mol *syn-anti* butadiene energy difference, eq. 4 evaluates the ring strain of CBD (56.0 kcal/mol) relative to butadiene. The inherent total destabilization energy of CBD, as evaluated by eq. 5 (48.4 kcal/mol) measures the ring strain (ca. 60 kcal/mol) and (net stabilizing) π conjugation energy of CBD (see Table 3-1).

Table 3-1. Conventional estimates for the strain energy, π resonance energy, and π antiaromaticity of CBD based on homodesmotic and isodesmic equations and new BLW estimates. Negative values indicate destabilization, positive values indicate stabilization.

	Ring strain	Resonance Energy	Antiaromaticity	Total destabilization
Conventional Estimate	ca. -33 kcal/mol	0 or “negative”	-35 to -45 kcal/mol	70 to 80 kcal/mol
BLW Estimate	ca. -60 kcal/mol	- +10.1 kcal/mol	-16.6 kcal/mol -	-74.4 kcal/mol ^a -48.4 kcal/mol ^b

^a Evaluation based on eq. 1a. ^b Evaluation based on eq. 5 (bond separation equation).

3.6 CONCLUSIONS

Our finding contrasts the prevalent literature view that CBD is highly destabilized by antiaromaticity. Instead, the high energy of CBD is due to its very strained σ -framework. CBD suffers from angle strain, torsional strain, and Pauli repulsion¹⁹ between the parallel π bonds. Despite the popular expectation for CBD as the antiaromatic paradigm, CBD is only modestly destabilized by antiaromaticity, but net stabilized by π conjugation. Planar 4n annulenes, like their comparable acyclic polyene models, are *stabilized* by π conjugation (antiaromaticity is only a minor effect).⁵⁻⁸ None of the four membered rings (i.e. cyclobutene, cyclobutane) typically used to model the strain energy of CBD, via balanced homodesmotic and isodesmic equations, resemble the structural uniqueness of CBD and thus give erroneous estimates. We emphasize Schleyer and Mo’s 2006 comment,¹⁸ that “instead of the conventional interpretation of CBD as the antiaromatic paradigm, it should be regarded as a unique molecule.”

3.7 REFERENCES

1. Emerson, G. F.; Watts, L.; Pettit, R. *J. Am. Chem. Soc.* **1965**, *87*, 131-133.
2. Masamune, S.; Nakamura, N.; Suda, M.; Ona, A. *J. Am. Chem. Soc.* **1973**, *95*, 8481-8483.
3. Gompper, R.; Holsboer, F.; Schmidt, W.; Seybold, G. *J. Am. Chem. Soc.* **1973**, *95*, 8479.
4. Breslow, R. *Chem. Eng. News* **1965**, *43*, 90-99.
5. Breslow, R. *Acc. Chem. Res.* **1973**, *6*, 393-398.
6. Wannere, C. S.; Moran, D.; Allinger, N. L.; Hess Jr., B. A.; Schaad, L. J.; Schleyer, P. v. R. *Org. Lett.* **2003**, *17*, 2983-2986.
7. Breslow, R. *Pure Appl. Chem.* **1971**, *28*, 111-130.
8. Schaad, L. J.; Hess Jr. B. A. *Chem. Rev.* **2001**, *101*, 1465-1476.
9. Fattahi, A.; Liz, L.; Tian, Z.; Kass, S. R. *Angew. Chem. Int. Ed.* **2006**, *45*, 4984-4988.
10. Cohen, N.; Benson, S. *Chem. Rev.* **1993**, *93*, 2419-2438.
11. Schurman, M. S.; Muir, S. R.; Allen, W. D.; Schaefer, H. F. III *J. Chem. Phys.* **2004**, *120*, 11586-11599.
12. Glukhovtsev, M. N.; Bach, R. D.; Laiter, S. *J. Mol. Struct.* **1997**, *417*, 123-129.
13. Deniz, A. A.; Peters, K. S.; Snyder, G. J. *Science* **1999**, *286*, 1119-1122.
14. Kovacevic, B.; Baric, D.; Maksic, Z. B.; Müller, T. *J. Phys. Chem. A* **2004**, *108*, 9126-9133.
15. Hohlneicher, G.; Packschies, L.; Weber, J. *Phys. Chem. Chem. Phys.* **2007**, *9*, 2517-2530.
16. Suresh, C. H.; Koga, N. *J. Org. Chem.* **2002**, *67*, 1965-1968.
17. Bally, T. *Angew. Chem. Int. Ed.* **2006**, *45*, 6616-6619.
18. Mo, Y.; Schleyer, P. v. R. *Chem. Eur. J.* **2006**, *12*, 2009-2020.
19. Politzer, P.; Grice, M. E.; Murray, J. S.; Seminario, J. M. *Can. J. Chem.* **1993**, *71*, 1123.

20. Mo, Y.; Wu, W.; Zhang Q. *J. Phys. Chem.* **1994**, 98, 10048-10053.
21. Baird, N. C. *J. Am. Chem. Soc.* **1972**, 94, 4941-4948
22. Gogonea, V.; Schleyer, P. v. R.; Schreiner, P. R. *Angew. Chem. Int. Ed.* **1998**, 37, 1945-1948.
23. Evangelista, F. A.; Allen, W. D.; Schaefer, H. F. III *J. Chem. Phys.* **2007**, 127, 24102-24119.
24. Wenthold, P. G.; Hrovat, D. A.; Borden, W. T.; Lineberger, W. C. *Science* **1996**, 272, 1456-1459.
25. Borden, W. T.; Davidson, E. R. *J. Am. Chem. Soc.* **1977**, 99, 4587-4594.
26. a) Mo, Y.; Peyerimhoff, S. D. *J. Chem. Phys.* **1998**, 109, 1687-1697; b) Mo, Y.; Zhang, Y.; Gao, J. *J. Am. Chem. Soc.* **1999**, 121, 5737-5742; c) Mo, Y.; Subramanian, G.; Ferguson, D. M.; Gao, J. *ibid* **2002**, 124, 4832-4837; d) Mo, Y.; Wu, W.; Song, L.; Lin, M.; Zhang, Q.; Gao, J. *Angew. Chem.* **2004**, 116, 2020-2024; *Angew. Chem. Int. Ed.* **2004**, 43, 1986-1990; e) Mo, Y. *J. Chem. Phys.* **2003**, 119, 1300-1306; f) Mo, Y.; Song, L.; Wu, W.; Zhang, Q. *J. Am. Chem. Soc.* **2004**, 126, 3974-3982; g) Mo, Y. *J. Org. Chem.* **2004**, 69, 5563-5567; h) Mo, Y.; Song, L.; Lin, Y. *J. Phys. Chem. A* **2007**, 111, 8291-8301.
27. NBO 5.0. Glendening, E. D.; Badenhoop, J. K.; Reed, A. E.; Carpenter, J. E.; Bohmann, J. A.; Morales, C. M.; Weinhold, F. Theoretical Chemistry Institute, University of Wisconsin, Madison (2001).

CHAPTER 4

WHY IS THE STRAIN ENERGY OF CYCLOPROPANE SO LOW?[†]

[†] Judy I. Wu, Frank Weinhold, Paul Schleyer.

To be submitted.

4.1 ABSTRACT

Cyclopropane is not stabilized by any special cyclic σ -aromaticity, but instead, benefits energetically from substantial geminal $\sigma_{\text{cc}} \rightarrow \sigma_{\text{cc}}^*$ (CCC) hyperconjugations (42.4 kcal/mol, three interactions, 14.1 kcal/mol each). This surprisingly large electron delocalization stabilization is the reason for cyclopropane's low conventional strain energy (27.6 kcal/mol, similar to that of cyclobutane, 26.6 kcal/mol). The larger cycloalkanes (C_nH_{2n} , $n = 4-6$) enjoy much less CCC geminal hyperconjugative stabilization (< 2 kcal/mol per interaction) due to their wider CCC bond angles, and thus less effective geminal $\sigma_{\text{cc}} \rightarrow \sigma_{\text{cc}}^*$ orbital overlap. Likewise, the 60° CCC bond angles of tetrahedrane encourage geminal $\sigma_{\text{cc}} \rightarrow \sigma_{\text{cc}}^*$ hyperconjugation. On the other hand, all of the Si_nH_{2n} ($n = 3-6$) silicon rings display only from modest (SiSiSi) geminal $\sigma_{\text{SiSi}} \rightarrow \sigma_{\text{SiSi}}^*$ hyperconjugation (ca. 3 kcal/mol per interaction). Substitution around the cyclopropane ring can influence the magnitudes of geminal hyperconjugative stabilizations; electropositive substituents enhance geminal hyperconjugation, electronegative substituents have the opposite effect. Nucleus independent chemical shifts (NICS) computations also reveal no evidence for any special σ -aromaticity in cyclopropane or in tetrahedrane.

4.2 INTRODUCTION

The origin of the unexpectedly low strain energy of cyclopropane remains a mystery. Baeyer's 1885 speculation, that the deviations of the ring angles of *assumed planar cycloalkanes* from the tetrahedral 109.5° introduces "strain," was first put forth to explain why three and four membered rings were unknown at the time.¹ Accordingly, Baeyer conjectured that increasing angle deviations of planar rings larger and smaller than cyclopentane should result in greater strain, as shown in Figure 4-1 (black dashed line and dotted grey line).

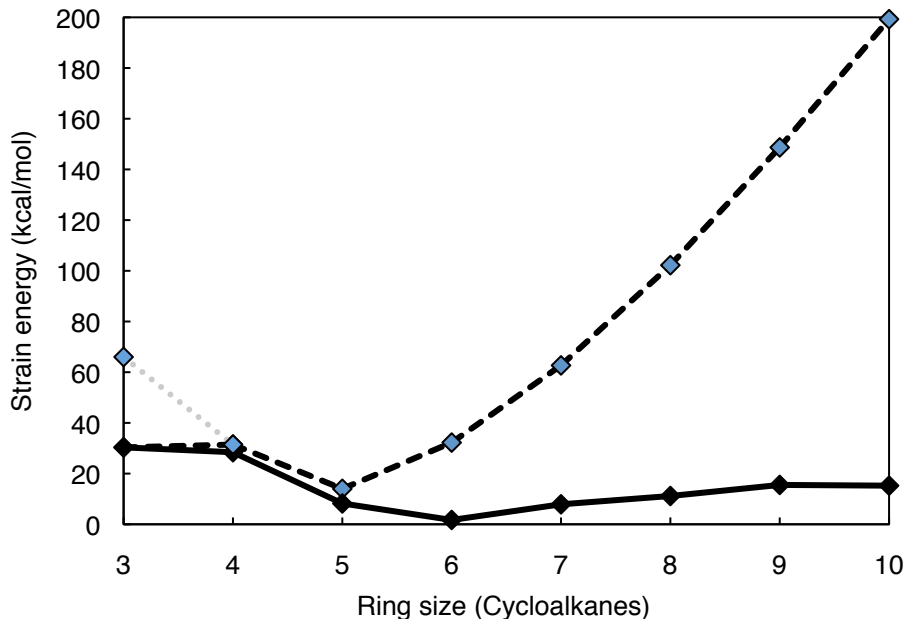


Figure 4-1. Strain energy vs. the number of carbons for cycloalkanes ($n = 3$ to 6) at their the assumed *planar* geometries (black dashed lines) and at their equilibrium geometries (black solid line). The strain energies are evaluated by $n \text{ C}_3\text{H}_8 \rightarrow n \text{ C}_2\text{H}_6 + \text{C}_n\text{H}_{2n}$, at MP2/6-311+G** (no ZPE correction). The dotted grey line indicates the expected strain energy relationship between cyclopropane and cyclobutane based on Baeyer's angle strain theory.

However, by 1950, reliable thermochemical measurements and the realization that rings (other than cyclopropane) were *not planar* did not agree with Baeyer's original strain theory.¹ When the strain energies of the cycloalkanes (C_nH_{2n} , $n = 3$ to 6) were derived by comparison to the assigned "strain-free" acyclic alkanes, via the following homodesmotic equation: $n \text{ C}_3\text{H}_8 \rightarrow \text{C}_n\text{H}_{2n} + n \text{ C}_2\text{H}_6$, cyclohexane (D_{3d} , $\angle\text{CCC}=111.5^\circ$, CSE: 0.2 kcal/mol, expt.) rather than cyclopentane (C_2 , $\angle\text{CCC}=103^\circ\text{-}106^\circ$, CSE: 6.3 kcal/mol, expt.) had the lowest conventional strain energy (CSE). (Note that cyclohexane, even at its D_{3d} equilibrium geometry, is only "strain-free" by convention!)² The larger cycloalkane rings ($n = 7$ to 10) also have only modest

ring strain as a result of their non-planarity (see Figure 4-1, black solid line). Nevertheless, the most striking discovery was the exceptionally low CSE of cyclopropane (27.6 kcal/mol, expt.) (D_{3h} , $\angle CCC=60.0^\circ$). Based on pure geometrical considerations, both the CSE's of cyclopentane and cyclobutane (26.6 kcal/mol, eq. 1b, expt.) (D_{2d} , $\angle CCC=88.8^\circ$) followed expectations reasonably well, but that of cyclopropane appeared to be much out of line (see Figure 4-1, grey dashed line). Why is the CSE of cyclopropane almost the same as cyclobutane?

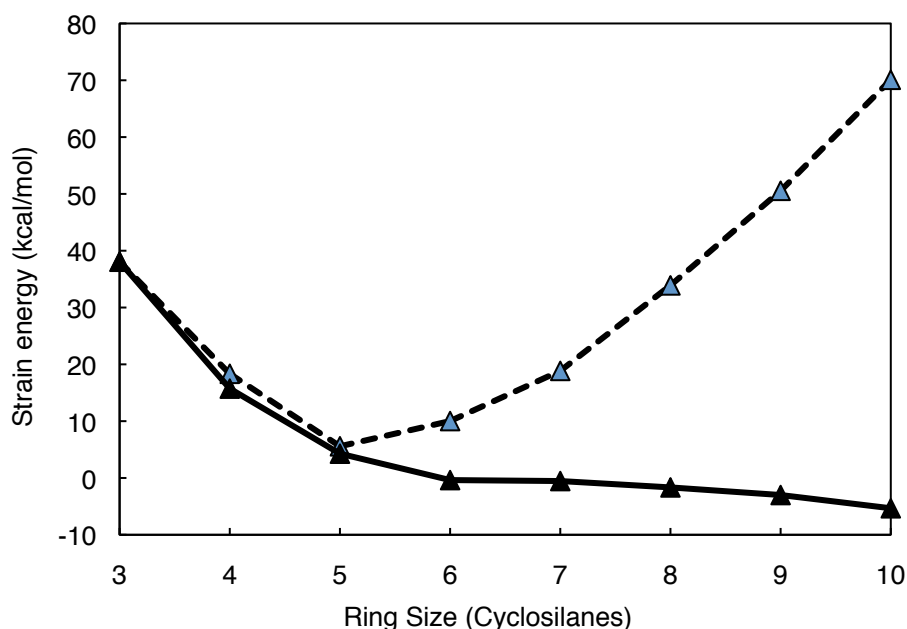


Figure 4-2. Strain energy vs. the number of silicons for silacycloalkanes ($n = 3$ to 6) at their the assumed *planar* geometries (black dashed lines) and at their equilibrium geometries (black solid line). The strain energies are evaluated by $n \text{ Si}_3\text{H}_8 \rightarrow n \text{ Si}_2\text{H}_6 + \text{Si}_n\text{H}_{2n}$, at MP2/6-311+G** (no ZPE correction).

On the other hand, the seemingly analogous silicon rings followed Baeyer's expectations¹ at least for the three, four, and five membered silicon rings (see Figure 4-2). This prompted

Schleyer's comment, in 1986, that "perhaps Baeyer should have been a silicon chemist!"³ Based on $n \text{ Si}_3\text{H}_8 \rightarrow n \text{ Si}_2\text{H}_6 + \text{Si}_n\text{H}_{2n}$, the CSE of silacyclopropane (38.1 kcal/mol) is more than twice that of silacyclobutane (15.7 kcal/mol) and much higher than that of silacyclopentane (4.3 kcal/mol, C_s), and silacyclohexane (−0.4 kcal/mol) (computations at MP2/6-311+G**, see Figure 4-2). Likewise, the CSE's of cyclopropene (53.7 kcal/mol, expt.) is much higher than that of cyclobutene (29.8 kcal/mol, expt.).⁴ Clearly, angle strain is not the only effect that governs the cycloalkane strain energies. But is cyclopropane particularly stabilized or is cyclobutane unusually destabilized? Why do the estimated silicon ring strain follow the expected trend based on angle deviations, but not the carbon rings?

Cyclopropane is chemically and structurally *special* among the cycloalkanes, and may be in many ways, more appropriately viewed as an olefinic "trimethylene ring." Note that Baeyer's 1885 paper¹ considered ethylene to be the smallest two membered ring, i.e., an olefinic "dimethylene ring."

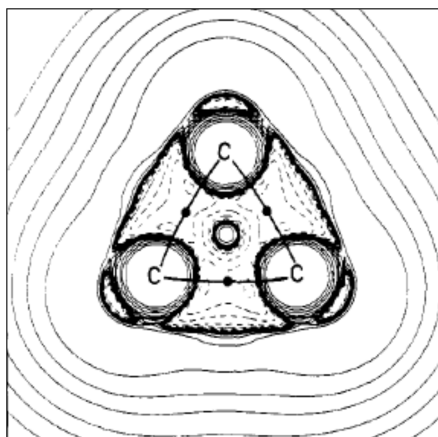


Figure 4-3. Contours of the Laplacian, $\nabla^2\rho(r)$, for cyclopropane (reproduced with permission from ref. 9). Bond paths are marked by thick solid lines, bond critical points are indicated by dots; $\nabla^2\rho(r) < 0$ (dashed lines) indicate a concentration of electron density.

Topologically, the σ -electron density distribution of cyclopropane closely resembles the π -density of ethylene (based on a “bent” bond picture). The Laplacian representation of the electron density, $\nabla^2\rho(r)$, for cyclopropane (see Figure 4-3, reproduced with permission from reference 9) reveal extended electron density toward the three membered ring center and away from the line directly connecting each of the C–C bonds (note also the slightly convexed C–C bond path of cyclopropane, Figure 4-3). Hence, the C–C bonds of cyclopropane are often viewed as being either highly “bent” or “alkene-like.” The Coulson-Moffit model describes the bent bonds of cyclopropane by three rehybridized carbons of high p character.⁵ Alternatively, the Walsh model illustrates C–C bonds of cyclopropane by a “ π -type” bonding, which utilizes three unhybridized methylene carbene-like orbitals.⁶ As a result of its weaker C–C bond, cyclopropane also displays double bond-like chemical reactivities and readily undergoes addition reactions that lead to ring opening.

Dewar first suggested that cyclopropane, due to its three sets of geminal CCC interactions and six skeletal σ -electrons, is “isoconjugate” with benzene.^{7, 8} The presence of σ -aromaticity (stabilization) in cyclopropane and σ -antiaromaticity (destabilization) in cyclobutane might be the reason for their similar strain energies.⁷ In support, Cremer et al. described the accumulation of electron density towards the cyclopropane ring center by the term *surface delocalization*, and conjectured that the angle deformation strain energy of cyclopropane might be partially relieved by such an effect.⁹ Although Dewar claimed that the σ -aromatic stabilization of cyclopropane might be as large as 55.1 kcal/mol in 1954,⁸ subsequent evaluations of the σ -aromaticity hypothesis using various lines of reasoning and degrees of sophistication all have resulted in much lower estimates (see Table 4-1).^{3, 10-13}

Table 4-1. Literature estimates of the σ -aromaticity of cyclopropane.

Estimates for σ -aromaticity	
Dewar (1954) ⁸	55.1 kcal/mol
Robert/Caserio (1964) ¹⁰	5 kcal/mol
Cremer (1985) ⁹	48 kcal/mol
Cremer/Gauss (1986) ¹¹	17 kcal/mol
Schleyer (1986) ³	13 kcal/mol
Exner/Schleyer (2001) ¹²	11.3 kcal/mol
Mo (2009) ¹³	−0.7 kcal/mol

Schleyer even expressed skepticism in 1986, that, “There is no need to invoke σ -aromaticity to explain the thermochemistry of cyclopropane.”³ Mo et al.’s recent VB computations found no significant aromatic σ -stabilization for cyclopropane.¹³ The computed σ -electron delocalization energy of cyclopropane (12.5 kcal/mol) was nearly the same as that of butane (13.2 kcal/mol), the extra cyclic resonance energy (ECRE) of cyclopropane is close to zero. Lazzeretti et al.’s¹⁴ recent detailed analysis of the magnetic behavior of cyclopropane also found “no evidence for strong diatropism and therefore no σ -aromaticity” in cyclopropane.

Could rehybridization be responsible for the low cyclopropane CSE^{10, 12} The Coulson-Moffitt model⁵ for cyclopropane predicts that rehybridization should weaken the C–C bonds but strengthen C–H bonds to a greater extent. Silicon rings benefit far less since second row atoms do not rehybridize well. NBO computations¹⁵ reveal that the cyclopropane C–C bonds have unusually high p character ($Csp^{3.41}$, computed at MP2/6-311+G**) compared to than ethane ($Csp^{2.33}$), and thus have weaker bond strengths. However, this is compensated by strengthened C–H bonds (cyclopropane: $Csp^{2.65}$, ethane: $Csp^{3.27}$), which have sp^2 -like character. In contrast, the weakened Si–Si bonds in silacyclopropane ($Sisp^{3.76}$) compared to disilane ($Sisp^{3.00}$) are not

compensated by much Si–H bond strengthening (*Sisp*^{2,40}, the Si–H bond of disilane has *Sisp*^{3,00}). Schleyer and Exner's detailed theoretical bond energy analysis¹² revealed that the overall CC bond weakening in cyclopropane is about 40.4 kcal/mol (relative to cyclohexane), while the C–H bond strengthening is only 11.7 (taken to be an estimate of the σ -aromaticity of cyclopropane). The net effect (28.7 kcal/mol) approximates the conventional strain energy of cyclopropane, but even C–H bond strengthening is insufficient in the quantitative sense to account for the cyclopropane strain anomaly. Cremer et al.'s estimated angle strain for cyclopropane (66 kcal/mol), based on computed CCC bending force constants and a 79° interpath CCC angle for cyclopropane (considering its bent C–C bonds), is almost 40 kcal/mol higher than the actual CSE (27.6 kcal/mol) of cyclopropane.⁹

Is cyclobutane anomalous? Dunitz and Schomaker proposed that repulsion between the non-bonded carbons in cyclobutane (as a result of their unusually short ca. 2.22 Å cross-ring distance) could lead to an unusually high strain energy,¹⁶ while such interactions are absent in cyclopropane and attenuated for the larger cycloalkanes. As a result, the C–C bonds of cyclobutane (1.556 Å)¹⁷ are much longer than the typical 1.54 Å alkane C–C distance, and in sharp contrast with cyclopropane's relatively short bent C–C bond (1.512 Å).¹⁸ Cyclopentane (average C–C bond distance: 1.546 Å)¹⁹ and cyclohexane (C–C bond length: 1.536 Å)²⁰ also have shorter C–C bond lengths compared to cyclobutane. However, the computed Si–Si bond distances of silacyclobutane (2.356 Å) also are longer than those of silacyclopentane (2.333 Å), silacyclopentane (2.347 to 2.360 Å), and silacyclohexane (2.346 Å) (MP2/6-311+G** geometry), but the strain energies of the silicon rings follow the expected Baeyer trend.

Hence, factors other than σ -aromaticity/antiaromaticity and rehybridization differences must be responsible for the similar strain energies of cyclopropane and cyclobutane. Wiberg and

Landis suggested that considerable $\sigma_{\text{cc}} \rightarrow \sigma_{\text{cc}}^*$ (CCC) geminal hyperconjugation in cyclopropane (ca. 30 kcal/mol, from six $\sigma_{\text{cc}}-\sigma_{\text{cc}}^*$ interactions) could compensate the large angle strain.²¹ Their computed NBO donor-acceptor interactions energies for a model propane (computed with systematic CCC angle deformation) revealed remarkable $\sigma_{\text{cc}}-\sigma_{\text{cc}}^*$ geminal hyperconjugation stabilization energies for CCC angles smaller than 90°. In effect, this recasts Dewar's arguments^{7,8} without invoking special cyclic “ σ -aromaticity” effects. However, Mo et al.'s more recent XMVB²² study did not find any “special stabilization” in cyclopropane.¹³ Instead, the computed delocalization energies (DE's) per CH₂ for cyclopropane (7.6 kcal/mol) and cyclobutane (6.9 kcal/mol) were quite similar. The corresponding data for Si₃H₆ and Si₄H₈ data are 4.1 kcal/mol and 3.2 kcal/mol, respectively (at HF/6-31G*).

The NBO¹⁵ vs. XMVB²² discrepancy is due the use of different theoretical reference wavefunctions (constructed artificially to describe a fully localized cyclopropane). In both methods, the electron delocalization stabilization of cyclopropane is derived by the energy difference between the fully delocalized wavefunction and the electronically constrained “localized” wavefunction. In the NBO donor-acceptor formalism, the localized reference adopts an enforced Lewis wavefunction. Thus, the accumulated electron density at the cyclopropane ring center is considered highly delocalized. On the other hand, the XMVB method utilizes the same basis functions to describe the spatial distribution of the electrons of in the delocalized and constrained wave functions. As a result, the central electron densities of cyclopropane are not viewed as being exceptionally delocalized. The justification of choosing one theoretical reference standard over another (e.g. for evaluating electron delocalization energies) is as arbitrary as the choice of particular reference molecules over other alternatives when deriving the

stabilization or destabilization energies of molecules by balanced homodesmotic or isodesmic equations. But different viewpoints can offer complementary insights.

In this paper, we investigate the cyclopropane ring strain anomaly from the NBO perspective. Detailed NBO analyses were carried out to examine the energetic impact of CCC geminal delocalization in cyclopropane as well as many closely related systems, i.e., cycloalkanes, silacycloalkanes, substituted cyclopropane, cubane and tetrahedrane. Dissected canonical molecular orbital nucleus independent chemical shifts (CMO-NICS) computations verified the absence of σ -aromaticity in cyclopropane.

4.3 METHODS

All geometries were optimized at the MP2/6-311+G** level employing the Gaussian03 program.²³ The CCC geminal delocalization energies for each of the $\sigma_{cc} \rightarrow \sigma_{cc}^*$ interactions were computed at the HF/6-311+G**//HF/6-311+G** level by the natural bond orbital (NBO) 5.0 program.¹⁵ For example, the total CCC geminal delocalization energy for cyclopropane is computed by the energy difference between a “localized” Lewis structure (i.e., by deleting the following six elements: $\sigma_{c1c2} \rightarrow \sigma_{c1c3}^*$, $\sigma_{c1c3} \rightarrow \sigma_{c1c2}^*$, $\sigma_{c2c3} \rightarrow \sigma_{c1c3}^*$, $\sigma_{c1c3} \rightarrow \sigma_{c2c3}^*$, $\sigma_{c1c2} \rightarrow \sigma_{c2c3}^*$, $\sigma_{c2c3} \rightarrow \sigma_{c1c2}^*$) and that of the fully delocalized cyclopropane wavefunction. Dissected nucleus independent chemical shifts (NICS)²⁴ for probing the σ -aromaticity of cyclopropane were computed employing the most sophisticated NICS(0)_{MOzz} index (NICS point placed at the center of the ring). The NICS(0)_{MOzz} index extracts the out-of-plane tensor component of isotropic NICS values, and includes contributions only from relevant molecular orbitals. Since caged compounds do not have specific “ring planes,” the aromaticity of tetrahedrane was

evaluated by NICS(0)_{MO} computed at the cage center. All NICS data were computed at the PW91/IGLOIII level.

4.4 THE “MISSING” STRAIN IN CYCLOPROPANE

No other cycloalkane display as much unfavorable structural features as cyclopropane. Cyclopropane suffers from angle strain, compression strain, and eclipsing strain. Besides having very narrow 60° CCC bonds angles, cyclopropane has much shorter C–C bond lengths (1.512 Å) compared to the typical alkane (ca. 1.54 Å) and is marred by six fully eclipsed CH's around its planar ring. The larger cycloalkanes have non-planar minimum geometries and thus have mostly staggered vicinal CH's. Clearly, cyclopropane's 27.6 kcal/mol CSE is much too low if no other stabilizing factors were present. But how much lower is cyclopropane's strain energy compared to its expected value, in view of the strain energies of cyclobutane, cyclopentane, and cyclohexane?

Simple considerations based on a linear extrapolation of the conventional strain energies (CSE) and average ring bond angles ($\angle\text{CCC}_{\text{avg}}$, computed at MP2/6-311+G**) of cyclohexane (CSE: 0.2 kcal/mol, $\angle\text{CCC}_{\text{avg}} = 111.05^\circ$), cyclopentane (CSE: 6.3 kcal/mol, $\angle\text{CCC}_{\text{avg}} = 104.2^\circ$), and cyclobutane (CSE: 26.6 kcal/mol, $\angle\text{CCC}_{\text{avg}} = 87.66^\circ$) suggest that the “expected” strain energy for cyclopropane (58.2 kcal/mol, see Figure 4-4) is at least twice its CSE (27.6 kcal/mol, $\angle\text{CCC}_{\text{avg}} = 60.00^\circ$). This is not far from Cremer's 66 kcal/mol estimate of cyclopropane's angle strain.⁹ On this basis, a ca. 30-40 kcal/mol stabilization is needed to rationalize cyclopropane's much too low CSE.

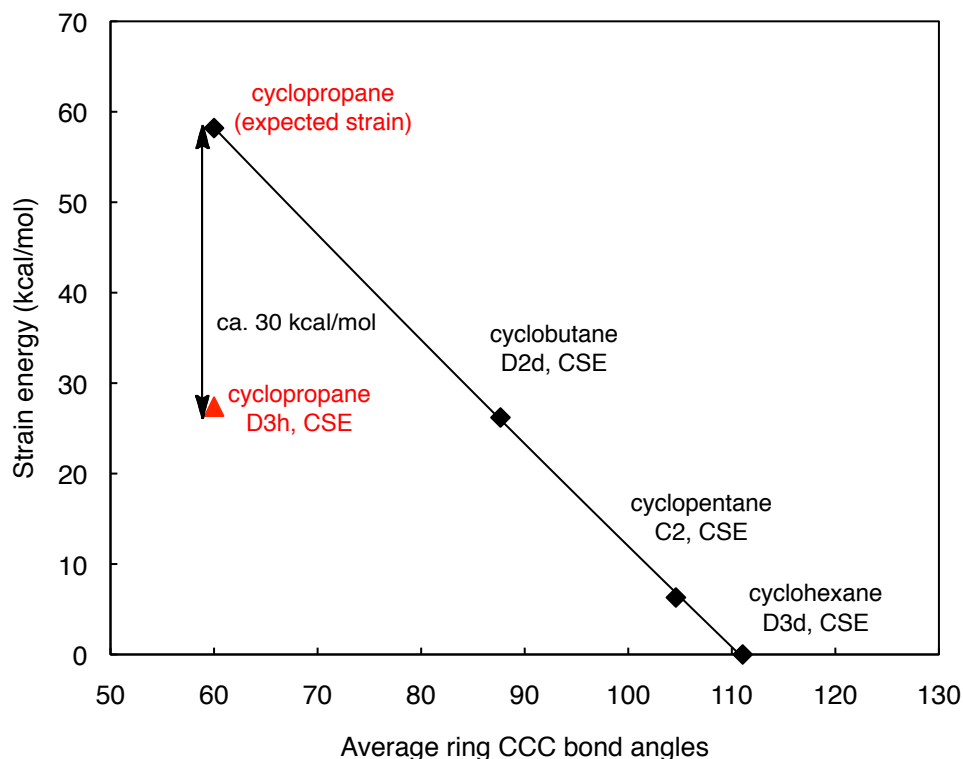


Figure 4-4. Conventional strain energy (based on $n \text{ C}_3\text{H}_8 \rightarrow n \text{ C}_2\text{H}_6 + \text{C}_n\text{H}_{2n}$, expt.) vs. the average ring CCC bonds angles (geometries computed at MP2/6-311+G**) of cyclopropane (D_{3h}), cyclobutane (D_{2d}), cyclopentane (C_2), and cyclohexane (D_{3d}). The expected cyclopropane ring strain (extrapolated by the CSE's of cyclobutane, cyclopentane, and cyclohexane) is ca. 30 kcal/mol higher than its CSE.

Traditionally, the CSE's of cycloalkanes are derived by comparing their heats of formation to the energies of acyclic linear alkanes through the following homodesmotic equation: (1) $n \text{ C}_3\text{H}_8 \rightarrow n \text{ C}_2\text{H}_6 + \text{C}_n\text{H}_{2n}$. However, equation 1 is conceptually flawed due to the neglect of protobranching effects (stabilizing interactions between 1,3-nonbonded alkyl groups).²⁵ Besides cyclopropane (zero protobranches),^{25, 26} other members in the cycloalkane family are stabilized by protobranching; cyclobutane has two protobranches, cyclopentane has

five protobranches, and cyclohexane has six protobranches. But these effects (or the absence of) are cancelled out to different extents by n numbers of protobranching on the left side of the equation (propane has one protobranching and appears n times). In addition, eq. 1 for cyclopropane evaluates the energetic consequence of compression strain and eclipsing strain; propane has only staggered vicinal CH's and a 1.531 Å C–C bond length, while cyclopropane has only eclipsed CH's and a short 1.512 Å C–C bond distance. But these effects are not present in the larger cycloalkane rings.

Table 4-2. Strain estimates for C_nH_{2n} ($n = 3$ to 6) rings based on various equations: **(1)** $n C_3H_8 \rightarrow n C_2H_6 + C_nH_{2n}$ and **(2)** $n C_2H_6 \rightarrow n CH_4 + C_nH_{2n}$ (evaluated by experimental heats of formation).²⁷ Equation **(1)** evaluates the conventional strain energies (CSE) of cycloalkanes. Equation **(2)** gives the bond separation equation (BSE) strain, and includes protobranching stabilization.

	CSE (1)	BSE (2)
C_3H_6 (D_{3h})	27.57 kcal/mol	19.50 kcal/mol
C_4H_8 (D_{2d})	26.55 kcal/mol	15.79 kcal/mol
C_5H_{10} (C_2)	6.27 kcal/mol	–7.18 kcal/mol
C_6H_{12} (D_{3d})	0.21 kcal/mol	–15.93 kcal/mol
NOTES	1. Angle strain included	1. Angle strain included
	2. Protobranching <i>imbalanced</i>	2. Protobranching stabilization included
	3. Compression strain included for C_3H_6	3. Compression strain included for C_3H_6
	4. Eclipsing strain included for C_3H_6	4. Eclipsing strain included for C_3H_6

Isodesmic bond separation equations (BSE), $n C_2H_6 \rightarrow n CH_4 + C_nH_{2n}$ (equation 2), correct for this problem partially ...offer a superior alternative for measuring the inherent strain energies of cycloalkanes, and *include* protobranching stabilization (two, five, and six in

cyclobutane, cyclopentane, and cyclohexane, respectively).²⁵ The BSE strain energies of cyclopropane, cyclobutane, cyclopentane, and cyclohexane are 19.5 kcal/mol, 15.8 kcal/mol, –7.2 kcal/mol, and –15.9 kcal/mol (see also Table 4-2). Cyclopentane and cyclohexane have negative BSE values as stabilizing protobranching effects overwhelm their subtle destabilizing angle strains. The expected cyclopropane ring strain (53.5 kcal/mol), derived by extrapolating the BSE's of cyclobutane, cyclopentane, and cyclohexane, is 34 kcal/mol higher than its BSE value (19.5 kcal/mol).

Note that strain is a *relative* energetic property that depends on the (rather arbitrary) choice of reference standard. Thus, the justification of one reference over another often relies on their structural and chemical similarity to the target molecule. Differences among various evaluation schemes for the cycloalkane ring strains are due to the inclusion of different energetic effects. The CSE (eqs. 1 and 2) and BSE (eq. 3) strain evaluations differ predominantly by excluding and including protobranching stabilizations, respectively. However, both equations are marred by imbalanced compression strain and eclipsing strain for cyclopropane.

Hence, one may evaluate the BSE of cyclopropane relative to two eclipsed ethanes (six eclipsed CH's) and one staggered ethane, instead of three staggered ethanes. The revised BSE for cyclopropane, based on two times the ethane rotational barrier (3 kcal/mol each), is only 13.6 kcal/mol. Alternatively, one could compare cyclopropane to ethylene. Based on $3/2 \text{ C}_2\text{H}_4 \rightarrow \text{C}_3\text{H}_6$ (eq. 3, balanced for six eclipsed CH's on both sides of the equation), cyclopropane displays *negative* strain (–6.1 kcal/mol)!²⁶ This is not surprising if one considers ethylene as the smallest two membered “dimethylene” ring. The C–C σ -bonds of ethylene (compressed from the typical alkane C–C distance, 1.54 Å, to a 1.330 Å length) surely suffer from more compression strain than the 1.512 Å C–C σ -bonds of cyclopropane.

Clearly, Baeyer (angle) strain is not the only factor that governs the energies of cycloalkanes, but other stabilizing (e.g. protobranching, hyperconjugation, as we emphasize below) and destabilizing (e.g. eclipsing strain and compression strain) effects also are important.

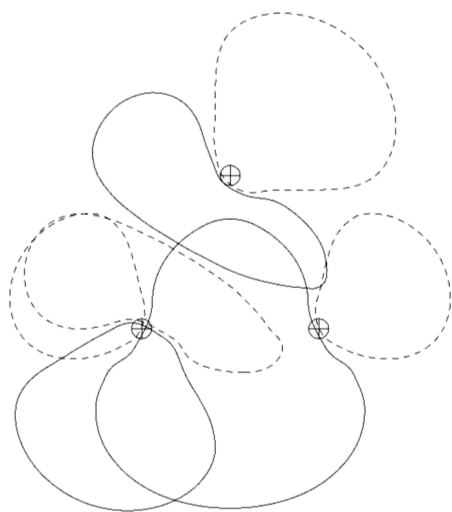
4.5 GEMINAL DELOCALIZATION AND SUBSTITUENT EFFECTS

Compared to the four, five, and six membered ring cycloalkanes, cyclopropane benefits from three CCC geminal hyperconjugation stabilization ($\sigma_{cc} \rightarrow \sigma_{cc}^*$) between each of the C–C bonds that share a common carbon atom. The NBO orbital deletion procedure (see Methods) reveals that cyclopropane is stabilized by CCC geminal electron delocalization by 42.3 kcal/mol (14.1 kcal/mol between each pair of C–C bonds, see Table 4-3) relative to its fully localized Lewis structure! This extra stabilization easily accounts for the majority of cyclopropane’s ca. 30-40 kcal/mol “missing strain” without the need to invoke any σ -aromaticity. In contrast, geminal $\sigma_{cc} \rightarrow \sigma_{cc}^*$ hyperconjugations between the C–C bonds of cyclobutane (0.1 kcal/mol per interaction), cyclopentane (0.9 kcal/mol per interaction), and cyclohexane (1.5 kcal/mol per interaction) are much less stabilizing (see Table 4-3). On the other hand, all of the silacycloalkanes have only modest geminal $\sigma_{SiSi} \rightarrow \sigma_{SiSi}^*$ hyperconjugation stabilization: silacyclopropane (3.1 kcal/mol per interaction), silacyclobutane (3.0 kcal/mol e per interaction), silacyclopentane (3.3 kcal/mol per interaction), silacyclohexane (3.1 kcal/mol per interaction) (see Table 4-3).

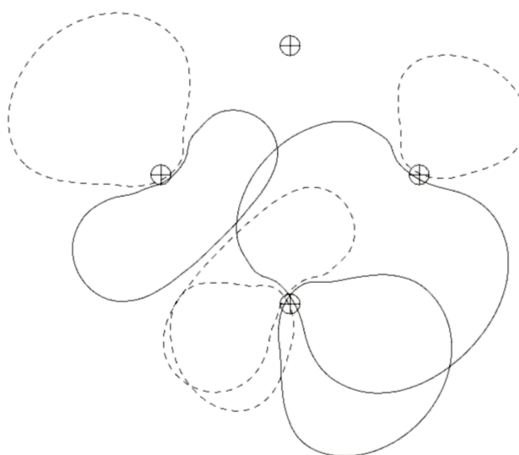
As pointed out already by Weinhold and Landis,²¹ the degree of geminal CCC hyperconjugation of hydrocarbons are closely related to their $\angle CCC$ angles; bond angles greater than 90° lead to diminished $\sigma_{cc}-\sigma_{cc}^*$ orbital overlap and reduced geminal $\sigma_{cc} \rightarrow \sigma_{cc}^*$ hyperconjugation, on the other hand, bond angles smaller than 90° encourage geminal $\sigma_{cc} \rightarrow \sigma_{cc}^*$ hyperconjugation. Cyclopropane’s 60° $\angle CCC$ bond angles, despite imposing unfavorable angle

strain, are beneficial for effective geminal $\sigma_{cc} \rightarrow \sigma_{cc}^*$ orbital overlap (see Figure 4-5a). The “bent” C–C bonds of cyclopropane also facilitate geminal $\sigma_{cc} \rightarrow \sigma_{cc}^*$ orbital overlap; the C–C bond electron density extends towards the three membered ring center (see Figure 4-5a). Note that even cyclobutane (see Figure 4-5b) reveals much less geminal $\sigma_{cc} \rightarrow \sigma_{cc}^*$ orbital overlap compared to cyclopropane. For the same reason, the highly strained tetrahedrane reveals substantial geminal $\sigma_{cc} \rightarrow \sigma_{cc}^*$ hyperconjugative stabilizations (104.2 kcal/mol, 12 interactions, 8.7 kcal/mol each), although to a lesser extent, per interaction, compared to cyclopropane. In sharp contrast, cubane enjoys much less geminal $\sigma_{cc} \rightarrow \sigma_{cc}^*$ hyperconjugation (12.7 kcal/mol, 24 interactions, only 0.5 kcal/mol each!).

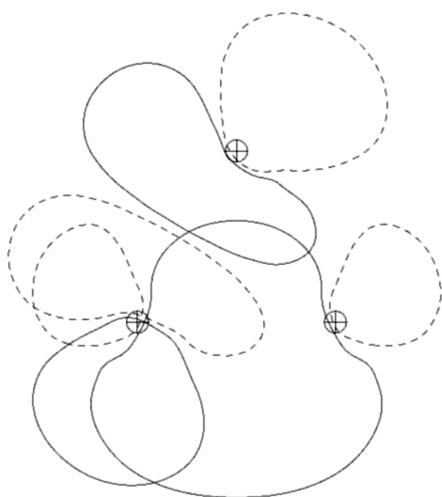
Substituents can influence the degree of geminal hyperconjugative stabilizations in cyclopropane^{28, 29} by reducing or enhancing effective geminal $\sigma_{cc} \rightarrow \sigma_{cc}^*$ orbital overlap; electropositive (BeH) substituents enhance geminal delocalization, electronegative (F) substituents have the opposite effect. Thus, perfluorocyclopropane has much reduced geminal $\sigma_{cc} \rightarrow \sigma_{cc}^*$ hyperconjugation (4.1 kcal/mol per interaction, see Table 4-3) compared to cyclopropane, due to less effective $\sigma_{cc}-\sigma_{cc}^*$ orbital overlap (see Figure 4-5c). Since perfluorination reduces favorable geminal $\sigma_{cc} \rightarrow \sigma_{cc}^*$ hyperconjugation in the three membered ring, the strain energies of the perfluoroalkanes, evaluated by $n \text{ C}_3\text{F}_8 \rightarrow n \text{ C}_2\text{F}_6 + \text{C}_n\text{F}_{2n}$, are follow expectations based on their CCC angle deviation from the tetrahedral 109.5° (see Figure 4-6). Conversely, $\text{C}_3(\text{BeH})_6$ displays even slightly greater geminal $\sigma_{cc} \rightarrow \sigma_{cc}^*$ hyperconjugation (16.6 kcal/mol per interaction, see Table 4-3) than cyclopropane, due to enhanced $\sigma_{cc}-\sigma_{cc}^*$ orbital overlap (see Figure 4-5d).



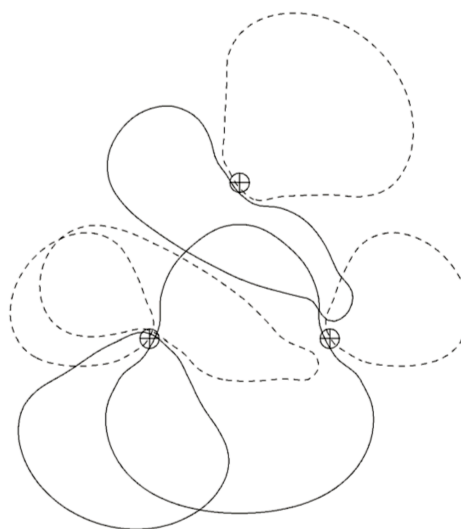
a) C_3H_6



b) C_4H_8



c) C_3F_6



d) $\text{C}_3(\text{BeH})_6$

Figure 4-5. Geminal $\sigma_{\text{cc}} \rightarrow \sigma_{\text{cc}}^*$ interactions in cyclopropane (C_3H_6), cyclobutane (C_4H_8 , D_{4h}), C_3F_6 , and $\text{C}_3(\text{BeH})_6$. Note the visibly more “bent” C–C bonding orbitals of the three membered rings (greater coefficients that extent to the center of the ring) compared to C_4H_8 .

Table 4-3. Interaction per geminal $\sigma_{cc} \rightarrow \sigma_{cc}^*$ hyperconjugation (HPC) for the cycloalkanes C_nH_{2n} , C_nF_{2n} , $C_n(BeH)_{2n}$, and silacycloalkanes Si_nH_{2n} , $n = 3$ to 6 series. (NBO data computed at the HF/6-311+G**//HF/6-311+G** level)

	P.G. (NIm)	HPC (kcal/mol)		P.G. (NIm)	HPC (kcal/mol)
C_3H_6	D_{3h} (0)	14.13	$C_3(BeH)_6$	D_{3h} (3)	16.57
C_4H_8	D_{2d} (0)	0.97	$C_4(BeH)_8$	D_{4h} (6)	0.77
C_5H_{10}	C_2 (0)	0.90	$C_5(BeH)_{10}$	D_{5h} (10)	0.25
C_6H_{12}	D_{3d} (0)	1.54	$C_6(BeH)_{12}$	D_{6h} (15)	0.03
C_3F_6	D_{3h} (0)	4.12	Si_3H_6	D_{3h} (0)	3.06
C_4F_8	D_{2d} (0)	0.01	Si_4H_8	D_{2d} (0)	3.03
C_5F_{10}	C_2 (0)	0.02	Si_5H_{10}	C_2 (0)	3.31
C_6F_{12}	D_{3d} (0)	0.08	Si_6H_{12}	D_{3d} (0)	3.05

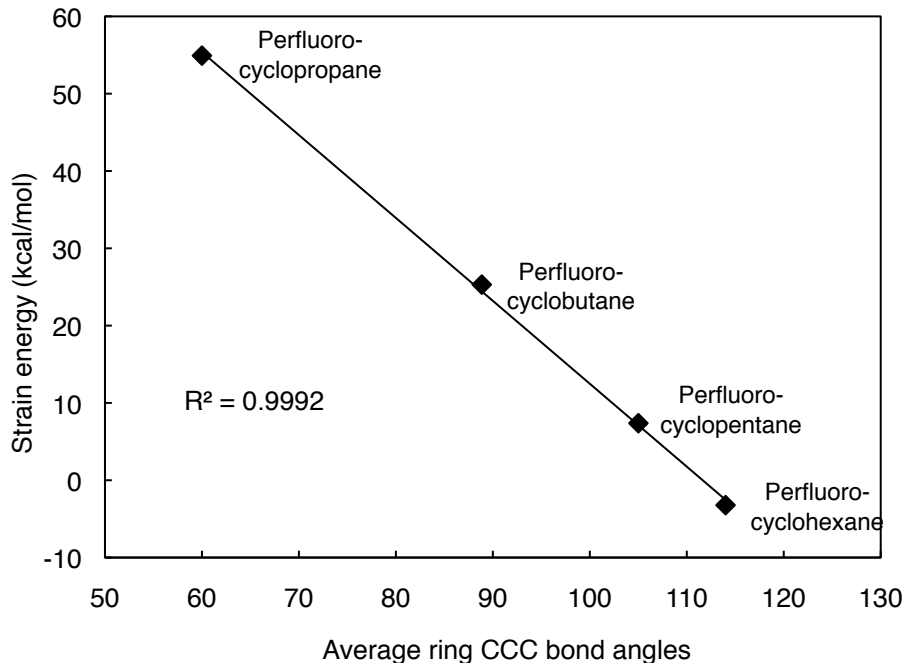


Figure 4-6. Computed strain energy vs. average ring CCC bond angles for perfluorocycloalkanes, All geometries and energies were computed at the MP2/6-31+G* level.

Cyclopropane's much lower CSE is the result of three highly stabilizing geminal $\sigma_{cc} \rightarrow \sigma_{cc}^*$ hyperconjugative interactions. This recasts Dewar's argument for special electron delocalization stabilization in cyclopropane without invoking any cyclic "σ-aromaticity." Geminal hyperconjugations are only "local" effects. Similarly, tetrahedrane and cubane do not exhibit "super" σ-aromaticity and σ-antiaromaticity. The former, like cyclopropane, is stabilized by significant geminal $\sigma_{cc} \rightarrow \sigma_{cc}^*$ hyperconjugation, while the latter, like cyclobutane, displays negligible geminal $\sigma_{cc} \rightarrow \sigma_{cc}^*$ hyperconjugation stabilization.

4.6 NUCLEUS INDEPENDENT CHEMICAL SHIFTS

Although cyclopropane appears to have many "aromatic-like" behavior: upfield proton chemical shifts (cyclopropane: 9.78 ppm, cyclohexane: 8.56 ppm),³⁰ exalted magnetic susceptibility (-6.0×10^{-6} , based on CH₂ increments),³¹ large magnetic susceptibility anisotropy,³² induced diatropic ring current,³³ and negative isotropic NICS(0) values (-42.9 ppm),³⁴ much of the supporting evidence for cyclopropane's "σ-aromaticity" are based on measurements not directly related to aromaticity. As pointed out many times in the literature, isotropic NICS(0) values perform poorly for characterizing π-aromaticity, especially for small rings, due to exceptional contributions from the in-plane tensor components (i.e., *xx* and *yy*) (see below).^{14, 35, 36} For such cases, the use of more sophisticated dissected NICS indices certainly is warranted!

Dissected canonical molecular orbital (CMO)-NICS(0)_{zz} analyses²⁴ (computed at the cyclopropane ring center) disprove the existence of σ-aromaticity in cyclopropane. NICS(0)_{MOzz} extracts the out-of-plane tensor component of the isotropic NICS and includes contributions only from CMO's relevant to σ- (MO's 8, 11, and 12, Walsh orbitals) or π- (MO's 7, 9, and 10) aromaticity (see Figure 4-7).

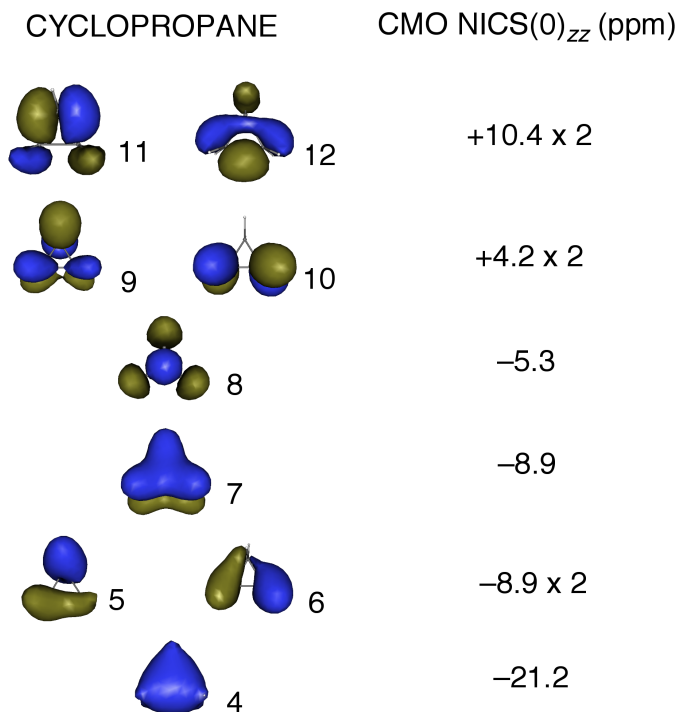


Figure 4-7. Dissected canonical molecular orbital (CMO)-NICS(0)_{zz} for cyclopropane, computed at the ring center (at PW91/IGLOIII); NICS(0) = -42.9 ppm, NICS(0)_{zz} = -30.2 ppm (including core orbital contributions), NICS(0)_{πzz} = -0.5 ppm (includes contributions from MO's 7, 9, 10), NICS(0)_{Walshzz} = +15.5 ppm (includes contributions from the Walsh-type MO's 8, 11, 12).

When only contributions from the orbitals with π symmetry (MO's 7, 9, 10) are considered, NICS(0)_{πzz} is only -0.5 ppm (see Figure 4-7). When only the three Walsh-type orbitals (MO's 8, 11, 12) are considered, the NICS(0)_{Walshzz} value (+15.5 ppm) is weakly *paratropic* (see Figure 3-7). Hence, there is no special σ - (or π -) aromaticity in cyclopropane! Although the total NICS(0)_{zz} value (-30.2 ppm) is highly diatropic, this is mainly due to large negative contributions coming from the lower lying CMO's (MO's 4, 5, and 6, see Figure 4-7) that are not related to aromaticity. The large isotropic NICS(0) value of cyclopropane (-42.9 ppm) certainly

does not reflect aromaticity, but is the result of overwhelming $\text{NICS}(0)_{xx}$ and $\text{NICS}(0)_{yy}$ contributions (-49.3 ppm each) [$\text{Isotropic NICS} = 1/3(\text{NICS}_{xx} + \text{NICS}_{yy} + \text{NICS}_{zz})$].

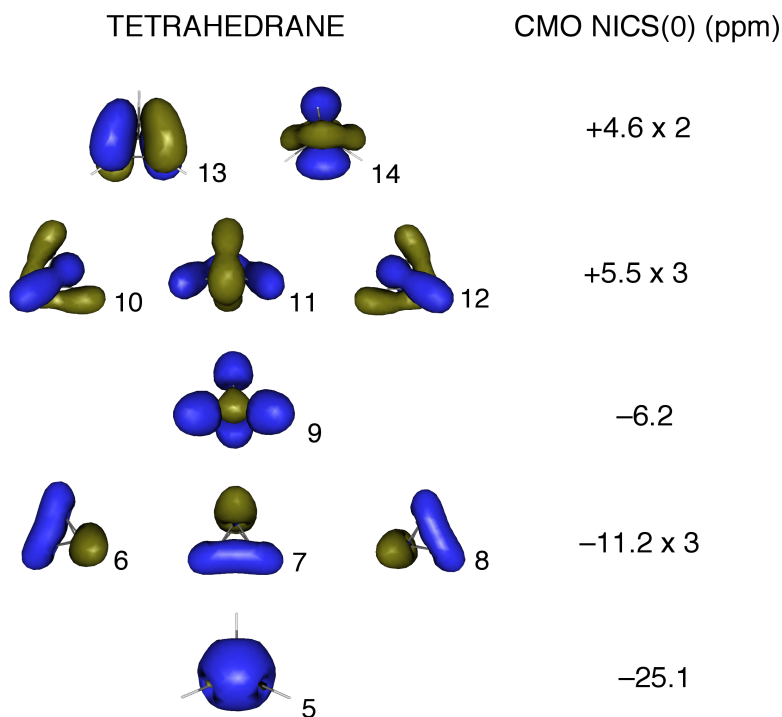


Figure 4-8. Dissected canonical molecular orbital (CMO)-NICS(0) of tetrahedrane, computed at the cage center (at PW91/IGLOIII); total NICS(0) = -47.5 ppm (including core orbital contributions), $\text{NICS}(0)_{\text{Walsh}} = +19.5$ ppm (includes contributions from the Walsh-type MO's 9, 10, 11, 12, 13, 14).

Likewise, dissected CMO-NICS reveals no special “super σ -aromaticity” for tetrahedrane. When only contributions from the Walsh-type orbitals (MO's 9, 10, 11, 12, 13, 14) are included, the $\text{NICS}(0)_{\text{Walsh}}$ value of tetrahedrane ($+19.5$ ppm) is not even diatropic. Tetrahedrane's large negative NICS(0) value (-47.5 ppm)³⁷ is predominantly due to large diatropic contributions

coming from the lower lying CMO's (MO's 5, 6, 7, 8, see Figure 4-8) that are not related to aromaticity.

4.7 CONCLUSIONS

Cyclopropane's 60° \angle CCC bond angles impose significant angle strain, but are advantageous for geminal CCC hyperconjugative interactions between each of its C–C bonds sharing a common carbon. Our detailed NBO analyses reveals that cyclopropane is highly stabilized by geminal $\sigma_{cc} \rightarrow \sigma_{cc}^*$ hyperconjugative interactions by 42.3 kcal/mol! None of the larger cycloalkanes rings (or the silicon rings in general) have such highly stabilizing $\sigma_{cc} \rightarrow \sigma_{cc}^*$ hyperconjugative interactions. Thus, cyclopropane does not have a “much too low” strain energy, but its expected high angle strain is overwhelmed by substantial electron delocalization stabilization. Note however, that the geminal CCC hyperconjugations of cyclopropane are a “local” rather than “cyclic” (i.e. σ -aromatic) effect. Dissected CMO-NICS also reveals no special diatropism in cyclopropane, when only contributions from the Walsh orbitals are considered. Likewise, tetrahedrane is *not* super σ -aromatic, as suggested erroneously by its large negative isotropic NICS value.³⁷

We stress again Schleyer's expressed skepticism in 1986, that, “There is no need to invoke σ -aromaticity to explain the thermochemistry of cyclopropane!”³ Although cyclopropane is not the σ -aromaticity paradigm it is an exemplary model for substantial σ -electron delocalization stabilization in non- π -conjugated molecules. This contributes to the increasing awareness that both σ - and π - electron delocalization can stabilize molecules effectively.

4.8 REFERENCES

1. Baeyer, A *Chem. Ber.* **1885**, 18, 2269-2281.
2. Schleyer, P. v. R.; Williams, J. E.; Blanchard, K. R., *J. Am. Chem. Soc.* **1980**, 92, 2377-2386.
3. Schleyer, P. v. R. in *Proceedings of the NATO Advanced Research Workshop on "Substituent Effects in Radical Chemistry"*; H. G. Viehe, Z. Janousek, R. Merenyi, Eds.; Louvain-la-Neuve, **1986**, pp 69-81.
4. Cohen, N.; Benson, S., *Chem. Rev.* **1993**, 93, 4219-2438.
5. Coulson, C. A.; Moffitt, W. E. *Philos. Mag.* **1949**, 40, 1-35.
6. Walsh, A. D. *Trans. Faraday Soc.* **1949**, 45, 179-190.
7. Dewar, M. J. S.; McKee, M. L. *Pure Appl. Chem.* **1980**, 52, 1431-1441.
8. Dewar, M. J. S.; Pettit, R. *J. Chem. Soc.* **1954**, 1625-1634
9. Cremer, D.; Kraka, E. *J. Am. Chem. Soc.* **1985**, 107, 3800-3810.
10. Robert, J. D.; Caserio, M. C. *Basic Principles of Organic Chemistry*; Benjamin Press: New York, 1964, pp 113.
11. Cremer, D.; Gauss, J. *J. Am. Chem. Soc.* **1986**, 108, 7467-7477.
12. Exner, K.; Schleyer, P. v. R. *J. Phys. Chem. A* **2001**, 105, 3407-3416.
13. Wu, W.; Ma, B.; Wu, J. I.; Schleyer, P. v. R.; Mo, Y. *Chem. Eur. J.* **2009**, 15, 9730-9736.
14. Pelloni, S.; Lazzeretti, P.; Zanasi, R. *J. Phys. Chem. A* **2007**, 111, 8163-8169.
15. NBO 5.0. Glendening, E. D.; Badenhoop, J. K.; Reed, A. E.; Carpenter, J. E.; Bohmann, J. A.; Morales, C. M.; Weinhold, F. Theoretical Chemistry Institute, University of Wisconsin, Madison (2001).
16. Dunitz, J. D.; Schomaker, V. *J. Chem. Phys.*, 20, **1952**, 1703-1707.

17. a) Vogelsanger, B.; Caminati, W. Bauder, A. *Chem. Phys. Lett.* **1987**, *141*, 245-250; b) Egawa, T.; Fukuyama, T.; Yamamoto, S.; Takabayashi, F.; Kambara, H.; Ueda, T.; Kuchitsu, K. *J. Chem. Phys.* **1987**, *86*, 6018-6026.
18. Demaison, J; Wlodarczak, G. *Struct. Chem.* **1994**, *5*, 57-66; b) Endo, Y.; Chiang, M. C.; Hirota, E. *J. Mol. Spectrosc.* **1987**, *126*, 63.
19. Adams, W. J.; Geise, H. J.; Bartell, L. S. *J. Am. Chem. Soc.* **1970**, *92*, 5013-5019; b) Han, S. J.; Kang, Y. K. *J. Mol Struct.* **1966**, *362*, 243-257.
20. Bialkowska-Jaworska, E.; Jaworski, M.; Kisiel, Z. *J. Mol. Struct.* **1995**, *350*, 247-254.
21. F. Weinhold, C. R. Landis in *Valency and Bonding: A Natural Bond Orbital Donor-Acceptor Perspective*, Cambridge University Press, **2005**, 271-272.
22. Song, L.; Mo, Y.; Zhang, Q.; Wu, W. *J. Comput. Chem.* **2005**, *26*, 514-521.
23. M. J. Frisch, G. W. Trucks, H. B. Schlegel, G. E. Scuseria, M. A. Robb, J. R. Cheeseman, J. A. Montgomery, Jr, T. Vreven, K. N. Kudin, J. C. Burant, J. M. Millam, S. S. Iyengar, J. Tomasi, V. Barone, B. Mennucci, M. Cossi, G. Scalmani, N. Rega, G. A. Petersson, H. Nakatsuji, M. Hada, M. Ehara, K. Toyota, R. Fukuda, J. Hasegawa, M. Ishida, T. Nakajima, Y. Honda, O. Kitao, H. Nakai, M. Klene, X. Li, J. E. Knox, H. P. Hratchian, J. B. Cross, V. Bakken, C. Adamo, J. Jaramillo, R. Gomperts, R. E. Stratmann, O. Yazyev, A. J. Austin, R. Cammi, C. Pomelli, J. W. Ochterski, P. Y. Ayala, K. Morokuma, G. A. Voth, P. Salvador, J. J. Dannenberg, V. G. Zakrzewski, S. Dapprich, A. D. Daniels, M. C. Strain, O. Farkas, D. K. Malick, A. D. Rabuck, K. Raghavachari, J. B. Foresman, J. V. Ortiz, Q. Cui, A. G. Baboul, S. Clifford, J. Cioslowski, B. B. Stefanov, G. Liu, A. Liashenko, P. Piskorz, I. Komaromi, R. L. Martin, D. J. Fox, T. Keith, M. A. Al-Laham, C. Y. Peng, A. Nanayakkara, M. Challacombe, P. M. W. Gill, B. Johnson, W. Chen, M.

- W. Wong, C. Gonzalez and J. A. Pople, GAUSSIAN 03 (Revision C.02), Gaussian, Inc., Wallingford CT, 2004.
24. a) Chen, ZF; Wannere, C. S.; Corminboeuf, C.; Puchta, R.; Schleyer, P. v. R. *Chem. Rev.* **2005**, *105*, 3842–3888; b) Fallah-Bagher-Shaidae, H.; Wannere, C. S.; Corminboeuf, C.; Puchta, R.; Schleyer, P. v. R. *Org. Lett.* **2006**, *8*, 863–866.
25. Wodrich, M. D.; Wannere, C. S.; Mo, Y.; Jarowski, P. D.; Houk, K. N.; Schleyer, P. v. R. *Chem. Eur. J.* **2007**, *13*, 7731-
26. Schleyer, P. v. R.; McKee, W. C. *J. Phys. Chem. A* **2010**, *114*, 3737-3740.
27. Experimental heats of formation taken from <http://cccbdb.nist.gov/>
28. Clark, T.; Spitznagel, G. W.; Klose, R.; Schleyer, P. v. R. *J. Am. Chem. Soc.* **1984**, *106*, 4412-4419.
29. Inagaki, S.; Ishitani, Y.; Kakefu, T. *J. Am. Chem. Soc.* **1994**, *116*, 5954-5958.
30. Wiberg, K. B.; Nist, B. J. *J. Am. Chem. Soc.* **1961**, *83*, 1226-1230.
31. Burke, J. J.; Lauterbur, P. C. *J. Am. Chem. Soc.* **1964**, *86*, 1870-1871.
32. Aldrich, P. D.; Kukolich, S. G.; Campbell, E. J.; Read, W. G. *J. Am. Chem. Soc.* **1983**, *103*, 15569-5576.
33. Fowler, P. W.; Baker, J.; Lillington, M. *Theor. Chem. Acc.* **2007**, *118*, 123-127.
34. Schleyer, P. v. R.; Maerker, C.; Dransfeld, A.; Jiao, H.; Hommes, N. J. R. v. E. *J. Am. Chem. Soc.* **1996**, *118*, 6317-6318.
35. Corminboeuf, C.; Heine, T.; Seifert, G.; Schleyer, P. v. R. *Phys. Chem. Chem. Phys.* **2004**, *6*, 273-276.
36. Cernusak, I. Fowler, P. W. Steiner, E. *Mol. Phys.* **1997**, *91*, 401-402.
37. Moran, D.; Manoharan, M.; Heine, T.; Schleyer, P. v. R. *Org. Lett.* **2003**, *5*, 23-26.

CHAPTER 5

THE EFFECT OF PERFLUORINATION ON THE AROMATICITY OF BENZENE AND
HETEROCYCLIC SIX MEMBERED RINGS[†]

[†] Reproduced with permission from Judy I. Wu, Frank G. Pühlhofer, Paul von Ragué Schleyer, Ralph Puchta, Boggavarapu Kiran, Michael Mauksch, Nico J. R. van Eikema Hommes, Ibon Alkorta, José Elguero, *J. Phys. Chem. A*. **2009**, *113* (24), pp 6789-6794.

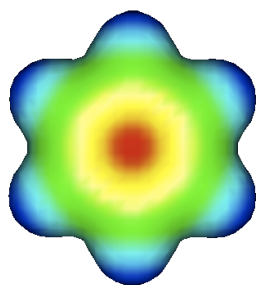
Copyright © 2009 American Chemical Society

5.1 ABSTRACT

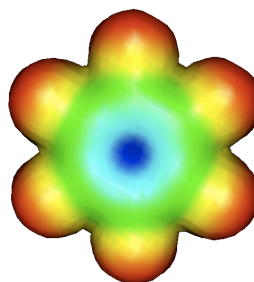
Despite having six highly electronegative F's, perfluorobenzene C_6F_6 is as aromatic as benzene. *Ab initio* block-localized wavefunction (BLW) computations reveal that both C_6F_6 and benzene have essentially the same extra cyclic resonance energies (ECRE's). Localized molecular orbital (LMO)-nucleus-independent chemical shifts (NICS) grids demonstrates that the F's induce only local paratropic contributions that are not related to aromaticity. Thus, all of the fluorinated benzenes ($C_6F_nH_{(6-n)}$, $n=1-6$) have similar ring-LMO-NICS $_{\pi zz}$ values. However, 1,3-difluorobenzene **2b** and 1,3,5-trifluorobenzene **3c** are slightly less aromatic than their isomers due to a greater degree of ring charge alternation. Isoelectronic C_5H_5Y heterocycles ($Y = BH^-$, N, NH^+) are as aromatic as benzene, based on their ring-LMO-NICS $_{\pi zz}$ and ECRE values, unless extremely electronegative heteroatoms (e.g. $Y = O^+$) are involved.

5.2 INTRODUCTION

Perfluorination alters the electrostatic potentials of benzene dramatically. As F's are highly electronegative, C_6H_6 and C_6F_6 display completely opposite molecular electrostatic potential (MEP) maps (below).



MEP map of C_6H_6



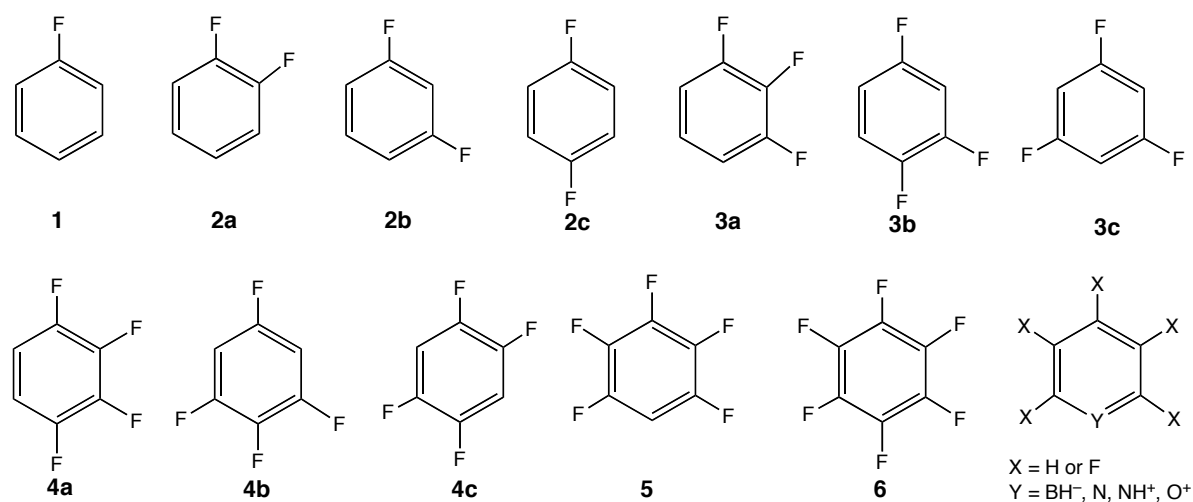
MEP map of C_6F_6

In particular, the MEP map of C_6F_6 reveals a rather electron deficient ring center (blue) and an electron rich exterior (red). Benzene shows the opposite MEP character. Since the aromaticity of benzene arises from its six delocalized π electrons, and the C_6F_6 ring center is more “electron deficient” compared to benzene, does this mean that C_6F_6 is less aromatic than benzene?

C_6H_6 and C_6F_6 behave quite differently when used as solvents for NMR measurements. Benzene ring currents¹ produce sizeable effects on the proton NMR chemical shifts of nearby solute 1H nuclei (aromatic solvent induced shifts),²⁻⁵ while C_6F_6 usually seems to be an "inert" solvent in this respect, either because it does not sustain an aromatic ring current⁶⁻⁸ or because the nature of its associations with solute molecules are very different from those of benzene.⁹⁻¹¹ Nikki has argued convincingly that C_6F_6 in certain instances produces ASIS (Aromatic Solvent Induced Shifts) in the opposite direction to that produced by benzene, as C_6H_6 (-8.7 ± 0.5 D Å, experimental)¹² and C_6F_6 ($+9.5 \pm 0.5$ D Å, experimental)¹² have opposite quadrupole moments and may interact with the dipoles of the solute molecules in opposite ways.^{9,10} C_6H_6 and C_6F_6 have quite different binding energies to cations and anions.¹³⁻¹⁹ The most recent reports support the greater importance of substituent-cation²⁰ or anion²¹ interactions over cation/anion- π interactions.

While various consequences of fluorinated alkanes,²²⁻²³ polycyclic aromatic hydrocarbons,²⁴⁻²⁷ cyclacenes²⁸ and phenylenes²⁹ have been reported, there are only a few comparative studies on the aromaticities of C_6H_6 versus C_6F_6 themselves.^{30,31} Fowler and Steiner computed the induced π ring current densities of C_6H_6 and C_6F_6 and found no significant differences between the two, except for the six independent local π circulations around the F's in

C_6F_6 .³⁰ In contrast, Laali evaluated a set of $C_6H_nF_{(6-n)}$ ($n=1-6$) compounds based on nucleus independent chemical shifts (NICS)³² computations (NICS(1)_{zz}), and found *diminished ring currents* for the more fluorinated species.³¹ To reconcile this discrepancy, we re-evaluated the aromaticities of the fluorinated benzenes (**1-6**: $C_6H_nF_{(6-n)}$, $n=1-6$), employing the more sophisticated NICS _{π zz}^{32c,32d} index and the block localized wavefunction (BLW)³³ method to characterize their aromatic stabilization energies. In addition, we evaluated the aromaticities of a set of heterocyclic six membered rings C_5X_5Y ($X = H, F$; $Y = BH^-, N, NH^+, O^+$) isoelectronic to benzene and pentafluorobenzene.



We answer the following questions in this paper: What effect does perfluorination have on the aromaticity of benzene? Can the ASIS effect be due to absence of ring current in C_6F_6 ? To what extent do hetero- ring atoms and fluorination perturb the aromaticities of heterocyclic six membered rings isoelectronic to benzene?

5.3 COMPUTATIONAL DETAILS

All geometries were optimized at the B3LYP/6-311+G** level as implemented in Gaussian98.³⁴ Harmonic vibrational frequencies, computed at the same DFT level, established the character of the stationary points. For all NICS computations, we employ the most highly recommended NICS _{π_{zz}} index which extracts the out-of-plane (zz) tensor component of the isotropic NICS and includes only the π MO contributions.^{32d} Negative NICS(0) _{π_{zz}} values due to diamagnetic shieldings indicate aromaticity. Positive NICS(0) _{π_{zz}} values due to paramagnetic shieldings indicate antiaromaticity.

The NICS _{π_{zz}} data for the fluorinated benzenes were computed employing both (localized molecular orbital) LMO³⁵ and (canonical molecular orbital) CMO³⁶ dissection. LMO NICS (at the PW91/IGLOIII level) were computed with the individual gauge for localized orbitals (IGLO) method³⁷ (implemented in the deMon NMR program)³⁸ utilizing the Pipek-Mezey localization algorithm.³⁹ CMO NICS employed the (gauge-including atomic orbital) GIAO method. LMO and CMO NICS are complementary, but the former (LMO) separates the total shielding of the molecule into individually localized MO contributions of bonds, lone pairs and core electrons, while the latter (CMO) dissects the total shielding of the molecule into each canonical MO contributions.

All BLW³³ computations were performed at the B3LYP/6-31G* level as implemented in the GAMESS R5 version.⁴⁰ The BLW method is specifically designed for evaluating resonance energies (RE), for cyclic or acyclic conjugated molecules, directly without recourse to reference compounds, but can also be used to derive the extra cyclic resonance energies (ECRE's),⁴¹ of aromatic molecules. Note that the *ab initio* VB based BLW computations preserve the concepts of valence bond theory, but is more efficient due to its molecular orbital (MO)-based

computations.³³ BLW computed RE's adopt the Pauling-Wheland⁴² definition and is the computed total energy difference between the completely delocalized conjugated molecule (fully optimized employing regular canonical molecular orbitals) and that of its most stable resonance contributor. The latter can be optimized employing BLW orbitals, constructed by partitioning all the electrons and basis functions into several subspaces to form sets of localized MO's, in which orbitals of the same subspaces are mutually orthogonal but those of different subspaces overlap freely. Depending on the partitioning scheme of the subgroups, the BLW procedure "disables" the intramolecular interactions among the selected subgroups and gives the total energy of the hypothetical resonance structure.³³ The ECRE's are derived from the BLW-RE's of the aromatic compounds minus that of its acyclic conjugated references with the same number and type of conjugation (see ECRE section).⁴¹

RESULTS AND DISCUSSION

The effect of fluorination on the aromaticity of C₆H₆ and a set of isoelectronic six membered rings C₆H₅Y (Y = CH, N, NH⁺, O⁺), containing first row heteroatoms, were evaluated both magnetically and energetically. Nucleus chemical independent shift (NICS) computations characterized the magnetic aromaticity for the sequentially fluorinated benzene analogs as well as the parent and perfluorinated heterocyclic six membered rings. Their extra cyclic resonance energies (ECRE's), related to the aromatic stabilization energies (ASE's), were computed based on Mo's *ab initio* block-localized wavefunction (BLW) procedure (see Methods).

5.4 NUCLEUS INDEPENDENT CHEMICAL SHIFTS

We evaluated the nucleus independent chemical shifts of C₆H₆ and C₆F₆, based on the most

sophisticated NICS _{π_{zz}} index,³² employing both LMO and CMO NICS (see Methods section). The LMO-NICS is especially useful for comparing the aromaticity of C₆F₆ vs. C₆H₆ as it can distinguish the NICS _{π_{zz}} contributions of the ring from those of the F lone pairs (see Methods).³⁵ The “ring”-LMO NICS(0) _{π_{zz}} values include only the contributions of the three double bonds within the six membered ring; “F”-LMO NICS(0) _{π_{zz}} values include only the contributions of the F’s. The total-LMO NICS(0) _{π_{zz}} includes both the ring and F contribution and may be compared with the canonical molecular orbital (CMO)-NICS(0) _{π_{zz}} data, which dissects the total shielding of the molecule into each canonical MO contributions, but cannot identify contributions coming from the ring and F’s for C₆F₆ separately.

Remarkably, the ring-LMO NICS(0) _{π_{zz}} values of C₆H₆ (−36.9 ppm) and C₆F₆ (−37.7ppm) are very similar (Table 5-1). Despite having six highly electronegative F’s, C₆F₆ is as aromatic as C₆H₆! The six peripheral Fs induce sizable paramagnetic shielding at the C₆F₆ ring center (F-LMO NICS(0) _{π_{zz}} = +8.4 ppm), but are these only local effects and do not perturb the aromaticity of the benzene ring (see discussion below). For this reason, the total-LMO NICS(0) _{π_{zz}} (the sum of both ring and F contributions) of C₆F₆ (−29.3 ppm) is quite different from C₆H₆ (−36.9 ppm), which when interpreted superficially, may suggest erroneously that C₆F₆ is less aromatic than benzene. The CMO NICS(0) _{π_{zz}} results for C₆F₆ (−28.9 ppm) and C₆H₆ (−36.2 ppm) are also misleading for the same reason. The in-plane NICS _{π_{zz}} grids for C₆F₆ and C₆H₆ (see Figure 5-1), with NICS points placed at positions radiating out from the ring center at 1 Å intervals through the ring C-C bonds, characterizes the local effects of the Fs (see Figure 5-1c). Aromatic molecules not only should be characterized by a negative NICS _{π_{zz}} value at the ring center; they should exhibit paramagnetic deshielding outside the ring as well. The NICS _{π_{zz}} values for each of the NICS grid points of C₆F₆ and C₆H₆ have similar magnitudes both inside (diatropic, red dots)

and outside (paratropic, green dots) the ring. However, the F-LMO NICS $_{\pi zz}$ grids for C₆F₆ reveal large paratropic contributions in the ring (+8.4 ppm) and close to the C-C bonds (+6.0 ppm) but negligible diatropic contributions outside the ring (less than –0.5 ppm).

Table 5-1. CMO and LMO NICS(0) $_{\pi zz}$ data for the C₆F_nH_(6-n) compounds (both computed at the PW91/IGLOIII level). In the LMO-NICS $_{\pi zz}$ column, “F’s” refers to contributions from the p_z lone pairs of the F substituents only; “Ring” refers to contributions from the three π MOs of the C₆ ring. “Total” refers to the total contributions from all π MOs (includes both “F” and “ring”), and may be compared to the CMO-NICS $_{\pi zz}$ results.

Compound	CMO-NICS(0) $_{\pi zz}$	LMO-NICS(0) $_{\pi zz}$		
		Total	Ring	F’s
Benzene	–35.9	–36.9	–36.9	-
1	–34.0	–34.8	–36.6	1.8
2a	–33.1	–33.9	–37.1	3.2
2b	–31.7	–32.2	–35.8	3.6
2c	–33.1	–33.4	–36.9	3.5
3a	–31.7	–32.3	–36.9	4.6
3b	–31.2	–31.9	–36.7	4.8
3c	–29.3	–29.5	–34.6	5.1
4a	–30.7	–31.5	–37.4	5.9
4b	–29.5	–30.0	–36.1	6.1
4c	–30.3	–31.0	–37.2	6.2
5	–29.3	–30.1	–37.1	7.0
6	–28.6	–29.3	–37.7	8.4

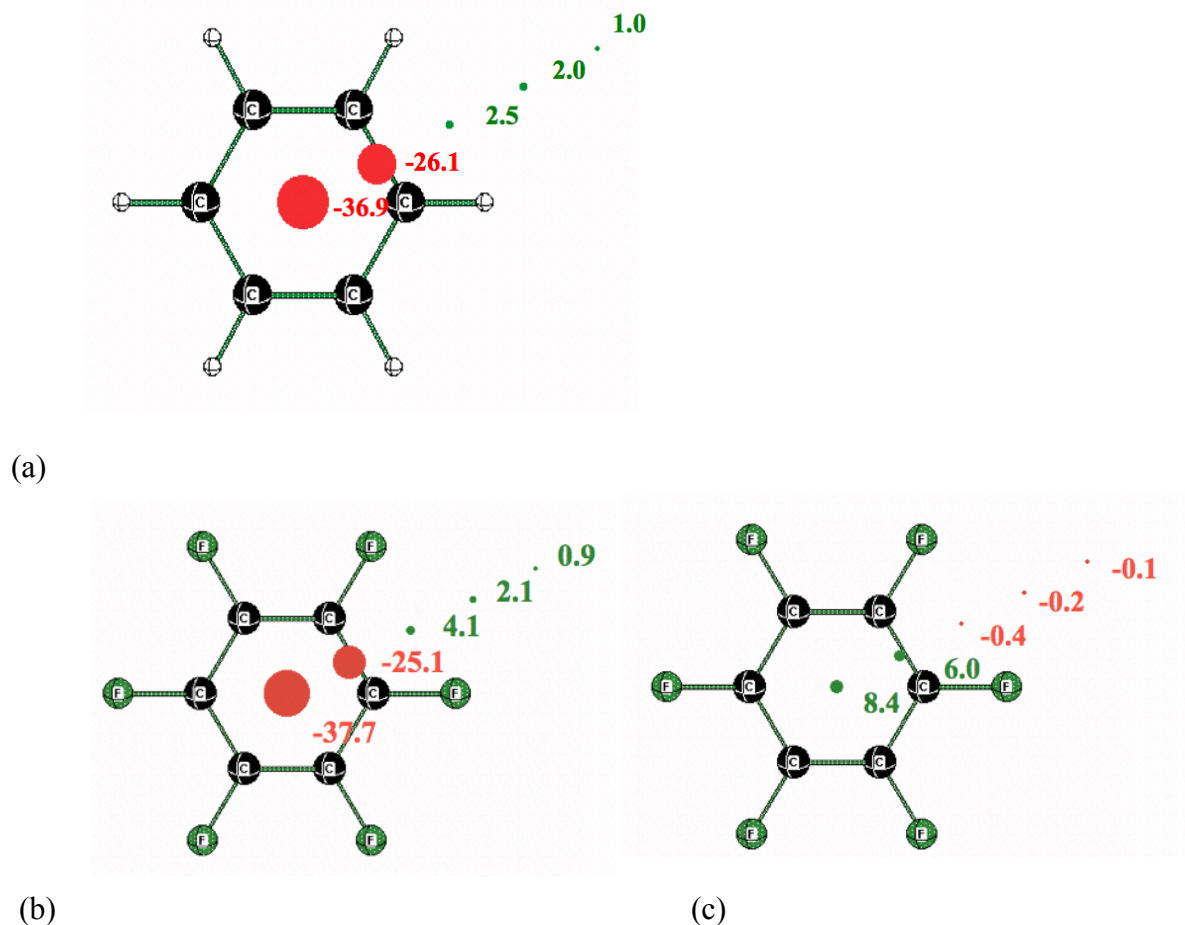


Figure 5-1. In plane LMO-NICS $_{\pi_{zz}}$ grid of C₆H₆ and C₆F₆ (NICS data computed at the PW91/IGLOIII level). (a) LMO-NICS $_{\pi_{zz}}$ grid of benzene. (b) “Ring” LMO-NICS $_{\pi_{zz}}$ grid of C₆F₆. (c) “F” IGLO-LMO-NICS $_{\pi_{zz}}$ grid of C₆F₆. The insignificant shielding outside the ring suggests that there are no induced paratropic ring currents coming from the Fs, but the Fs induce only local paramagnetic deshieldings.

LMO-NICS $_{\pi_{zz}}$ computations confirm, in agreement with Fowler’s ring current density plots of C₆H₆ and C₆F₆,³⁰ that perfluorination does not change the π ring current of benzene. The aromaticity of C₆H₆ and C₆F₆ are essentially the same, while the F’s induce only local paramagnetic deshieldings not related to aromaticity.

Since perfluorination has no significant effect on the aromaticity of benzene, the ring-LMO NICS(0)_{πzz} values of the sequentially fluorinated benzene derivatives (C₆F_nH_(6-n), n=1-6) also give similar values (ranging from –34.6 to –37.7 ppm, see Table 5-1) compared to benzene (–36.9 ppm). However, the F-LMO NICS(0)_{πzz} values are more positive for species with more Fs (see Table 5-1), as they induce greater local paramagnetic deshielding. For this reason, both the CMO NICS(0)_{πzz} and total-LMO NICS(0)_{πzz} values become less negative for the more fluorinated benzene derivatives (see Table 5-1).

Note that both **2b** and **3c** have the lowest total energies among the di- and tri-fluorobenzenes, but also have the *least negative* diatropic ring-LMO NICS(0)_{πzz} values (see Table 5-1), and thus are less aromatic than their isomers. Interestingly, the ordering for aromaticity (e.g. **2a** > **2c** > **2b**, **3a** > **3b** > **3c**) and thermochemical stability (e.g. **2b** > **2c** > **2a**, **3c** > **3b** > **3a**), both for the di- and tri- fluorobenzenes, are completely opposite! The weakened aromaticity of **2b** and **3c** is due to their greater charge alternation in the C₆ ring, which arises from the highly electronegative F's pulling electrons away from the substituted C atoms. Thus, all of the fluorinated carbons have partial positive charges, while the unsubstituted carbons have partial negative charges. As an extreme example, borazine has significant ring charge alternation due to the electronegativity difference between the ring atoms, and is not very aromatic (NICS(0)_{πzz} = –9.2 ppm, compared to –36.9 for benzene). Hence, charge alternation can be thermodynamically favorable for cyclic conjugated systems, but is unfavorable in terms of aromaticity. Although fluorination does not perturb the aromaticity of C₆H₆, partially fluorinated benzene derivatives can have weakened aromaticity due to alternating charges in the C₆ ring.

The ring-LMO NICS(0)_{πzz} values of the heterocyclic C₅H₅Y (ranging from –31.4 to –36.4 ppm) and C₅F₅Y (–28.9 to –35.9 ppm) compounds (X = H, F; Y = BH[–], N, NH⁺, O⁺) do not

differ much from benzene (−36.9 ppm) and pentafluorobenzene **5** (−37.1 ppm) (see Table 5-2); those of $C_5H_5O^+$ (−31.4 ppm) and $C_5F_5O^+$ (−28.9 ppm) are slightly less negative due to the greater electronegativity difference between the ring carbons and O (which is even more electronegative with the positive charge). At the extreme, both $C_5H_5F^{2+}$ (−15.7 ppm) and $C_5F_6^{2+}$ (−12.9 ppm) have significantly less negative ring-LMO-NICS(0) $_{\pi zz}$ values. Note that the ring-LMO NICS(0) $_{\pi zz}$ values of each of the C_5H_5Y species are almost the same as their fluorinated C_5F_5Y counterparts (see Table 5-2). Thus, perfluorination has no significant effect on the aromaticities of the heterocyclic six membered rings containing only one first row element. Aromaticity is not easily perturbed, and for benzene, is weakened only when unrealistic highly electronegative/electropositive heteroatoms (like F^{2+}), which we have omitted from this study, are incorporated into the ring.

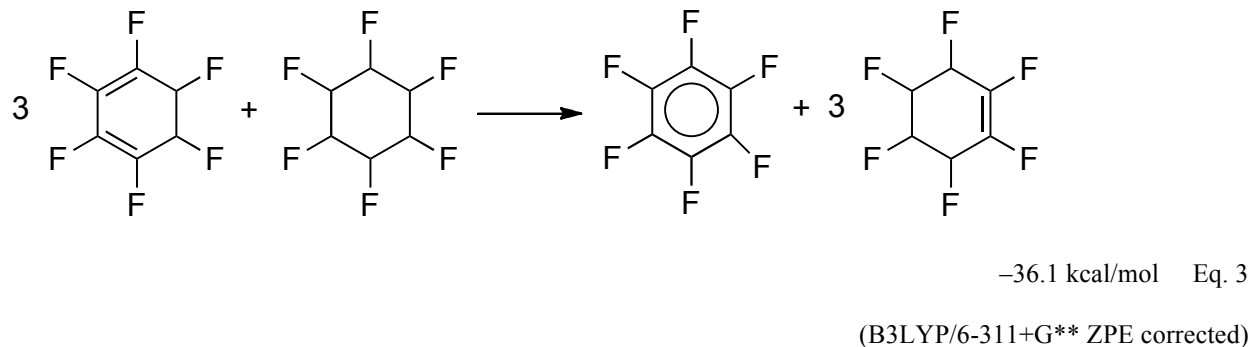
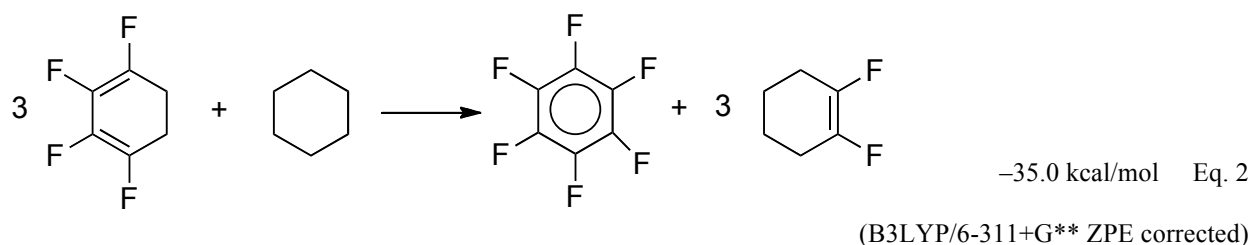
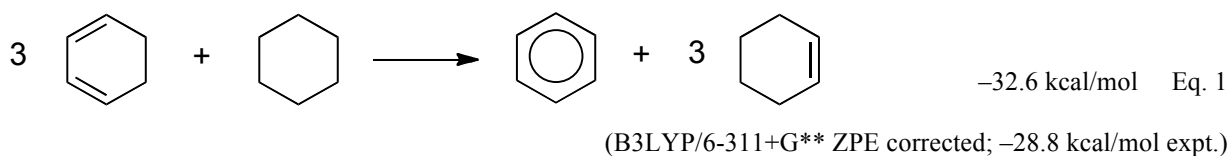
Table 5-2. Ring LMO-NICS(0) $_{\pi zz}$ values for C_5X_5Y compounds (X= H or F; Y = BH[−], CH, N, NH⁺, O⁺) (NICS data computed at the PW91/IGLOIII level).

Y	Ring LMO-NICS(0) $_{\pi zz}$	
	X = H	X = F
BH [−]	−32.1	−35.0
CH	−36.9	−37.1
N	−36.4	−35.9
NH ⁺	−34.8	−33.0

5.5 EXTRA CYCLIC RESONANCE ENERGY

The aromatic stabilization energies of C_6H_6 and C_6F_6 were estimated based on their extra cyclic resonance energies (ECRE's),⁴¹ which measures the extra stabilization associated with the aromaticity of the cyclic conjugated systems. ECRE's can be derived from the BLW computed

RE's of the cyclic conjugated aromatic compound minus that of its appropriate acyclic references, which represent the same number and type of conjugation present in the aromatic system, and thus cancel out all energetic effects other than aromaticity.⁴¹ For example, the ECRE of benzene (29.3 kcal/mol) is derived from the RE of benzene (61.4 kcal/mol) minus that of three syn butadienes (−10.7 kcal/mol each). Similarly, the ECRE of C₆F₆ (28.5 kcal/mol) can be derived from the RE of C₆F₆ (61.8 kcal/mol) minus the BLW-RE sum of three syn-1,2,3,4-tetrafluorobutadienes (worth 11.1 kcal/mol each). Remarkably, the ECRE values for C₆H₆ and C₆F₆ are almost the same! Hence, C₆F₆ is, energetically, as aromatic as C₆H₆.



The aromatic stabilization energy (ASE) of C_6F_6 can also be evaluated based on the recommended hyperhomodesmotic equation⁴³ (Equation 1) adopted for benzene.⁴⁴ Thus, equation 1 has equal numbers of C-C bond types and equal numbers of each type of carbon atom (sp^3 , sp^2 , sp) with zero, one, two or three hydrogens attached on both side, and is balanced also for the number of conjugations and hyperconjugations.⁴³ For C_6F_6 , equations 2 and 3 are derived from equation 1 and also retain balanced C-C, C-F bond types and carbon hybridizations. Based on equations 1-3, the estimated ASE for C_6F_6 (−35.0 kcal/mol, eq. 2; −36.1 kcal/mol, eq. 3) also is close to that of benzene (−32.6 kcal/mol, eq. 1).

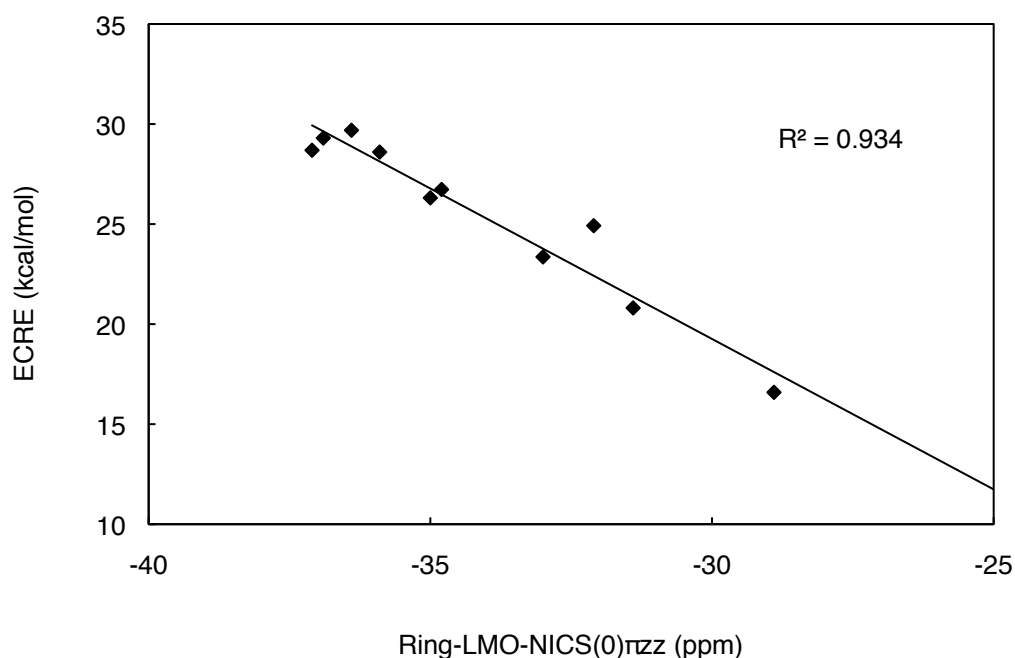


Figure 5-2. ECRE vs. ring-LMO NICS(0) π_{zz} values for heterocyclic six membered rings C_5X_5Y ($X = H, F$; $Y = BH^-, CH, N, NH^+, O^+$). All ECRE data were computed with the BLW method at the B3LYP/6-31G* level, all NICS(0) π_{zz} values were computed with the LMO-NICS method at the PW91/IGLOIII level.

The ECRE's⁴¹ of the heterocyclic C₅H₅Y (20.8 to 29.7 kcal/mol) and C₅F₅Y (16.6 to 28.6 kcal/mol) (Y = BH⁻, N, NH⁺, O⁺) species also do not too deviate much from benzene (29.3 kcal/mol) and **5** (28.7 kcal/mol). The ECRE's of C₅H₅O⁺ (20.8 kcal/mol) and C₅F₅O⁺ (16.6 kcal/mol) are particularly smaller due to the electronegativity difference between the ring atoms, as discussed earlier. The ECRE's of C₅H₅Y also do not differ much from their fluorinated C₅F₅Y derivatives, thus perfluorination does not change the aromatic stabilization energies of the heterocyclic six membered rings. Notably, the NICS_{πzz} and ECRE results correlate remarkably well, for the C₅X₅Y species (R² = 0.934, see Figure 5-2). Hence, for benzene, the substitution of a single ring carbon by other first row ring heteroatoms has only little effect on aromatic stabilization energy, except in extreme cases when highly electronegative heteroatoms are incorporated.

5.6 CONCLUSIONS

Perfluorination has no significant effect on the aromaticity of benzene, either energetically or magnetically. The computed ring-LMO NICS_{πzz} and ECRE values for C₆H₆ and C₆F₆ are essentially the same. For this reasons, the aromatic solvent induced shifts (ASIS)²⁻⁵ effect for C₆H₆ and C₆F₆ cannot be due to the absence of ring currents in C₆F₆, but other reasons, for example, the different solute-substituent interactions for C₆F₆, could be responsible.

Although CMO and LMO NICS are complementary and are generally in very good agreement with each other, LMO-NICS are superior for evaluating substituent effects for aromatic systems, as it distinguishes the ring and substituent contributions separately. The F-LMO-NICS grid of C₆F₆ reveals that Fs induce only local paratropic contributions in the ring center, but are not related to aromaticity. Thus, Laali's conclusion suggesting diminished ring

currents for the sequentially fluorinated benzenes³¹ is incorrect. All of the fluorinated benzenes **1-6** have very similar ring-LMO NICS(0)_{πzz} values (−34.6 to −37.7 ppm). **2b** and **3c** are slightly less aromatic (less negative ring-LMO NICS(0)_{πzz} values) than the other di- and tri-fluorobenzenes as they have a greater degree of alternating ring charges. For comparison borazine is only very weakly aromatic (NICS(0)_{πzz} = −9.2 ppm). The aromaticities of heterocyclic six membered rings (containing only one first row heteroatom), isoelectronic to benzene, are weakened only when strongly electronegative heteroatoms (e.g. O+) are involved. Remarkably, the aromaticity of benzene is quite persistent and is not easily perturbed by substituents⁴⁵ or heteroatoms⁴⁶ in the ring.

5.7 REFERENCES

1. a) Jackman, L. M. *Applications of Nuclear Magnetic Resonance Spectroscopy in Organic Chemistry*, Pergamon Press, London, **1959**, 125; b) Jackman, L. M.; Sternhell, S. *Applications of Nuclear Magnetic Resonance Spectroscopy in Organic Chemistry*, 2nd Edition, Pergamon Press, Oxford, **1969**, 95.
2. a) P. Laszlo, *Progr. NMR Spectroscopy*, **1967**, 3, 231-402; b) Ronayne, J.; Williams, D. *H. Annu. Rep. NMR Spectrosc.* **1969**, 2, 83-124.
3. R. D. Bertrand, R. D. Compton, J. G. Verkade, *J. Am. Chem. Soc.* **1970**, 92, 2702–2709.
4. E. M. Engler, P. Laszlo *J. Am. Chem. Soc.* **1971**, 93, 1317-1327.
5. H. Stamm, H. Jäckel *J. Am. Chem. Soc.* **1989**, 111, 6544-6550.
6. L. Pauling *J. Chem. Phys.* **1936**, 4, 673-677.
7. J. A. Pople *J. Chem. Phys.* **1956**, 24, 1111.
8. A. H. Cowley, M. C. Damasco, J. A. Mosbo, J. G. Verkade, J. G. *J. Am. Chem. Soc.* **1972**, 94, 6715-6717.
9. K. Nikki, N. Nakahata, N. Nakagawa *Tetrahedron Lett.* **1975**, 3811-3812.
10. K. Nikki, N. Nakagawa *Bull. Chem. Soc. Japan* **1978**, 51, 3267-3272.
11. M. A. Suhm, H. Weingärtner *Chem. Phys. Lett.* **1989**, 159, 193-198.
12. M. R. Battaglia, A. D. Buckingham, J. H. Williams, *Chem. Phys. Lett.* **1981**, 78, 421-423.
13. I. Alkorta, I. Rozas, J. Elguero *J. Org. Chem.* **1997**, 62, 4687-4691.
14. I. Alkorta, I. Rozas, J. Elguero *J. Am. Chem. Soc.* **2002**, 124, 8593-8598.
15. D. Quiñonero, C. Garau, A. Frontera, P. Ballester, A. Costa, P. M. Deyà *Chem. Phys. Lett.* **2002**, 359, 486-492.
16. D. Quiñonero, C. Garau, C. Rotger, A. Frontera, P. Ballester, A. Costa, P. M. Deyà

- Angew. Chem. Int. Ed.* **2002**, *41*, 3389-3392.
17. I. Alkorta, J. Elguero *J. Phys. Chem. A* **2003**, *107*, 9428-9433.
 18. C. Garau, D. Quiñonero, A. Frontera, P. Ballester, A. Costa, P. M. Deyà *New. J. Chem.* **2003**, *27*, 211-214.
 19. C. Garau, A. Frontera, D. Quiñonero, P. Ballester, A. Costa, P. M. Deyà *Chem. Phys. Lett.* **2004**, *392*, 85-89.
 20. S. E. Wheeler, K. N. Houk *J. Am. Chem. Soc.* **2009**, *131*, 3126-3127.
 21. A. Clements, M. Lewis *J. Phys. Chem. A* **2006**, *110*, 12705-12710.
 22. O. Mó, M. Yáñez, M. Eckert-Maksic, Z. B. Maksic *J. Org. Chem.* **1995**, *60*, 1638-1646.
 23. a) P. P. Bera, L. Horny, H. F. Schaefer *J. Am. Chem. Soc.* **2004**, *126*, 6692-6702; b) P. Ankan, C. S. Wannere, V. Kasalova, P. v. R. Schleyer, H. F. Schaefer *J. Am. Chem. Soc.* **2005**, *127*, 15457-15469.
 24. S. Martin-Santamaria, H. S. Rzepa *J. Chem. Soc. Perkin Trans. 2* **2000**, *12*, 2372-2377
 25. C. J. Kastrup, S. P. Oldfield, H. S. Rzepa *Chem. Commun.* **2002**, *6*, 642-643.
 26. Y. Xie, H. F. Schaefer, F. A. Cotton *Chem. Commun.* **2003**, *1*, 102-103.
 27. X. Feng, QS Li, J. Gu, A. Cotton, Y. Xie, H. F. Schaefer *J. Phys. Chem. A* **2009**, *113*, 887-894.
 28. L. Türker *J. Mol. Struct. (Theochem)* **2002**, *587*, 57-61.
 29. Y. Sakamoto, T. Suzuki, A. Miura, H. Fujikawa, S. Tokito, Y. Taga *J. Am. Chem. Soc.* **2000**, *122*, 1832-1833.
 30. P. W. Fowler, E. Steiner *J. Phys. Chem.* **1997**, *101*, 1409-1413.
 31. T. Okazaki, K. K. Laali *Org. Biomol. Chem.*, **2006**, *4*, 3085-3095.
 32. a) P. v. R. Schleyer, C. Maerker, A. Dransfeld, H. J. Jiao, N. J. r. V. E Hommes, *J. Am.*

- Chem. Soc.* **1996**, 118, 6317-6318; b) P. v. R. Schleyer, H. J. Jiao, N. J. r. V. E Hommes, V. G. Malkin, O. L. Malkina, O. L. *J. Am. Chem. Soc.* **1997**, 119, 12669-12670; c) C. Corminboeuf, T. Heine, G. Seifert, P. v. R. Schleyer, *Phys. Chem. Chem. Phys.* **2004**, 6, 273-276; d) H. Fallah-Bagher-Shaidaei, C. S. Wannere, C. Corminboeuf, R. Puchta, P. v. R. Schleyer, *Org. Lett.* **2006**, 8, 863-866; e) Z. Chen, C. S. Wannere, C. Corminboeuf, R. Puchta, P. v. R. Schleyer, *Chem. Rev.* **2005**, 105, 3842-3888.
33. a) Y. Mo, S. D. Peyerimhoff, *J. Chem. Phys.* **1998**, 109, 1687-1697; b) Y. Mo, Y. Zhang, J. Gao, *J. Am. Chem. Soc.* **1999**, 121, 5737-5742; c) Y. Mo, G. Subramanian, D. M. Ferguson, J. Gao, *ibid* **2002**, 124, 4832-4837; d) Y. Mo, W. Wu, L. Song, M. Lin, Q. Zhang, J. Gao, *Angew. Chem.* **2004**, 116, 2020-2024; *Angew. Chem. Int. Ed.* **2004**, 43, 1986-1990; e) Y. Mo, *J. Chem. Phys.* **2003**, 119, 1300-1306; f) Y. Mo, L. Song, W. Wu, Q. Zhang, *J. Am. Chem. Soc.* **2004**, 126, 3974-3982; g) Y. Mo, *J. Org. Chem.* **2004**, 69, 5563-5567; h) Mo, Y.; Song, L.; Lin, Y. *J. Phys. Chem. A* **2007**, 111, 8291-8301.
34. Frisch, M. J.; Trucks, G. W.; Schlegel, H. B.; Scuseria, G. E.; Robb, M. A.; Cheeseman, J. R.; Zakrzewski, V. G.; Montgomery, Jr., J. A.; Stratmann, R. E.; Burant, J. C.; Dapprich, S.; Millam, J. M.; Daniels, A. D.; Kudin, K. N.; Strain, M. C.; Farkas, O.; Tomasi, J.; Barone, V. M.; Cossi, R.; Cammi, B.; Mennucci, C.; Pomelli, C.; Adamo, S.; Clifford, J.; Ochterski, Petersson, G. A.; Ayala, P. Y.; Cui, Q.; Morokuma, K.; Malick, D. K.; Rabuck, A. D.; Raghavachari, K.; Foresman, J. B.; Cioslowski, J.; Ortiz, J. V.; Baboul, A. G.; Stefanov, B. B.; Liu, G.; Liashenko, A.; Piskorz, P.; Komaromi, I.; Gomperts, R.; Martin, R. L.; Fox, D. J.; Keith, T.; Al-Laham, M. A.; Peng, C. Y.; Nanayakkara, A.; Challacombe, M.; Gill, P. M. W.; Johnson, B.; Chen, W.; Wong, M. W.; Andres, J. L.;

- Gonzalez, C.; Head-Gordon, M.; Replogle, E. S.; Pople, J. A. Gaussian, Inc., Pittsburgh PA, 1998.
35. P. v. R. Schleyer, M. Manoharan, Z. X. Wang, B. Kiran, H. Jiao, R. Puchta, N. J. R. v. E. Hommes *Org. Lett.* **2001**, 3, 2465-2468.
 36. a) C. Corminboeuf, T. Heine, J. Weber, *J. Org. Lett.* **2003**, 5, 1127-1130; b) D. Moran, M. Manoharan, T. Heine, P. v. R. Schleyer *Org. Lett.* **2003**, 5, 23-26; c) T. Heine, P. v. R. Schleyer, C. Corminboeuf, G. Seifert, R. Reviakine, J. Weber *J. Phys. Chem. A*, **2003**, 107, 6470-6475.
 37. Kutzelnigg, W. *Isr. J. Chem.* **1980**, 19, 193.
 38. a) V. G. Malkin, O. L. Malkina, M. E. Casida, D. R. Salahub, *J. Am. Chem. Soc.* **1994**, 116, 5898-5908; b) J. Pipek, P. J. Mezey, *J. Chem. Phys.* **1989**, 90, 4916-4927.
 39. J. Pipek, P. J. Mezey, *J. Chem. Phys.* **1989**, 90, 4916-4927.
 40. Gamess (Version R5): M. W. Schmidt, K. K. Baldridge, J. A. Boatz, S. T. Elbert, M. S. Gordon, J. H. Jensen, S. Koseki, N. Matsunaga, K. A. Nguyen, S. J. Su, T. L. Windus, M. Dupuis, J. A. Montgomery, *J. Comput. Chem.* **1993**, 14, 1347-1363.
 41. Y. Mo, P. v. R. Schleyer, *Chem. Eur. J.* **2006**, 12, 2009-2020.
 42. L. C. Pauling, G. W. Wheland, *J. Chem. Phys.* **1933**, 1, 362-374; b) L. C. Pauling, *The Nature of the Chemical Bond*, 3rd ed., Cornell University Press, Ithaca, NY, **1960**; c) G. W. Wheland, *J. Am. Chem. Soc.* **1941**, 85, 431-434; d) G. W. Wheland, *The Theory of Resonance*, Wiley, New York, **1944**; e) G. W. Wheland, *Resonance in Organic Chemistry*, Wiley, New York, **1955**.
 43. S. E. Wheeler, K. N. Houk, P. v. R. Schleyer, W. D. Allen *J. Am. Chem. Soc.* **2009**, 131, 2547-2560.

44. M. D. Wodrich, C. S. Wannere, Y. Mo, P. D. Jarowski, K. N. Houk, P. v. R. Schleyer, *Chem. Eur. J.* **2007**, *13*, 7731-7744.
45. a) A. R. Campanelli, A. Domenicano, F. Ramonda *J. Phys. Chem. A* **2003**, *107*, 6429-6440; b) T. M. Krygowski, K. Ejsmont, B. T. Stepien, M. K. Cyranski, J. Poater, M. Solà *J. Org. Chem.* **2004**, *69*, 6634–6640; c) T. M. Krygowski, B. T. Stepien *Chem. Rev.* **2005**, *105*, 3482-3512; d) T. M. Krygowski, H. Szatylowicz *Trends in Organic Chemistry* **2006**, *11*, 37-53.
46. a) A. Mehlhorn, J. Fabian *Croatica Chemica. Acta.* **1981**, *54*, 427-434; b) C. W. Bird *Tetrahedron* **1985**, *41*, 1409-1414; c) R. Hosmane, J. F. Liebman *Tetrahedron Letters* **1991**, *32*, 3949-3952; d) B. Y. Simkin, V. I. Minkin, M. N. Glukhovtsev *Advances in Heterocyclic Chemistry* **1993**, *56*, 303-428; e) C. W. Bird *Tetrahedron* **1993**, *49*, 8441-8448; f) M. Z. Kassaei, N. Jalalimanesh, S. M. Musavi *J. Mol. Struct. (Theochem)* **2007**, *816*, 153-160.

CHAPTER 6

WHY ARE PERFLUOROCYCLOBUTADIENE AND
SOME OTHER (CF)_n^q RINGS NON-PLANAR?[†]

[†] Reproduced with permission from Judy I. Wu, Francesco A. Evangelista, Paul von Ragué Schleyer, *Org. Lett.* **2010**, 12 (4), pp 768-771.

Copyright © 2010 American Chemical Society

6.1 ABSTRACT

Although surprising, the non-planarity of C_{2h} C_4F_4 is not unique. While C_6F_6 is planar, other members of the $(CF)_n$ family, e.g., $C_5F_5^-$, $C_6F_6^{\bullet-}$, $C_7F_7^{\bullet}$, and triplet $C_7F_7^-$ are not. C_{2h} C_4F_4 is not aromatic, as claimed, but its antiaromaticity is reduced relative to the planar D_{2h} form due to decreased π antibonding and enhanced cross-ring π overlap. The non-planar C_{2h} geometry also benefits from the relief of repulsive FC-CF bond eclipsing interactions.

6.2 INTRODUCTION

Why is perfluorocyclobutadiene nonplanar?¹⁻⁴ Petersson et. al.¹ first discovered the unexpected C_{2h} symmetry of C_4F_4 , by observing a 595 cm^{-1} ring-puckering mode with negative dichroism in its vibrational spectrum; this would be IR inactive in D_{2h} symmetry. Their computed 11.6° out-of-plane angles of the C-F bonds (B3LYP/cc-pVDZ) result in substantial FCCF staggering across the single CC bonds (see Figure 6-1). The authors, noting the reminiscence to “the nonplanarity of the calculated structure of the perfluoroallyl radical”⁵ attributed the non-planarity of C_4F_4 to rehybridization,¹ “Electron withdrawal by the highly electronegative fluorines favors pyramidalization of the carbons by increasing the p -character of the C–F bonds, and this tendency is reinforced by the resulting attenuation of the cyclic conjugation in the π system.” However, similar rehybridization occurs in perfluorobenzene (C_6F_6) and in perfluoroethylene (C_2F_4), but both have planar geometries.^{6, 7}

Could non-planar C_4F_4 be aromatic? The remarkable conclusion “that aromaticity and the second-order Jahn-Teller effect (SOJTE)⁸ are primarily responsible for the non-planarity of C_4F_4 ” was put forward by Seal and Chakrabarti (SC) in 2007 on the basis of extensive analyses of the effects of planarization on several energetic and magnetic properties.^{2,4} SC interpreted the

C_{2h} HOMO as showing “complete π -delocalization around the ring carbons.” This was attributed to the mixing of s and p_π orbitals and “is responsible for the aromatic nature of C_4F_4 .” For non-planar C_{2h} C_4F_4 , SC reported a diamagnetic -7.2 ppm isotropic NICS(0)⁹ (in the ring center) and -2.1 ppm NICS(1)_{zz}¹⁰ (for the zz tensor component, perpendicular to the ring plane, 1 Å above the ring center). These negative (i.e., “aromatic”, diatropic) values contrasted with the positive (i.e., “antiaromatic”, paramagnetic) $+3.5$ NICS(0) and $+1.3$ ppm NICS(1)_{zz} data corresponding to the D_{2h} form. (As we document below, SC’s NICS evidence for the aromaticity of the C_{2h} form was misinterpreted and even erroneous.)

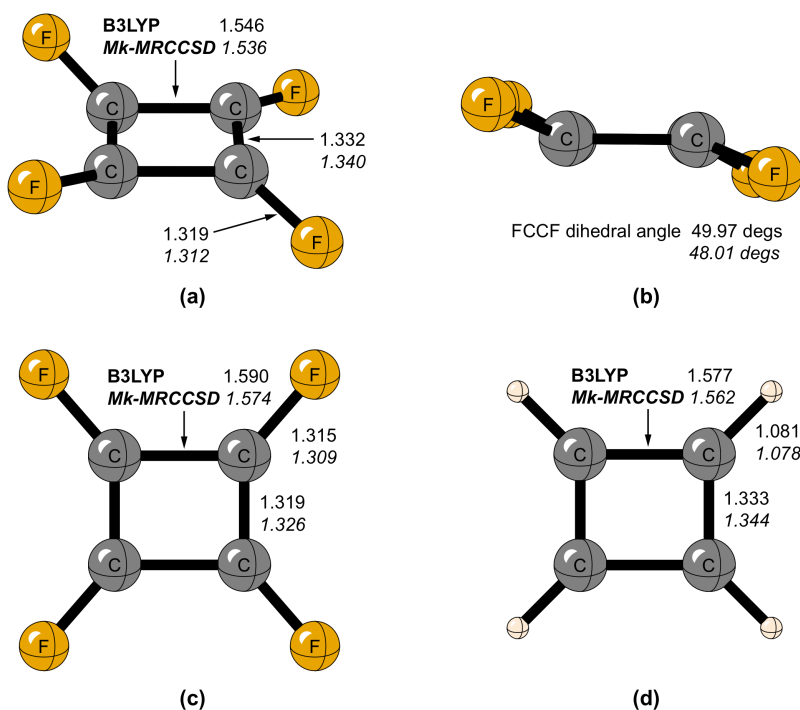


Figure 6-1. Geometries of C_{2h} C_4F_4 (a-b), D_{2h} C_4F_4 (c), and cyclobutadiene (d), computed at B3LYP/6-311+G** and Mk-MRCCSD/cc-PVTZ (in italics). Graphic prepared by HFSmol.¹¹

SC's aromaticity claim was challenged by Koehler, Herges, and Stanger (KHS) shortly afterwards based on “energetic considerations, NICS-scans, and ACID analyses.”³ According to KHS's refutation, C₄F₄ failed to show any special stability relative to CBD energetically, and its NICS_{zz} scan only revealed weakened paratropicity compared to cyclobutadiene. Thus, according to KHS, C₄F₄ is not aromatic, but at most only might be somewhat less antiaromatic than CBD.³ KHS suggested that F electron withdrawal in *C*_{2h} C₄F₄ was more effective than in planar *D*_{2h} C₄F₄ (due to greater *p* character in the CF bond hybridization). This reduced the “destabilizing interaction between the two double bonds” to a greater extent and favored the nonplanar *C*_{2h} form.

Table 6-1. GIAO-Nucleus Independent Chemical Shifts (NICS) data for *D*_{2h} and *C*_{2h} C₄F₄ and cyclobutadiene (CBD) (computed at PW91/IGLOIII//B3LYP/6-311+G**), all units are in ppm.

NICS data	<i>C</i> _{2h} C ₄ F ₄	<i>D</i> _{2h} C ₄ F ₄	<i>D</i> _{2h} CBD
NICS(0)	−7.3	−4.3	+26.4
NICS(1)	+5.1	+9.1	+17.7
NICS(0) _{zz}	+47.5	+48.3	+108.6
NICS(1) _{zz}	+24.2	+33.1	+54.6
NICS(0) _{πzz}	+30.6	+41.0	+58.3
NICS(1) _{πzz}	+26.6	+35.9	+51.33

However, KHS³ did not remark on the startling discrepancy between their ca. +32 ppm NICS(1)_{zz} value for *D*_{2h} C₄F₄, and the +1.3 ppm value (−2.1 ppm for *C*_{2h} C₄F₄) presented in SC's original paper.² Our computed PW91/IGLOIII NICS(1)_{zz} data for *D*_{2h} (+33.1 ppm) and *C*_{2h}

(+24.2 ppm) C₄F₄ (see Table 6-1) supports KHS's data. SC mistook an in-plane (*xx*, *yy*) tensor component of the isotropic NICS for the perpendicular (*zz*) tensor component analyses (as explained in footnote 12).

In their rebuttal,⁴ SC also did not comment on this NICS(1)_{*zz*} discrepancy with KHS, but plotted changes in diamagnetic susceptibility, kinetic energy, and nucleus-electron interaction energy in going from *D*_{2h} to *C*_{2h} C₄F₄. Although this evidence only indicates general trends, it was interpreted as supporting their original² “prediction of the aromatic behavior” of *C*_{2h} C₄F₄. Their claimed 18 kcal/mol decrease in kinetic energy upon puckering was interpreted to reveal “greater delocalization in non-planar C₄F₄.”

Petersson, *et al.*'s¹ original rehybridization argument seemed reasonable superficially. Thus, the *Csp*^{1.94} hybridization of the CBD C–H bonds (close to *sp*²) contrasts with the *Csp*^{2.59} hybridization of the *C*_{2h} C₄F₄ C–F bonds (close to *sp*³) (PW91/IGLOIII NLMO¹³ data). But this difference does not explain the non-planarity of C₄F₄ satisfactorily since *sp*³ hybridization does not necessarily favor local pyramidal geometries. Especially when highly electronegative F substituents are present, geometry and hybridization based on the ratio of localized orbital occupancies (NLMO) do not have a simple relationship,¹⁴ e.g., the carbon in tetrahedral CF₄ (*sp*^{2.33}) is roughly *sp*² rather than *sp*³ hybridized.¹⁵ The C–F bonds of the antiaromatic fluorocyclobutadiene (*sp*^{2.80}), 1,4-difluorocyclobutadiene (*sp*^{2.73}), 1,3-difluorocyclobutadiene (*sp*^{2.68}), and 1,2-difluorocyclobutadiene (*sp*^{2.67}), have even more *p* character than *C*_{2h} (*sp*^{2.59}) and *D*_{2h} (*sp*^{2.51}) C₄F₄, but only trifluorocyclobutadiene (*sp*^{2.58}, *sp*^{2.60}, and *sp*^{2.64}) is very slightly non-planar.

6.3 RESULTS AND DISCUSSION

Our definitive multireference coupled cluster computations (Mk-MRCCSD/cc-PVTZ)¹⁶ find that the D_{2h} C_4F_4 transition structure is only 2.0 kcal/mol higher in energy than the C_{2h} minimum (this confirms KHS's³ 2.05 kcal/mol difference at B3LYP/6-311+G*). The energy required to deform the D_{2h} C_4H_4 minimum into a simulated C_4F_4 -like C_{2h} C_4H_4 geometry was estimated by fixing all angles to those of C_{2h} C_4F_4 and then optimizing the CC and CH bond lengths. The 6.4 kcal/mol higher energy results largely from angle strain of the puckered CH's. But what is responsible for the non-planarity of C_4F_4 ? Is C_{2h} C_4F_4 really aromatic? Why do some perfluorinated rings, e.g. C_4F_4 , favor non-planar geometries, whereas others, e.g. C_6F_6 , are planar?

Planar C_4F_4 differs markedly from CBD and the partially fluorinated cyclobutadienes in having four repulsive eclipsed vicinal F...F interactions around the ring. The data in Figure 6-2 show that this repulsion destabilizes D_{2h} C_4F_4 by +22.7 kcal/mol (eq. 2) relative to four C_4FH_3 fluorocyclobutadienes! The Figure 6-2 data also agrees with KHS's conclusion that fluorine substitution disfavors C_4F_4 versus C_4H_4 energetically. However, this steric repulsion between the two single C–C bond FC–CF's is partially relieved in non-planar C_{2h} C_4F_4 . Since fluorocyclobutadiene C_4FH_3 is not destabilized relative to CBD (see Figure 6-2, eq. 1), the energetic effect of FC–CH and HC–CH eclipsing are about the same. As expected from energetic additivity (see Figure 6-2), the overall FC–CF repulsion is only half as large in trifluorocyclobutadiene (+11.7 kcal/mol, see eq. 3); it is less for 1,2- (+7.0 kcal/mol, eq. 4) as well as 1,4- (+4.2 kcal/mol, eq. 5) difluorocyclobutadiene, and is negligible for 1,3-difluorocyclobutadiene (–0.4 kcal/mol, eq. 6) since there are no eclipsed FC–CF's.

Similarly, due to the effect of the two vicinal FC–CF repulsions involving the central C–F, the perfluoroallyl radical favors a non-planar geometry,⁵ even though the 1,1,3,3-tetrafluoroallyl radical is planar. Tetra-tert-butyl cyclobutadiene¹⁷ and tetra-nitrocyclobutadiene²

also are non-planar because of their very bulky substituents. Despite having larger Cl atoms, the C_4Cl_4 minimum is planar (D_{2h} symmetry) as the ClC–CCl Cl's are much further apart (3.867 Å) than the FC–CF F's in D_{2h} C_4F_4 (3.313 Å) (at B3LYP/6-311+G*). However, the triplet C_4Cl_4 minimum is slightly non-planar (C_{2h} symmetry).

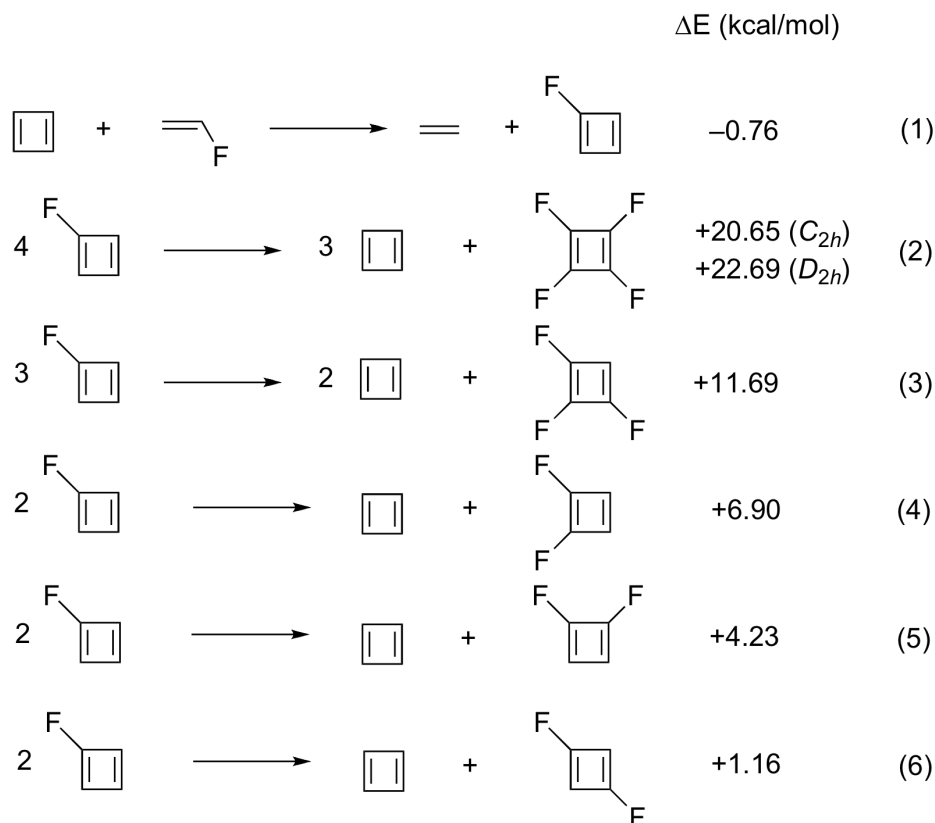


Figure 6-2. Homodesmotic evaluations of the vicinal FCCF repulsion in fluorinated cyclobutadienes (B3LYP/6-311+G** + ZPE data). Note that the additivity relationships: (4) + (5) \sim (3) and 2(4) + 2(5) \sim (2, D_{2h}) reveal no special energetic effects.

Compared to its D_{2h} transition state, we agree that C_{2h} C_4F_4 benefits from having somewhat better molecular orbital features. As noted by SC,^{2,4} the twisting of the HOMO in C_{2h} C_4F_4 decreases its unfavorable π anti-bonding cross-ring interaction and increases the overlap

between the π lobes of the same sign. However, SC's suggestion that aromatic character results is exaggerated; we agree with KHS that the effect only reduces antiaromaticity somewhat. The alleviation of vicinal FC–CF repulsion, accompanied by decreased antibonding character of the HOMO (note the significantly shortened CC single bond in C_{2h} C_4F_4 , from 1.590Å to 1.546Å, see Figure 6-1), results in a more compact carbon ring framework in C_{2h} C_4F_4 . Hence, the non-planar C_4F_4 has greater nuclear-nuclear (nn) / electron-electron (ee) repulsion but even greater nuclear-electron (ne) attraction than the planar D_{2h} form (see Table 6-2).

Table 6-2. Energy components (nuclear-nuclear, electron-electron, nuclear-electron, potential, kinetic and total energy) of D_{2h} and C_{2h} C_4F_4 (computed at B3LYP/6-311+G*//B3LYP/6-311+G* and MP2/6-311+G*//MP2/6-311+G*, italics). The C_{2h} preference is “attractive” dominant (due to greater nuclear-electron interaction).

Energy Components	C_{2h} (a.u.)	D_{2h} (a.u.)
Nuclear-nuclear (nn)	355.02230	351.68198
“repulsive”	<i>355.41574</i>	<i>351.54584</i>
Electron-electron (ee)	559.65627	556.58299
“repulsive”	<i>559.36813</i>	<i>555.82719</i>
Nuclear-electron (ne)	–2015.94748	–2009.53043
“attractive”	<i>–2015.83756</i>	<i>–2008.42403</i>
Potential Energy	–1101.26892	–1101.26546
(nn + ee + ne)	<i>–1101.05369</i>	<i>–1101.05100</i>
Kinetic Energy	549.72089	549.72087
(KE)	<i>550.50586</i>	<i>550.50927</i>
Total Energy	–551.54803	–551.54459
	<i>–550.54783</i>	<i>–550.54173</i>

Nevertheless, these energy component analyses give only limited insight to the origin of C_4F_4 puckering, as they reflect the energy lowering associated with all geometric changes in the molecule, which are not identifiable individually. We find that the kinetic energy change going from C_{2h} to D_{2h} C_4F_4 is only 0.01 kcal/mol (see Table 6-2), in contrast to SC's report of 18 kcal/mol (this discrepancy is explained in footnote 18).

SC's conclusion that C_{2h} C_4F_4 is aromatic also was supported misleadingly by the small negative isotropic C_{2h} C_4F_4 NICS(0) value (−7.3 ppm) (see Table 6-1), as well as their erroneous NICS(1)_{zz} and D_{2h} NICS(0) data.^{2, 10} Canonical molecular orbital (CMO) analyses NICS(0)_{πzz}¹⁹⁻²⁰ evaluate the diatropicity/paratropicity of planar as well as non-planar molecules accurately and are more soundly based than other NICS based indices, as only contributions perpendicular to the ring plane (zz) of the relevant CMO's are included. Thus, both C_{2h} (NICS(0)_{πzz} = +30.6 ppm, at PW91/IGLOIII, zz is the tensor component perpendicular to the plane of the carbon ring) and D_{2h} (+41.0 ppm) C_4F_4 are clearly antiaromatic (NICS(0)_{πzz} = +58.3 ppm for CBD, at the same level) (see Figure 6-3). Similar to non-planar C_4F_4 , the 4 π electrons $C_3H_3^-$ also has puckered CH bonds and reduced antiaromaticity (NICS(0)_{πzz} = +30.4 ppm).

As recognized in 1997²¹ and emphasized many times since,¹⁹ isotropic NICS (an average of the *xx*, *yy*, and *zz* tensor contributions)⁹ are seriously contaminated by contributions of the in-plane *xx* and *yy* tensor components, especially at the centers of small rings. Only the perpendicular *zz* tensor components are related to aromaticity in such cases, but these may not dominate. Specifically, the diatropicity of the *in-plane* NICS(0)_{xx} (−39.0 ppm and −21.0 ppm) and NICS(0)_{yy} (−19.1 ppm and −40.3 ppm) tensor components in C_{2h} and D_{2h} C_4F_4 , respectively, overwhelm the paratropicity of the more relevant NICS(0)_{zz} (+47.5 ppm and +48.3 ppm) contributions (see Table 6-1).

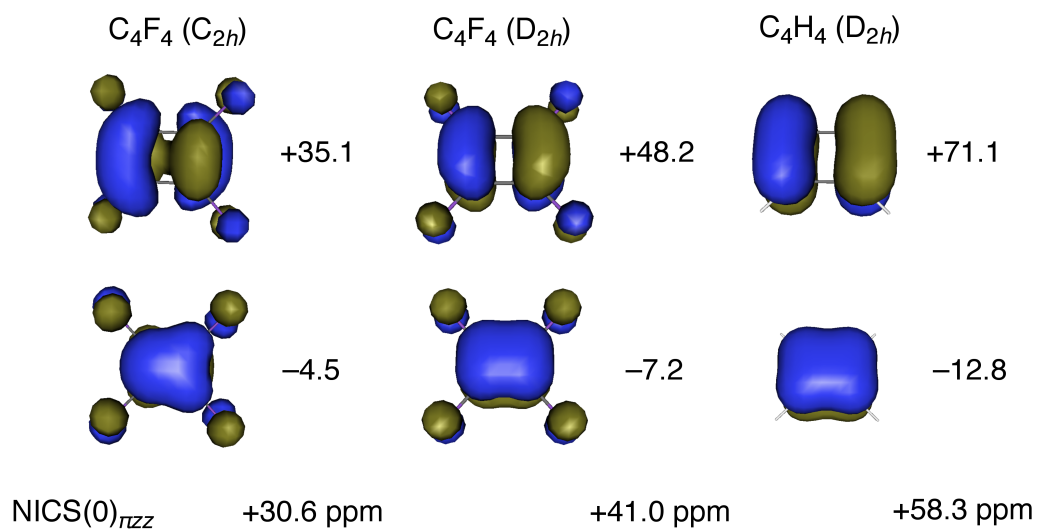


Figure 6-3. NICS $_{zz}$ data for the π MO's of C_4F_4 (C_{2h} and D_{2h}) and cyclobutadiene (CBD) and their total NICS(0) $_{\pi zz}$ values. All canonical molecular orbital (CMO) NICS data were computed at the PW91/IGLOIII level.

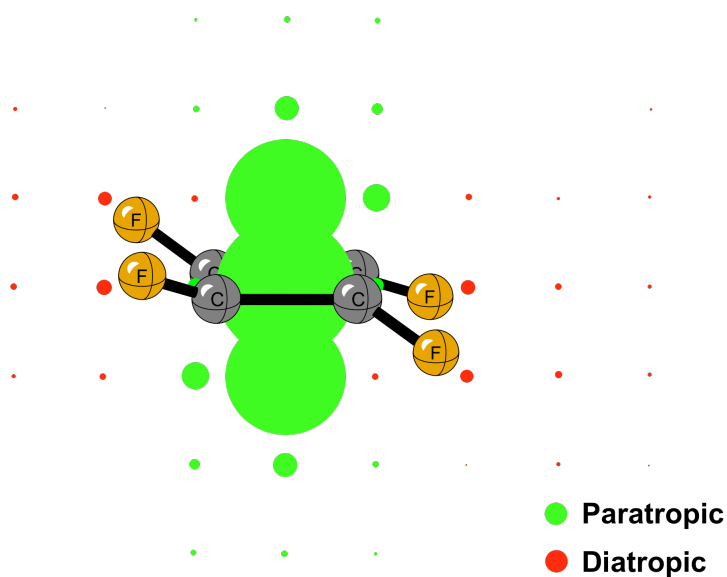


Figure 6-4. NICS $_{\pi zz}$ grid of antiaromatic C_{2h} C_4F_4 (at PW91/IGLOIII).

Isotropic NICS(1)^{19, 21} data (at points 1 Å above the ring center) alleviate this problem somewhat. Indeed, the NICS(1) values for both C_{2h} (+5.1 ppm) and D_{2h} (+9.1 ppm) C_4F_4 are *positive* (see Table 6-1), indicating weak antibonding (paratropic) character. When only the perpendicular tensor component is considered, both NICS(0)_{zz} and NICS(1)_{zz} are positive for C_{2h} and D_{2h} C_4F_4 (+24.2 ppm and +33.1 ppm, respectively; Table 6-1). The NICS_{zz} scans of KHS provide similar information, but the NICS(0)_{πzz} data in Table 6-1 and Figure 6-3 are definitive, as only the π MO contributions are included (note the NICS_{πzz} grid, Figure 6-4).

The smaller NICS(0)_{πzz} value of *planar* D_{2h} C_4F_4 (+41.0 ppm) than D_{2h} CBD (+58.3 ppm) is due to the significant differences in their CC bond lengths (see Figure 6-1). The NICS(0)_{πzz} value of CBD is reduced from +58.3 to +49.2 ppm when the D_{2h} C_4F_4 CC bond lengths are imposed. Hence, at least part of the reduced antiaromaticity in D_{2h} C_4F_4 , compared to CBD, can be attributed to the increase in CC bond length alternation due to fluorine substitution.²² *Therefore, C_4F_4 is non-planar due to the alleviation of the vicinal FC–CF eclipsing strain at the single CC bonds and to partial relief of antiaromaticity.*

However, the non-planarity of C_4F_4 is not unique. Non-planar geometries are favored by $C_5F_5^-$ (6 π) $C_6F_6^{\bullet-}$ (7 π),²⁴ $C_7F_7^\bullet$ (7 π), $C_7F_7^-$ (8 π , triplet), and $C_8F_8^{2-}$ (10 π), even though their $(CH)_n^q$ counterparts are planar (see Figure 6-5). Other perfluorinated rings have planar geometries, i.e. $C_5F_5^+$ (4 π electrons), $C_5F_5^\bullet$ (5 π), $C_6F_6^{\bullet+}$ (5 π),²³ C_6F_6 (6 π), and $C_7F_7^+$ (6 π). In general, fluorinated anions tend to be non-planar (as in CF_3^-), but cations favor planarity (as in CF_3^+). Larger perfluorinated rings have smaller F...F distances, but also much shorter CC “single bond” lengths (less than 1.48 Å for all perfluorinated five, six, and seven membered ring species, compared to 1.590 Å in C_4F_4); larger CC bond orders resist FCCF twisting. Vicinal FC–

CF repulsion is relieved by puckering more easily in antiaromatic species, while non-planarity is resisted. e.g., by C_6F_6 , due to aromaticity reduction.

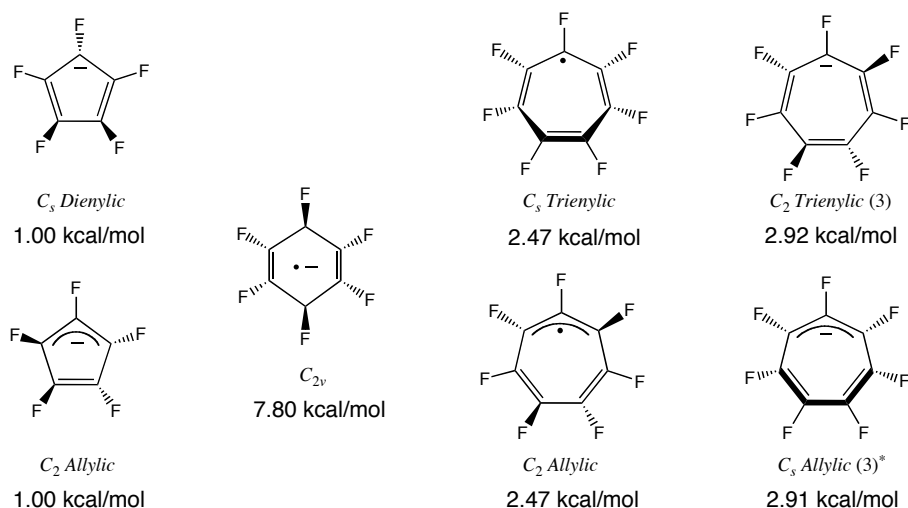


Figure 6-5. Planarization energies for non-planar $(CF)_n^q$ species (at B3LYP/6-311+G*) with planar hydrocarbon analogs.*The allylic $C_7H_7^-$ triplet (C_s) has one negligible imaginary frequency (-4.86 cm^{-1}).

Consequently, it is remarkable that the aromatic $C_5F_5^-$, despite having six π electrons, is non-planar. We attribute this to the pyramidalizing effect of its negative charge. The D_{5h} geometry of $C_5F_5^-$ ($NICS(0)_{\pi_{zz}} = -24.3\text{ ppm}$) is a second order (E_1) “monkey” saddle point on the potential energy surface involved in the stereomutation of the nearly isoenergetic dienylic C_s ($NICS(0)_{\pi_{zz}} = -15.9\text{ ppm}$) and allylic C_2 ($NICS(0)_{\pi_{zz}} = -16.6\text{ ppm}$) minima. Both these minima have small planarizing energies (ca. 0.7 kcal/mol) to the D_{5h} form, and are connected through a C_1 transition state ($NICS(0)_{\pi_{zz}} = -16.6\text{ ppm}$). All $C_5F_5^-$ forms are aromatic, the non-planar ones slightly less so. In contrast, the $C_5F_5^+$, despite having 4 π electrons, has a planar minimum due to its positive charge. The 5 π electron $C_5F_5^\bullet$ also is planar.

6.4 CONCLUSIONS

We conclude that C_4F_4 prefers C_{2h} instead of D_{2h} symmetry for two reasons: reduced antiaromaticity due to the less unfavorable π overlap across the ring and reduced vicinal FC–CF repulsions. Such repulsions tend to deplanarize perfluorinated $(\text{CF})_n$ rings, but obviously not their hydrocarbon (or less fluorinated) analogs. Non-planar $(\text{CF})_n$ rings only have small planarizing energies since planar geometries maximize π delocalization. In view of *the delicate balance between opposing factors*^[3] exemplified by the behavior of a broader set of neutral and charged $(\text{CF})_n$ rings, the non-planarity of C_4F_4 is not “*special*” at all.

6.5 REFERENCES

1. E. J. Petersson, J. C. Fanuele, M. R. Nimlos, D. M. Lemal, G. B. Ellison, J. G. Radziszewski, *J. Am. Chem. Soc.* **1997**, *119*, 11122-11123.
2. P. Seal, S. Chakrabarti, *J. Phys. Chem. A* **2007**, *111*, 715-718. The reported NICS(1)_{zz} datum for C_{2h} C₄F₄ (ca. -2 ppm) is in error. Our recomputed values are +24.2 ppm (C_{2h} C₄F₄) and +33.1 ppm (D_{2h} C₄F₄).
3. F. Koehler, R. Herges, A. Stanger, *J. Phys. Chem. A* **2007**, *111*, 5116-5118.
4. P. Seal, S. Chakrabarti, *J. Phys. Chem. A* **2007**, *111*, 5119-5121.
5. J. H. Hammons, M. B. Coolidge, W. T. Borden, *J. Phys. Chem.* **1990**, *94*, 5468-5470.
6. A. Almenningen, O. Bastiansen, R. Seip, M. Hans, *Acta. Chem. Scand.* **1964**, *18*, 2115-2124.
7. J. L. Carlos Jr., R. R. Carl Jr., S. H. Bauer, *J. Chem. Soc. Faraday Trans. 2* **1974**, *70*, 177-187.
8. The possibility of having a second order Jahn-Teller effect (SOJTE) in C₄F₄ is unlikely. The D_{2h} HOMO-LUMO gap is not small at all (ca. 0.15 a.u., HOMO energy -0.22361 a.u.), at C_{2h} it is 0.13 a.u. (HOMO energy -0.24001 a.u.). Moreover, the SOJTE requirement (see R. G. Pearson *Proc. Nat. Acad. Sci.* **1975**, *72*, 2104-2106) is not met: the HOMO (a_g) and LUMO (b_g) orbitals of C_{2h} C₄F₄ do not have the same symmetry Seal and Chakrabarti's original argument stating that there is "a manifestation of the electron-phonon or vibronic coupling" in C₄F₄, based on the dominating "attractive" E_(n-e) in C_{2h} C₄F₄, is not direct evidence for SOTJE.
9. P. v. R. Schleyer, C. Maerker, A. Dransfeld, H. J. Jiao, N. J. r. V. E. Hommes *J. Am. Chem. Soc.* **1996**, *118*, 6317-6318.

10. C. Corminboeuf, T. Heine, G. Seifert, P. v. R. Schleyer, *Phys. Chem. Chem. Phys.* **2004**, *6*, 273-276.
11. S. E. Wheeler, HFSmol; University of Georgia: Athens, GA, 2008.
12. SC's erroneous "NICS(1)_{zz}" value for C_{2h} C_4F_4 (−2.1 ppm) corresponds to the in-plane NICS(1)_{yy} (−1.4 ppm) in our PW91/IGLOIII computation (NICS(1)_{xx} = −7.6 ppm). Although *zz* is the conventional out-of-plane designation, it does not always represent the perpendicular tensor component in the NICS output, since the "xx, yy, and zz" assignment depends on the orientation of the molecule.
13. NBO 5.X. E. D. Glendening, J. K. Badenhoop, A. E. Reed, J. E. Carpenter, J. A. Bohmann, C. M. Morales, and F. Weinhold (Theoretical Chemistry Institute, University of Wisconsin, Madison, WI, 2003); A. E. Reed, L. A. Curtis, F. Wienhold, *Chem. Rev.* **1988**, *88*, 899-926.
14. K. B. Wiberg, M. A. Murcko, *J. Mol. Struct. (Theochem)* **1988**, *169*, 355-365.
15. A. E. Reed, P. v. R. Schleyer, *J. Am. Chem. Soc.* **1987**, *109*, 7362-7373.
16. F. A. Evangelista, W. D. Allen, and H. F. Schaefer *J. Chem. Phys.* **2007**, *127*, 24102-24119.
17. M. Balci, M. L. McKee, P. v. R. Schleyer *J. Phys. Chem.* **2000**, *104*, 1246-1255.
18. Kinetic energy components are very sensitive to molecular geometries (whether or not they are fully relaxed). SC reported an 18 kcal/mol kinetic energy change in going from C_{2h} to D_{2h} C_4F_4 at MP2/6-311+G*//B3LYP/6-311+G* and 8.5 kcal/mol at B3LYP/6-311+G*. These values are artifacts of computing the energetic components at geometries optimized at different levels (see Table 4-2). In contrast, our re-computations give 2.14

kcal/mol at MP2/6-311+G*//MP2/6-311+G* and only 0.01 kcal/mol at B3LYP/6-311+G*//B3LYP/6-311+G*. There is no kinetic energy difference!

19. H. Fallah-Bagher-Shaidaei, C. S. Wannere, C. Corminboeuf, R. Puchta, P. v. R. Schleyer, *Org. Lett.* **2006**, 8, 863-866.
20. Z. Chen, C. S. Wannere, C. Corminboeuf, R. Puchta, P. v. R. Schleyer, *Chem. Rev.* **2005**, 105, 3842-3888.
21. P. v. R. Schleyer, H. Jiao, N. J. R. v. E. Hommes, V. G. Malkin, O. L. Malkina, *J. Am. Chem. Soc.* **1997**, 119, 12669-12670.
22. Unlike C₄F₄, perfluorination of benzene has essentially no effect on either its geometry or aromaticity (see J. I. Wu, F. G. Pühlhofer, P. v. R. Schleyer, R. Puchta, B. Kiran, M. Mauksch, N. J. R. v. Hommes, E. I. Alkorta, J. Elguero, *J. Phys. Chem. A* **2009**, 113, 6789-6794).
23. V. P. Vysotsky, G. E. Salnikov, L. N. Shchegoleva, *Int. J. Quant. Chem.* **2004**, 100, 469-476.
24. L. N. Shchegoleva, I. V. Beregovaya, P. V. Schastnev, *Chem. Phys. Lett.* **1999**, 312, 325-332.

CHAPTER 7

4N PI ELECTRONS BUT STABLE: N,N-DIHYDRODIAZAPENTACENES[†]

[†] Reproduced with permission from Judy I. Wu, Chaitanya S. Wannere, Yirong Mo, Paul von Ragué Schleyer, Uwe, H. F. Bunz, *J. Org. Chem.* **2009**, *74* (11), pp 4343-4349.

Copyright © American Chemical Society

7.1 ABSTRACT

Despite having $4n$ π electrons, dihydrodiazapentacenes are more viable than their $4n+2$ π azapentacene counterparts. *Ab initio* valence bond block-localized wavefunction (BLW) computations reveal that despite having $4n$ π electrons dihydrodiazapentacenes are stabilized and benefit substantially from four dihydropyrazine ethenamine (enamine) conjugations. Almost all of these dihydrodiazapentacenes have large negative overall nucleus independent chemicals shifts NICS(0) _{π zz} values even though their dihydropyrazine rings (e.g. for **6-H**₂) are modestly antiaromatic, as their paratropic contributions are attenuated by delocalization throughout the system.

7.2 INTRODUCTION

Polycyclic six membered ring molecules with $4n$ π electrons elicit attention, especially when their $4n+2$ π electron counterparts are unstable. Remarkably, the $4n$ π electron dihydrodiazapentacenes (**5b-H**₂, **5c-H**₂, **6-H**₂ and **7-H**₂) have been known since the late 19th century,¹⁻⁷ but attempts to synthesize their aromatic $4n+2$ π electron counterparts (**5b**, **5c**, **6** and **7**) have not succeeded (see Figure 7-1).⁸⁻⁹ Although **4b** and **4b-H**₂ (Figure 7-2) were redox-interconvertible, Hinsberg noted that **6-H**₂ could not be oxidized to **6** (Figure 7-1).⁴ The $4n+2$ π azaacenes resemble the parent acenes¹⁰ in being increasingly unstable as the number of rings increase, however very recently a tetraazapentacene derivative has been synthesized by Bunz et al.⁹ How can the peculiar viability of the $4n$ π electron dihydrodiazapentacenes be rationalized?

The larger parent acenes usually have small HOMO-LUMO gaps and are not persistent¹¹⁻¹⁴ unless protected by bulky substituents at strategic positions.¹⁵⁻¹⁸ Furthermore, Houk and Wudl, noted that heptacene and the higher acenes had singlet diradicaloid character.¹³

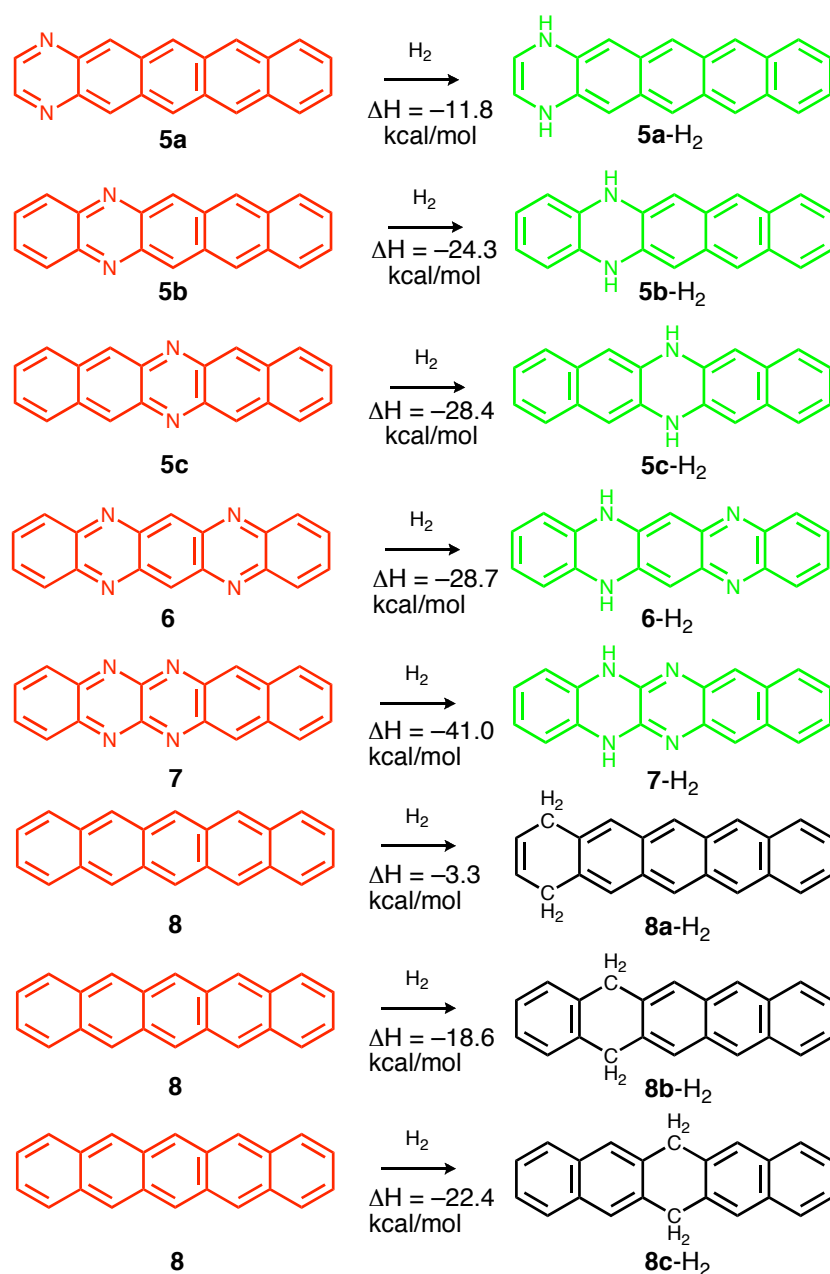


Figure 7-1. Heats of hydrogenation for the diazapentacenes **5-7** and pentacene **8** reduced to the dihydroazaacenes **5(a-c)-H₂-7-H₂** and dihydropentacenes **8(a-c)-H₂** (all data are computed at the B3LYP/6-311+G** level including ZPE correction). Compounds with a $4n+2$ π perimeter are traditionally aromatic (in red); formally antiaromatic compounds have a $4n$ π perimeter (in green).

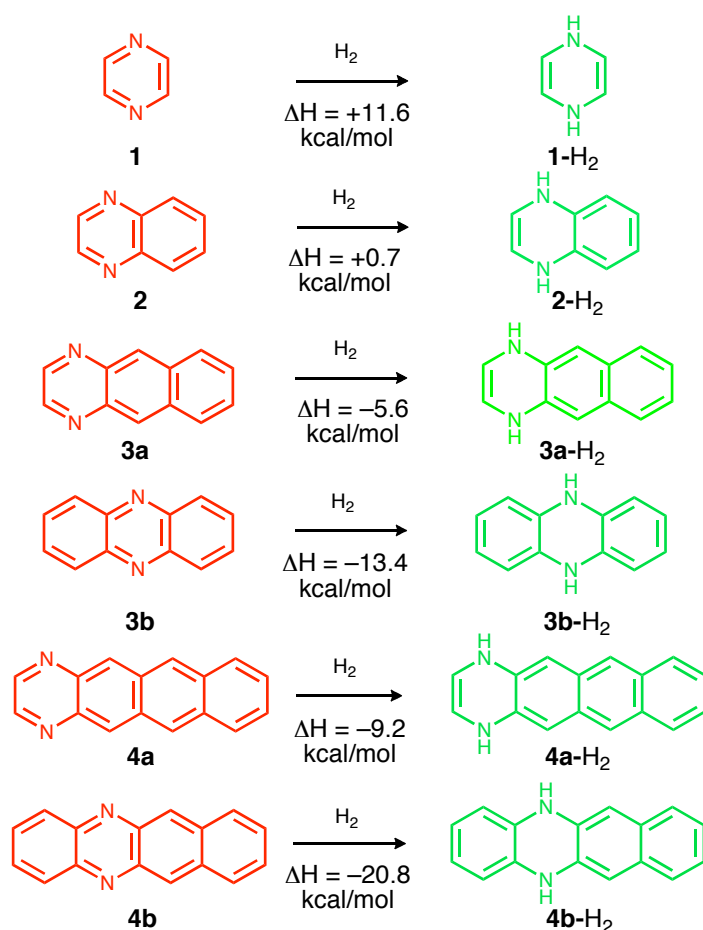


Figure 7-2. Heats of hydrogenation for the smaller azaacenes **1-4** reduced to dihydroazaacenes **1-H₂-4(a-b)-H₂** (all data are computed at the B3LYP/6-311+G** level including ZPE correction). Compounds with a $4n+2$ π perimeter are traditionally aromatic (in red); formally antiaromatic compounds have a $4n$ π perimeter (in green).

By analogy, the azaacenes (**5b**, **5c**, **6** and **7**, Figure 7-1) are to show a small band gap and increased reactivity. So what makes the $4n$ π electron dihydrodiazapentacenes so viable and perhaps more stable than their formally aromatic $4n+2$ π azapentacene derivatives? The dihydrodiazapentacenes (24 π electrons) have more π electrons than the azapentacenes (22 π electrons) at the cost of incorporating a formally antiaromatic 8π electron dihydropyrazine

moiety. But rather than having three butadiene-like conjugations, each of the dihydropyrazine rings have four ethenamine (enamine) conjugations instead. How large are these ethenamine stabilizations? Are they sufficient to overcome the energetic penalty of the unfavorable $4n$ π electron count?

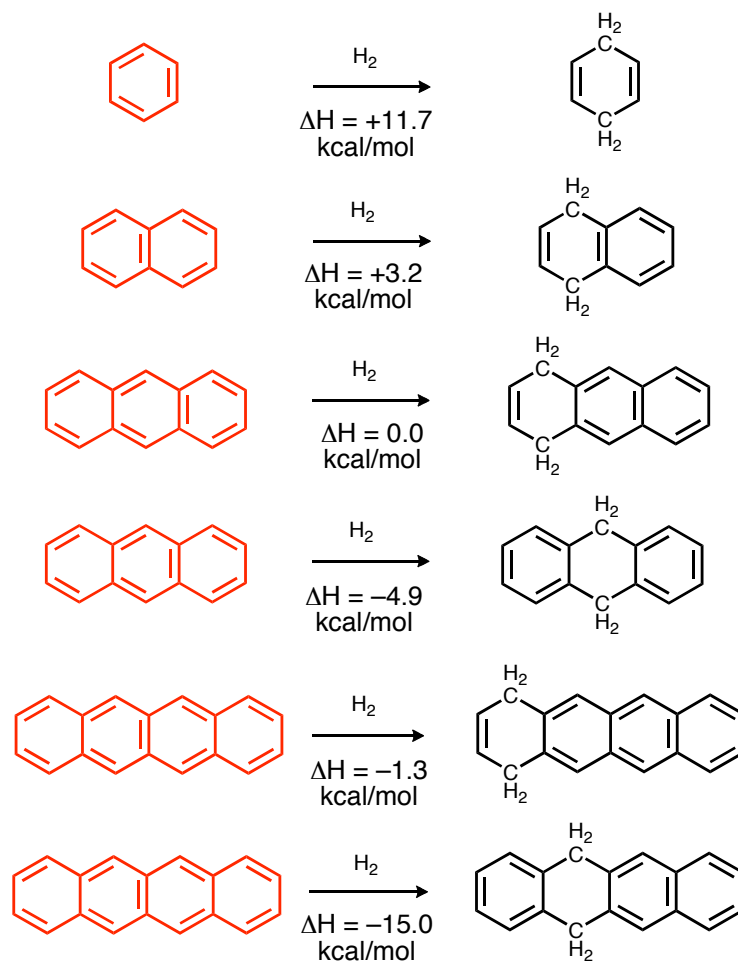


Figure 7-3. Heats of hydrogenation for the smaller acenes reduced to dihydroacenes (all data are computed at the B3LYP/6-311+G** level including ZPE correction).

The planarity of the dihydrodiazapentacenes suggests that they are not very antiaromatic. Thus, Nuckolls postulated that the unusual stability of both **5b**-H₂ and **5c**-H₂ was related to breaching

the π conjugation of the pentacene framework into smaller aromatic subunits.⁶ While both **5b**-H₂ and **5c**-H₂ can have two Clar rings,¹⁹ but **5b** and **5c** only one, is this explanation adequate to resolve the unusual stability of the $4n$ π dihydrodiazapentacenes?

Current interest in these nitrogen-containing heteroacenes^{20–23} arises from their potential applications as organic thin film transistors.²⁴ Nevertheless, there has not been any systematic studies explaining the unexpected existence of the $4n$ π electron dihydrodiazapentacenes. The questions we wish to answer in this paper are: What is responsible for the viability of the formally antiaromatic $4n$ π dihydrodiazapentacenes? To what extent does the ethenamine moieties confer energetic stabilization? Despite having $4n$ π electrons, do the dihydrodiazapentacenes still benefit from aromaticity?

RESULTS AND DISCUSSION

We computed the heats of hydrogenation for both the $4n+2$ π electron azaacenes and their parent acenes (number of rings $N = 1$ to 5) by evaluating the cross ring 1,4-hydrogenation reaction energies for each of the different rings of the various compounds. The resonance energies (REs) and aromatic stabilization energies of the $4n$ π dihydrodiazapentacenes and $4n+2$ π azapentacenes were evaluated based on Mo's *ab initio* block-localized wavefunction (BLW)²⁵ procedure (see Methods). Nucleus chemical independent shift (NICS)²⁶ computations (see Methods) characterized the magnetic aromaticity of these $4n$ and $4n+2$ π species.

7.3 HEATS OF HYDROGENATION

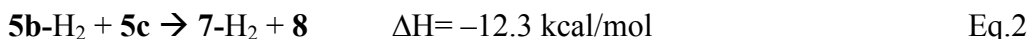
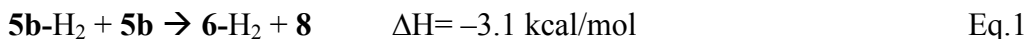
As expected from the instability of the larger acenes, the computed $\Delta H(H_2)$ for the azaacenes and their parent acenes become increasingly exothermic as the number of rings increase (Figures 7-1,

7-2, and 7-3). The $\Delta H(H_2)$ for pyrazine **1** and benzene are endothermic, due to the loss of aromaticity in dihydropyrazine and 1,4-cyclohexadiene (Figures 7-2 and 7-3). Although dihydropyrazine **1-H₂** is destabilized by antiaromaticity (eight π electrons), it is stabilized by four ethenamine conjugations involving the N lone pairs, while 1,4-cyclohexadiene is non-aromatic, and it is stabilized by four hyperconjugations instead. Thus, the $\Delta H(H_2)$ values for pyrazine and benzene are essentially the same.

In contrast, the $\Delta H(H_2)$ for the larger azaacenes (N = 3 to 5) are more exothermic than their acene parents (by 5 to 8 kcal/mol, Figure 7-1). Unlike **1-H₂**, the ring π electrons of the dihydropyrazine moieties of the dihydrodiazaacenes are not confined to a single a six-membered ring, but can delocalize to adjacent benzenoid rings. For this reason, the dihydropyrazine rings of the $4n \pi$ dihydrodiazaacenes are expected to be less antiaromatic (see also ECRE section, below). Hence, the fully conjugated dihydrodiazaacenes are stabilized to a greater extent compared to their corresponding dihydroacenes, involving hyperconjugation.

Note that the $\Delta H(H_2)$ for various azaacene and acene isomers differ depending on the position of the hydrogenated ring. Those with a reduced “inner ring” (e.g. **5(b-c)-H₂** and **8(b-c)-H₂**) have greater $\Delta H(H_2)$ ’s than those with the “outer ring” hydrogenated (e.g. **5a-H₂** and **8a-H₂**); as the former results in two Clar rings, but the latter only in one (see Figure 7-1). Clar’s rule states that isomers with a maximum number of sextet rings are advantageous energetically.¹⁹ Thus, the $\Delta H(H_2)$ of **3b**, **4b**, **5b** and **5c** are twice as exothermic as their 1,4-dihydro isomers, **3a**, **4a** and **5a**. The acenes demonstrate the same trend. The $\Delta H(H_2)$ for the tetraazapentacenes (**6** and **7**) are especially exothermic. Both **6-H₂** and **7-H₂** enjoy an internal stabilization between the dihydropyrazine and pyrazine ring, as the NH group lone pair of the dihydropyrazine rings alleviates the sigma electron withdrawing effect of the electron deficient pyrazine ring. This

synergistic stabilization is smaller for **6** (−3.1 kcal/mol, eq. 1) but quite large for **7** (−12.3 kcal/mol, eq. 2).



In agreement with the absent experimental reports of $4n+2$ π electron diazapentacenes, their heats of hydrogenation leading to the $4n$ π electron dihydrodiazapentacenes are highly exothermic. Pentacene also behaves similarly, but has less exothermic heats of hydrogenation compared to that of the corresponding diazapentacenes. Dihydrodiazapentacenes are stabilized by conjugation and leave the dihydropyrazine moieties less antiaromatic than **1-H₂**.

7.4 RESONANCE ENERGY

The resonance energies (PWRE) of the dihydrodiazapentacenes and diazapentacenes were evaluated, based on the Pauling-Wheland definition,²⁷ by the total energy difference between the fully conjugated compound and that of its most stable resonance contributor, employing the BLW procedure (see Methods). Remarkably, $4n$ π dihydrodiazapentacenes (**5a-H₂**, **5b-H₂**, **5c-H₂**, **6-H₂** and **7-H₂**) have significantly greater PWRE's (30 to 55 kcal/mol, see Table 7-1) than their corresponding $4n+2$ π derivatives (**5a**, **5b**, **5c**, **6** and **7**) (Table 7-1), as they benefit from the conjugated ethenamine (**9**)-like subunits of their dihydropyrazine rings. Each 4π electron ethenamine moiety has a conjugated CC double bond and an N lone pair. Note that there are four ethenamine subunits in each dihydropyrazine ring, but none for the pyrazine rings of the $4n+2$ π diazapentacenes (as their N lone pairs are in the ring plane). Based on the BLW computed

PWRE for ethenamine **9**, each of these conjugations is worth 20 kcal/mol; this value is remarkably large compared to the PWRE of butadiene **10** (12.2 kcal/mol). Thus, the PWRE of aniline (80.3 kcal/mol, C_{2v}) also is greater than styrene (71.5 kcal/mol). Since this feature is present four times for each dihydropyrazine ring, the ethenamine stabilization for each dihydrodiazapentacene might approach 80 kcal/mol. This could account for 25 to 30% of the total PWRE of the dihydrodiazapentacenes and is comparable to the PWRE of benzene (61.4 kcal/mol)! For the same reason, the smaller $4n\pi$ dihydrodiazacenes (number of annulated rings: $N = 2$ to 4) also have PWRE's 10 to 45 kcal/mol greater than their $4n+2\pi$ congeners (Table 7-1).

Note that the PWRE's of the dihydrodiazapentacenes depend on the positions of their dihydropyrazine rings, due to the number of Clar rings available. Both **5b**-H₂ (291.3 kcal/mol) and **5c**-H₂ (296.1 kcal/mol) have greater PWRE's than **5a**-H₂ (274.2 kcal/mol). The smaller dihydrodiazacenes ($N = 2$ to 4) with reduced "inner" dihydropyrazine moieties also have greater PWRE's than their 1,4- dihydro isomers. As expected from Clar's rule, isomers with a maximum number of sextet rings energetically more stable.¹⁹ Hence, dihydrodiazacenes with reduced "inner" dihydropyrazine moieties benefit from having two (instead of one) Clar rings (see the discussion in ECRE section). Both **5b**-H₂ and **5c**-H₂ have two Clar rings, and thus are energetically more favorable than **5a**-H₂, which has only one.

On a per ring basis, the PWRE's of both the diazacene and dihydrodiazacene series (number of rings $N = 2$ to 5) decrease as the number of annulated rings increase (Figure 7-4),¹⁰ but all of the $4n\pi$ dihydrodiazacenes (Figure 7-4, green and blue rhomboids) have greater PWRE's *per ring* than their corresponding $4n+2\pi$ azacenes (Figure 7-4, red triangles), as they are stabilized by the ethenamine conjugation. The number and positions of the pyrazine rings do not affect the PWRE's of the various azapentacene isomers (e.g. **5a**, **5b** and **5c**), but those of the

dihydrodiazapentacenes differ significantly depending on the positions of their dihydropyrazine ring and numbers of Clar rings available (see above).

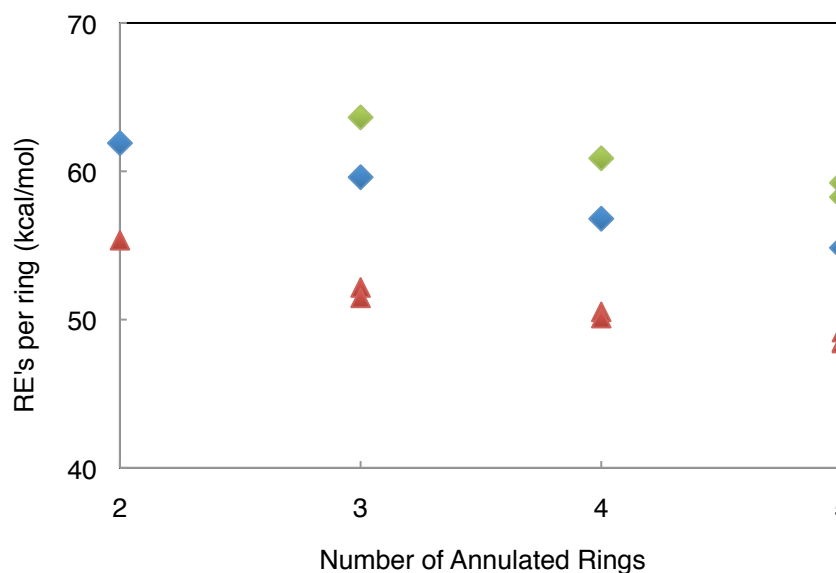


Figure 7-4. Resonance energies (RE's) per ring vs. the number of annulated rings ($N = 2$ to 5) for the dihydroazaacenes (**2**-H₂ to **5(a-c)**-H₂, blue and green rhomboids) and diazacenes (**2** to **5(a-c)**, red triangles). The 1,4-dihydroazaacenes (**2**-H₂, **3a**-H₂, **4a**-H₂ and **5a**-H₂) are in blue; their isomers with reduced inner rings (**3b**-H₂, **4b**-H₂ and **5(b-c)**-H₂) are in green. All BLW data are computed at the B3LYP/6-31G* level.

Despite having $4n$ π electrons, dihydrodiazapentacenes have considerably larger REs than the $4n+2$ π azapentacenes due to the ethenamine conjugations. Clar's rule rationalizes the different PWRE values for various dihydrodiazapentacene isomers, but is inadequate to explain the 30 to 55 kcal/mol PWRE difference between the related $4n$ π and $4n+2$ π species. Thus, the PWRE difference between phenanthrene (165.2 kcal/mol, two Clar rings) and anthracene (157.5

kcal/mol, one Clar ring) is less than 10 kcal/mol. Like the parent acenes and $4n+2$ π electron azaacenes, the larger $4n$ π electron dihydrodiazacenes also become increasingly unstable as the number of rings increase,¹⁰ but are stabilized substantially by the ethenamine conjugations.

7.5 EXTRA CYCLIC RESONANCE ENERGY

The ECRE²⁸ measures the aromatic stabilization (destabilization) energy for cyclic conjugated compounds, and is derived from the BLW computed RE of the aromatic (or antiaromatic) compound minus the RE sums of appropriate number and types of acyclic conjugation (including ethenamine) references (see Methods). Thus, all energetic effects other than aromaticity (or antiaromaticity) are cancelled out in the ECRE procedure.²⁸ Positive ECRE's indicate aromaticity and negative ECRE's indicate antiaromaticity.²⁸ For example, the ECRE of benzene (+29.3 kcal/mol) is derived from the RE of benzene (61.4 kcal/mol) minus the RE sum of three *syn*-butadienes (10.7 kcal/mol each), as they resemble the three butadiene conjugations of benzene.

Remarkably, all of the $4n$ π electron dihydrodiazapentacenes have *positive* ECRE's (see Table 7-1) and thus are stabilized by aromaticity. Since all energetic effects other than aromaticity are cancelled out in the ECRE procedure, the ECRE difference between the $4n+2$ π dihydrodiazapentacenes and their corresponding $4n+2$ π azapentacenes depends only on the different number of Clar rings present and the antiaromaticity of the dihydropyrazine rings of the dihydroazapentacens. Thus, the ECRE difference between **5a**-H₂ (+65.3 kcal/mol) and **5a** (+70.5 kcal/mol) accounts for the antiaromaticity of the dihydropyrazine ring, as both species can have only one Clar ring. Note that this 5.2 kcal/mol destabilization is only half the ECRE (−11.7 kcal/mol) of parent dihydropyrazine, planar-**1**-H₂ (see Table 7-1).

Table 7-1. PWREs and ECREs of the azaacenes (**1** to **7**) and dihydroazaacenes (**1**-H₂ to **7**). All BLW data are computed at the B3LYP/6-31G* level.

Cmpd.	PWRE (kcal/mol)	ECRE (kcal/mol)
1	59.8	+30.0
1 -H ₂	50.3	-1.1
planar- 1 -H ₂	56.9	-11.7
2	110.7	+48.8
planar- 2 -H ₂	123.8	+20.2
3a	156.5	+58.5
planar- 3a -H ₂	178.8	+38.7
3b	154.4	+59.2
planar- 3b -H ₂	190.9	+52.3
4a	202.1	+67.8
planar- 4a -H ₂	227.2	+52.0
4b	200.4	+70.1
planar- 4b -H ₂	243.5	+68.4
5a	245.8	+70.5
5a -H ₂	274.2	+65.3
5b	242.5	+70.1
5b -H ₂	291.3	+82.5
5c	242.1	+76.7
5c -H ₂	296.1	+84.5

By contrast, both **5b**-H₂ and **5c**-H₂ have *more positive* ECRE values (ca 10 kcal/mol) than their 4n+2 π **5b** and **5c** counterparts (see Table 7-1) and thus are more aromatic! Both **5b**-H₂ and **5c**-H₂ benefit from having two (instead of one) Clar rings, although they also suffer from the antiaromaticity of their dihydropyrazine rings (ca. 5 kcal/mol). Thus, the Clar stabilization for **5b**-H₂ and **5c**-H₂ is about 15 kcal/mol (ca 3 kcal/mol per ring). This may be compared to the ECRE per ring difference (2.9 kcal/mol) between phenanthrene (165.2 kcal/mol, two Clar rings) and anthracene (157.5 kcal/mol, one Clar ring).

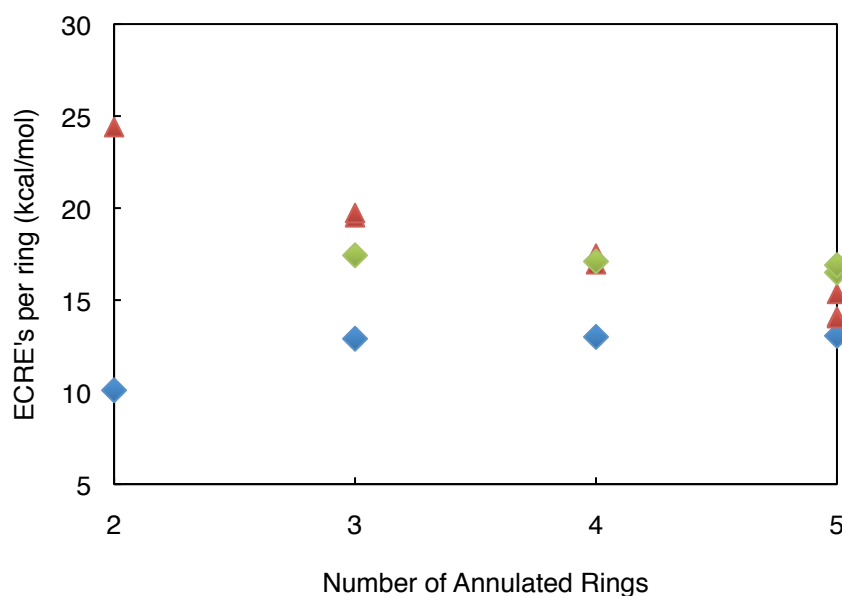


Figure 7-5. Extra cyclic resonance energies (ECRE's) per ring vs. the number of annulated rings (N = 2 to 5) for dihydroazaacenes (**2**-H₂ to **5(a-c)**-H₂, blue and green rhomboids) and diazaacenes (**2** to **5(a-c)**, red triangles). The 1,4-dihydroazaacenes (**2**-H₂, **3a**-H₂, **4a**-H₂ and **5a**-H₂, blue rhomboids) can have only one Clar ring, and thus have less ECRE per ring compared to their isomers (**3b**-H₂, **4b**-H₂ and **5(b-c)**-H₂, green rhomboids) with two Clar rings. All BLW data are computed at the B3LYP/6-31G* level.

The ECRE per ring of the diazaacenes (Figure 7-5, red triangles) decrease linearly across the series (N=1 to N=5), as expected for the acenes,¹⁰ since larger $4n+2$ π systems have less aromatic stabilization per ring. The positions of the pyrazine rings do not influence the aromaticity of these species significantly. However, the ECRE per ring of the $4n$ π dihydroazadiacenes are similar for N = 3, 4 and 5, but depend on the positions of the dihydropyrazine rings. The **b** and **c** isomers have greater ECRE's (Figure 7-5, green rhomboids) than their 1,4-dihydro relatives (**a** isomers, Figure 7-5, blue rhomboids), since they can have two (instead of one) Clar rings, and thus are more aromatic.

Remarkably, the interspersed 8π electron dihydropyrazine ring of the dihydrodiazapentacenes **5(a-c)-H₂** is not destabilized by antiaromaticity appreciably, but it is stabilized by its ethenamine conjugations and its placement results in a greater number of Clar rings for **5b-H₂** and **5c-H₂**.

7.6 NUCLEUS INDEPENDENT CHEMICAL SHIFTS

We evaluated NICS for **6**, **6-H₂**, **8** and planar-**8-H₂** employing the localized molecular orbital (LMO) NICS with the most sophisticated NICS _{π zz} index (see Methods).^{26c, 26d} NICS points were computed at each of the individual heavy atom ring centers of the polycyclic compounds. The LMO approach separates the total shielding of the molecule into the localized molecular orbital contributions of bonds, lone pairs and core electrons,²⁹ and thus are especially useful for evaluating the aromaticities of the individual rings of polycyclic aromatic compounds, since they can distinguish the *local* and *remote* contributions of the π system to a specific ring. *Local* NICS(0) _{π zz} values include only the contributions of the double bonds and lone pairs that are directly associated with the designated ring, while the *remote* NICS(0) _{π zz} values include only

those that are not directly involved. The *total* NICS(0)_{πzz} incorporates all of the individual LMO contributions (both *local* and *remote* NICS(0)_{πzz}) and characterizes the aromaticity of the designated ring. The overall aromaticity of the molecule is evaluated by the *total* NICS(0)_{πzz} sums (ΣNICS(0)_{πzz}) of all of the rings.

As expected by their 4n+2 π electrons count, both **6** and **8** are aromatic and have large diatropic *total* ΣNICS(0)_{πzz} values (−182.3 ppm for **6** and −183.2 ppm for **8**) (see Figure 7-6). Note that the replacement of the four Ns in **6** has very little effect on its aromaticity, as compared to **8**. As shown in Figure 7-3, the *local* NICS(0)_{πzz} of the individual benzenoid rings are largely diatropic and do not differ much from the *total* NICS(0)_{πzz} values (see Figure 7-6). The central Clar rings (ring C) of both **6** and **8** have the most negative *total* NICS(0)_{πzz} values, and are the most aromatic (see Figure 6-6).³⁰ This is in line with Fowler's ring current plots of the linear acenes, which show diatropic current density concentration towards the central ring.³¹ Thus, the *remote* NICS(0)_{πzz} values are small for the outer ring (ring A), but slightly diatropic for the inner rings (rings B and C).

Planar-**8**-H₂ also is overall aromatic (*total* ΣNICS(0)_{πzz} = −136.0 ppm), but less so than **6** and **8** as it involves a non-aromatic cyclohexadiene ring (ring B; *total* NICS(0)_{πzz} = +6.5 ppm) (see Figure 7-6, bottom). Ring B reduces the global aromaticity of planar-**8**-H₂, but has very little effect on the aromaticities of its adjacent benzenoid rings. Thus, all of the rings have small *remote* NICS(0)_{πzz} values. By contrast, the aromaticity of **6**-H₂ (*total* ΣNICS(0)_{πzz} = −68.4 ppm) is greatly reduced by the delocalized paratropic contribution of ring B. Note the significant *remote* NICS(0)_{πzz} of rings A (+14.0 ppm) and C (+8.8 ppm) (see Figure 7-6). However, the remote contributions of the benzenoid rings to ring B is rather small (*remote* NICS(0)_{πzz} = +4.4 ppm, Figure 7-6).

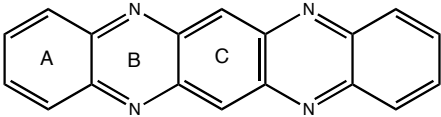
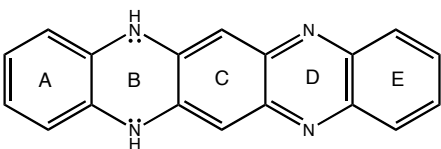
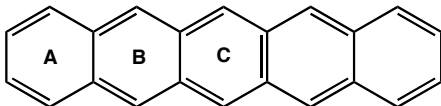
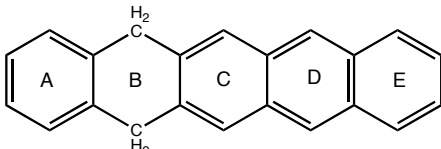
						6
Remote	-2.9	-5.5	-5.0	-	-	$\Sigma \text{NICS}(0)_{\pi_{zz}} = -18.8$
Local	-24.9	-34.8	-41.1	-	-	$\Sigma \text{NICS}(0)_{\pi_{zz}} = -163.5$
Total	-27.8	-40.3	-46.1	-	-	$\Sigma \text{NICS}(0)_{\pi_{zz}} = -182.3$
						6-H ₂
Remote	+14.0	+4.4	+8.8	+10.1	+3.0	$\Sigma \text{NICS}(0)_{\pi_{zz}} = +40.3$
Local	-34.4	+18.6	-23.3	-36.5	-33.1	$\Sigma \text{NICS}(0)_{\pi_{zz}} = -108.7$
Total	-20.4	+23.0	-14.5	-26.4	-30.1	$\Sigma \text{NICS}(0)_{\pi_{zz}} = -68.4$
						8
Remote	-0.7	-4.3	-4.7	-	-	$\Sigma \text{NICS}(0)_{\pi_{zz}} = -14.7$
Local	-26.9	-36.9	-40.9	-	-	$\Sigma \text{NICS}(0)_{\pi_{zz}} = -168.5$
Total	-27.6	-41.2	-45.6	-	-	$\Sigma \text{NICS}(0)_{\pi_{zz}} = -183.2$
						planar-8-H ₂
Remote	+1.0	-2.4	-1.3	-2.2	-1.4	$\Sigma \text{NICS}(0)_{\pi_{zz}} = -6.3$
Local	-35.4	+8.9	-33.1	-39.6	-30.5	$\Sigma \text{NICS}(0)_{\pi_{zz}} = -129.7$
Total	-34.4	+6.5	-34.4	-41.8	-31.9	$\Sigma \text{NICS}(0)_{\pi_{zz}} = -136.0$

Figure 7-6. LMO NICS(0)_{π_{zz}} data (computed at the PW91/IGLOIII level) for the individual rings of **6**, **6-H₂**, **8** and planar-**8-H₂**. *Local* refers to NICS(0)_{π_{zz}} values including only π MOs that belong to the designated ring. The *remote* NICS(0)_{π_{zz}} are defined by the π MO contributions that are not directly involved with the designated ring. The *total* NICS(0)_{π_{zz}} incorporates all of the individual LMO contributions. The sums of the *local*, *remote* and *total* NICS(0)_{π_{zz}} values of the individual rings, ΣNICS(0)_{π_{zz}}, are presented at the end of each corresponding row.

Remarkably, the diatropic contributions of the benzenoid rings are localized, but the paratropicity of the 8π electron dihydropyrazine ring is delocalized and experienced throughout the system.^{32–33} The Clar rings (rings A and D for both **6**-H₂ and planar-**8**-H₂, ring C for **6** and **8**) are distinguished by their more negative *local* and *total* NICS(0) _{π_{zz}} values compared to their adjacent benzenoid rings. Note also that the *total* NICS(0) _{π_{zz}} value (+23.0 ppm) for ring B of **6**-H₂ is remarkably less than the *total* NICS(0) _{π_{zz}} of planar-**1**-H₂ (+70.6 ppm). Thus, the dihydropyrazine ring of **6**-H₂ is much less antiaromatic than planar-**1**-H₂.

Despite having $4n$ π electrons, the individual benzenoid rings of dihydrodiazapentacenes display magnetic characteristics of aromaticity. The antiaromaticity of the dihydropyrazine ring is attenuated.³² The behavior of the $[n]$ phenylenes,^{33–35} in which the aromaticity of the benzenoid rings are weakened by the adjacent antiaromatic cyclobutadiene subunits, is similar. The dihydrodiazapentacenes differ, since their ethenamine contributions are strongly stabilizing, independent of their effects on the aromaticity.

7.7 CONCLUSIONS

Our RE and ECRE evaluations of the $4n$ π electron dihydrodiazapentacenes reveal that they are stabilized by aromaticity as well as by the ethenamine conjugations of their dihydropyrazine rings. However, the internal 8π electron dihydropyrazine rings in these $4n$ π electron species are slightly antiaromatic according to our NICS data (Figure 7-6). The dihydrodiazapentacenes with “inner” dihydropyrazine moieties (**5b**-H₂, **5c**-H₂) can have two Clar rings and thus are more aromatic than those with an outer dihydropyrazine ring (**5a**-H₂) as well as the $4n+2$ π electron diazapentacenes (**5a-c**). Like their parent acenes and azaacene derivatives,^{10,13} dihydrodiazacenes are more viable due to the stabilizing ethenamine conjugation.

Dihydrodiazapentacenes are magnetically aromatic overall, although less than their $4n+2$ π counterparts (see Figure 7-6 for numerical values). The dihydrodiazacenes differ from other formal $4n$ π systems like the benzannulated cyclobutadienes, which show antiaromatic properties (magnetic effects, higher energies, etc.). The dihydrodiazapentacenes are different since the stabilizing ethenamine moieties compensate for the $4n$ π electron ring character. Our study rationalizes the long known(!) but puzzling existence of the dihydrodiazapentacenes and provides a conceptual basis for designing larger viable heteroacenes and cyclacenes, with potential applications as organic-thin film transistors.²⁴

7.8 METHODS

All geometries were optimized at the B3LYP/6-311+G** level as implemented in Gaussian98.³⁶ Harmonic vibrational frequencies, computed at the same DFT level, established the character of the stationary points. Both NICS²⁶ and BLW²⁵ were computed employing the planar geometries of all compounds. Although **1**-H₂, **2**-H₂, **3(a-b)**-H₂, **4(a-b)**-H₂, and **8**-H₂ are not planar, their non-planar minima are not much lower in energy; the planarization energies of **1**-H₂ (C_{2v} ; 3.3 kcal/mol lower in energy than D_{2h} form) and **8**-H₂ (C_s ; 2.7 kcal/mol lower in energy than the C_{2v} form) are small, while those of **2**-H₂, **3(a-b)**-H₂ and **4(a-b)**-H₂ are negligible (less than 0.5 kcal/mol). **5(a-c)**-H₂, **6**-H₂, **7**-H₂ and **1-8** all have planar minima.

NICS²⁶ were computed with the individual gauge for localized orbitals (IGLO) method²⁹ (implemented in the deMon NMR program)³⁷ at the PW91/IGLOIII level, employing the Pipek-Mezey localization algorithm.³⁸ We employ most recommended NICS _{π zz} index which extracts the out-of-plane (zz) tensor component of the isotropic NICS and includes only the π MO

contributions.^{26c,26d} Negative NICS(0)_{πzz} values due to diamagnetic shieldings indicate aromaticity. Positive NICS(0)_{πzz} values due to paramagnetic shieldings indicate antiaromaticity.

Both the RE and the ECRE were computed employing Mo's *ab initio* valence bond (VB) based block localized wavefunction (BLW) method.²⁵ All BLW computations were performed at the B3LYP/6-31G* DFT level^{25h} as implemented in the GAMESS R5 version.³⁹ The BLW method preserves the concepts of VB theory, but is more efficient, especially for studying the conjugations and aromaticities of large systems, due to its molecular orbital (MO)-based computations.²⁵

BLW can compute RE's directly without recourse to reference compounds, by comparing the total energy of the fully delocalized structure (completely optimized employing regular canonical molecular orbitals) to its most stable hypothetical resonance structure, optimized following the imposed constraints. The latter is optimized employing BLW orbitals,²⁵ constructed by partitioning all the electrons and basis functions into several subspaces to form sets of localized MO's, in which orbitals of the same subspaces are mutually orthogonal but those of different subspaces overlap freely. This procedure "disables" the intramolecular interactions among the selected subgroups and gives the total energy of the hypothetical localized structure.²⁵ The ECRE's are derived from the RE's of monocyclic or polycyclic aromatic compounds by comparison with acyclic conjugated references with the same number and type of conjugation (see below).⁴⁰

Note that RE's and ECRE's are conceptually different. The ECRE measures the extra stabilization (or destabilization) associated with aromaticity (or antiaromaticity),²⁸ but the RE measures the overall π conjugation stabilization, which *includes* the energetic consequences related to aromaticity and antiaromaticity.^{25,27} We adopt the Pauling-Wheland resonance energy

definition, defined as the total energy difference between the fully delocalized conjugated compound and that of its most stable resonance contributor.²⁷ By definition, the RE's are always positive, but the ECRE's can be either positive or negative. Positive ECRE's indicate aromaticity and negative ECRE's indicate antiaromaticity. ECRE's of non-aromatic systems are close to zero.

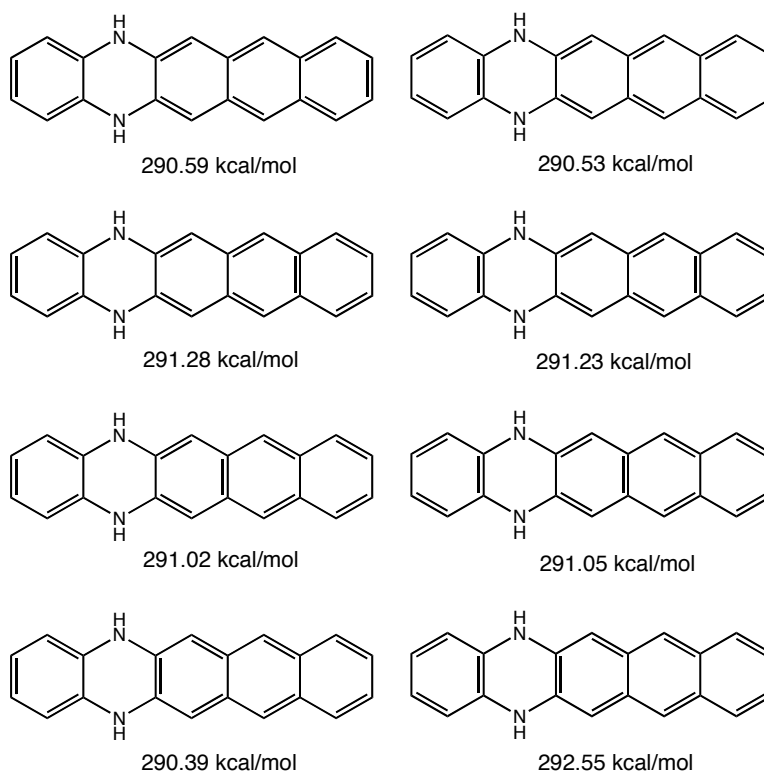
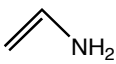
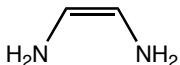
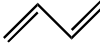
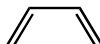
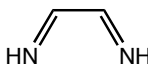
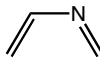
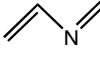



Figure 7-7. Different PWRE values of various BLW localizations for **5b-H₂**.

As polycyclic compounds can have several different resonance contributors, different localization schemes can be applied. However, we select a BLW localization scheme for each of the compounds based on the natural bond length alternations of their perimeter; C–C bonds longer than 1.40 Å are assigned a single bond, those that are less than 1.40 Å are assigned double bonds, the remaining double bonds are added to appropriate positions to complete the

conjugation. While other BLW localization schemes are possible, their RE values are nearly identical to those based on the scheme defined here (see **5b**-H₂ example, Figure 7-7). Based on the selected BLW localization scheme, the Clar rings are assigned to the sextet rings (with three double bonds within a ring). When two adjacent sextet rings share a common double bond, the Clar ring is assigned to the one with smaller bond length alternation around the ring.

Table 7-2. PWREs of acyclic references (**9-14**) used for evaluating ECRE. All BLW data are computed at the B3LYP/6-31G* level.

Compounds	Structures	PWRE (kcal/mol)
9		+16.0
Planar- 9		+20.0
10		+25.7
Planar- 10		+34.3
Anti- 11		+12.2
Syn- 11		+10.7
Avg- 11	(Anti-10 + Syn-10)/2	+11.5
12		+7.8
Syn- 13		+11.0
Anti- 13		+13.5
Avg- 14	(2 × Planar-8 + Planar-9)/2	+37.2
15		+11.2

The ECRE's of the dihydrodiazacenes and diazacenes are evaluated by their RE's minus the RE sums of appropriate number and types of acyclic conjugation references, which are

selected based on the specific BLW localization scheme applied for each of the polycyclic compounds (see Figure 7-7).^{28,40} For benzenoid rings, each Clar ring is assigned three syn butadienes (**syn-11**); the Kekule rings are assigned 1 syn and two anti butadienes, but 1 syn and two “averages” (**avg-11**, the averaged RE of syn and anti butadiene) for those adjacent to a Clar ring. The butadiene units that interact with the Clar rings are neither syn nor anti, but are averaged. This removes ambiguities in selecting appropriate acyclic references.⁴⁰

For the dihydropyrazine moieties, the choice of acyclic references depend on the positions of the dihydro rings: those with two adjacent Kekule rings are assigned four ethenamines, but those with only one adjacent kekule ring are assigned two ethenamines and one diaminoethylene. When two ethenamines interact with an adjacent Clar ring, they are taken as an average between two ethenamines and one diaminoethylene (**avg-14**). On this basis, all energetic effects other than aromaticity and antiaromaticity are cancelled out in the ECRE procedure. Thus, **5b-H₂** (RE = 291.3 kcal/mol, Table 7-1) has eight **syn-11**, four **avg-11**, two **9** and two **avg-14** conjugation units (see Table 7-2). The resulting ECRE value derived for **5b-H₂**, based on the REs of these acyclic references, is 82.5 kcal/mol (Table 7-1).

7.9 REFERENCES

1. Fischer, O.; Hepp, E. *Chem. Ber.* **1890**, *23*, 2789-2798
2. Fischer, O.; Hepp, E. *Chem. Ber.* **1900**, *33*, 1485-1498.
3. Sawtschenko, L.; Jobst, K.; Neudeck, A.; Dunsch, L. *Electrochim. Acta* **1996**, *41*, 123-131.
4. Hinsberg, O. *Liebigs Annalen der Chemie*, **1901**, *319*, 257-286.
5. Badger, G. M.; Pettit, R. *J. Chem. Soc.* **1951**, *73*, 3211-3215.
6. Miao, Q.; Nguyen, T. Q.; Someya, T.; Blanchet, G. B.; Nuckolls, C. *J. Am. Chem. Soc.* **2003**, *125*, 10284-10287.
7. Seillan, C.; Brisset, H.; Siri, O. *Org. Lett.* **2008**, *10*, 4013-4016.
8. a) Dutt, S. *J. Chem. Soc.* **1926**, 1171-1184; b) Wudl, F.; Koutenis, P. A.; Weitz, A.; Ma, B.; Strassner, T.; Houk, K. N.; Khan, S. I. *Pure Appl. Chem.* **1999**, *71*, 295-302.
9. a) Miao, S.; Appleton, A. L.; Berger, N.; Barlow, S.; Marder, S. R.; Hardcastle, K. I.; Bunz U. H. F. *Chem. Eur. J.* **2009**, *15*, 4990-4993; b) Kummer, F.; Zimmermann, H. *Ber. Bunsen Ges. Phys. Chem.* **1967**, *71*, 1119-1127.
10. Moran, D.; Stahl, F.; Bettinger, H. F.; Schaefer, H. F.; Schleyer, P. v. R. *J. Am. Chem. Soc.*, **2003**, *125*, 6746-6752.
11. Herwig, P. T.; Müllen, K. *Adv. Mater.* **1999**, *11*, 480-484.
12. Schleyer, P. v. R.; Manoharan, M.; Jiao, H. J.; Stahl, F. *Org. Lett.* **2001**, *3*, 3643-3646.
13. Bendikov, M.; Duong, H. M.; Starkey, K.; Houk, K. N.; Carter, E. A.; Wudl, F. *J. Am. Chem. Soc.* **2004**, *126*, 7416-7417.
14. Perepichka, D. F.; Bendikov, M.; Meng, H.; Wudl, F. *J. Am. Chem. Soc.* **2003**, *125*, 10190-10191.

15. Payne, M. M.; Parkin, S. R.; Anthony, J. E. *J. Am. Chem. Soc.* **2005**, *127*, 8028-8029.
16. Payne, M. M.; Delcamp, J. H.; Parkin, S. R.; Anthony, J. E. *Org. Lett.* **2004**, *6*, 1609-1612.
17. Anthony, J. E.; Brooks, J. S.; Eaton, D. L.; Parkin, S. R. *J. Am. Chem. Soc.* **2001**, *123*, 9482-9483.
18. Odom, S. A.; Parkin, S. R.; Anthony J. E. *Org. Lett.* **2003**, *5*, 4245-4248.
19. a) Clar, E. *Chem. Ber.* **1949**, *82*, 495-514; b) Clar, E. *The Aromatic Sextet*, Wiley, London, **1972**.
20. Winkler, M.; Houk, K. N. *J. Am. Chem. Soc.* **2007**, *129*, 1805-1815.
21. Tadokoro, M.; Yasuzuka, S.; Nakamura, M.; Shinoda, T.; Tatenuma, T.; Mitsumi, M.; Ozawa, Y.; Toriumi, K.; Yoshino, H.; Shiomi, D.; Sato, K.; Takui, T.; Mori, T.; Murata, K. *Angew. Chem. Int. Ed.* **2006**, *45*, 5144-5147.
22. Jenekhe, S. A. *Macromolecules* **1991**, *24*, 1-10.
23. Nishida, J.; Naraso; Murai, S.; Fujiwara, E.; Tada, H.; Tomura, M.; Yamashita, Y. *Org Lett.* **2004**, *6*, 2007-2010.
24. a) Nelson, S. F.; Lin, Y. Y.; Gundlach, D. J.; Jackson, T. N. *Appl. Phys. Lett.* **1998**, *72*, 1854-1856; b) Dimitrakopoulos, C. D.; Malenfant, P. R. L. *Adv. Mater.* **2002**, *14*, 99-117; c) Dimitrakopoulos, C. D.; Mascaró D. J. *IBM J. Res. Development* **2001**, *45*, 11-27; d) Reese, C.; Bao, Z. N. *J. Mater. Chem.* **2006**, *16*, 329-333; e) Roberson, L. B.; Kowalik, J.; Tolbert, L. M.; Kloc, C.; Zeis, R.; Chi, X. L.; Fleming, R.; Wilkins, C. *J. Am. Chem. Soc.* **2005**, *127*, 3069-3075.
25. a) Mo, Y.; Peyrimhoff, S. D. *J. Chem. Phys.* **1998**, *109*, 1687-1697; b) Mo, Y.; Zhang, Y.; Gao, J. *J. Am. Chem. Soc.* **1999**, *121*, 5737-5742; c) Mo, Y.; Subramanian, G.;

- Ferguson, D. M.; Gao, J. *Am. Chem. Soc.* **2002**, *124*, 4832-4837; d) Mo, Y.; Wu, W.; Song, L.; Lin, M.; Zhang, Q.; Gao, J. *Angew. Chem. Int. Ed.* **2004**, *43*, 1986-1990; e) Mo, Y. *J. Chem. Phys.* **2003**, *119*, 1300-1306; f) Mo, Y.; Song, L.; Wu, W.; Zhang, Q. *J. Am. Chem. Soc.* **2004**, *126*, 3974-3982; g) Mo, Y. *J. Org. Chem.* **2004**, *69*, 5563-5567; h) Mo, Y.; Song, L.; Lin, Y. *J. Phys. Chem. A* **2007**, *111*, 8291-8301.
26. a) Schleyer, P. v. R.; Maerker, C.; Dransfeld, A.; Jiao, H. J.; Hommes, N. J. r. V. *J. Am. Chem. Soc.* **1996**, *118*, 6317-6318; b) Schleyer, P. v. R.; Jiao, H. J.; Hommes, N. J. r. V. E.; Malkin, V.; G. Malkina, O. L. *J. Am. Chem. Soc.* **1997**, *119*, 12669-12670; c) Corminboeuf, C.; Heine, T.; Seifert, G.; Schleyer, P. v. R. *Phys. Chem. Chem. Phys.* **2004**, *6*, 273-276; d) Fallah-Bagher-Shaidaei, H.; Wannere, C. S.; Corminboeuf, C.; Puchta, R.; Schleyer, P. v. R. *Org. Lett.* **2006**, *8*, 863-866; e) Chen, Z.; Wannere, C. S.; Corminboeuf, C.; Puchta, R.; Schleyer, P. v. R. *Chem. Rev.* **2005**, *105*, 3842-3888.
27. Pauling, L. C.; Wheland, G. W. *J. Chem. Phys.* **1933**, *1*, 362-374; b) Pauling, L. C. *The Nature of the Chemical Bond*, 3rd ed., Cornell University Press, Ithaca, NY, **1960**; c) Wheland, G. W. *J. Am. Chem. Soc.* **1941**, *85*, 431-434; d) G. W. Wheland, *The Theory of Resonance*, Wiley, New York, **1944**; e) Wheland, G. W. *Resonance in Organic Chemistry*, Wiley, New York, **1955**.
28. Mo, Y. Schleyer, P. v. R. *Chem. Eur. J.* **2006**, *12*, 2009-2020.
29. Schleyer, P. v. R.; Manoharan, M.; Wang, Z. X.; Kiran, B.; Jiao, H.; Puchta, R.; Hommes, N. J. R. v. E. *Org. Lett.* **2001**, *3*, 2465-2468.
30. Schleyer, P. v. R.; Manoharan, M.; Jiao, H.; Stahl, F. *Org. Lett.* **2001**, *3*, 3643-3646.

31. a) Steiner, E.; Fowler, P. W. *Int. J. Quant. Chem.* **1996**, *60*, 609-616; b) Steiner, E.; Fowler, P. W. *J. Phys. Chem. A* **2001**, *105*, 9553-9562; c) Steiner, E.; Fowler, P. W. Havenith, R. W. A. *J. Phys. Chem. A* **2002**, *106*, 7048-7056.
32. a) Miao, S.; Schleyer, P. v. R.; Wu, J. I.; Hardcastle, K. I.; Bunz, U. H. F. *Org. Lett.* **2007**, *9*, 1073-1076; b) Miao, S.; Brombosz, S. M.; Schleyer, P. v. R.; Wu, J. I.; Barlow, S.; Marder, S. R.; Hardcastle, K. I.; Bunz, U. H. F. *J. Am. Chem. Soc.* **2008**, *130*, 7339-7344.
33. a) Diercks, R.; Vollhardt, K. P. C. *J. Am. Chem. Soc.* **1986**, *108*, 3150-3152; b) Holmes, D.; Kumaraswamy, S.; Matzger, A. J.; Vollhardt, K. P. C. *Chemistry Eur. J.* **1999**, *5*, 3399-3412.
34. Maksic, Z. B.; Kovacek, D.; Eckert-Maksic, M.; Böckmann, M.; Klessinger, M. *J. Phys. Chem.* **1995**, *99*, 6410-6416.
35. Schulman, J. M.; Disch, R. L.; Jiao, H.; Schleyer, P. v. R. *J. Phys. Chem. A* **1998**, *102*, 8051-8055.
36. Frisch, M. J.; Trucks, G. W.; Schlegel, H. B.; Scuseria, G. E.; Robb, M. A.; Cheeseman, J. R.; Zakrzewski, V. G.; Montgomery, Jr., J. A.; Stratmann, R. E.; Burant, J. C.; Dapprich, S.; Millam, J. M.; Daniels, A. D.; Kudin, K. N.; Strain, M. C.; Farkas, O.; Tomasi, J.; Barone, V. M.; Cossi, R.; Cammi, B.; Mennucci, C.; Pomelli, C.; Adamo, S.; Clifford, J.; Ochterski, Petersson, G. A.; Ayala, P. Y.; Cui, Q.; Morokuma, K.; Malick, D. K.; Rabuck, A. D.; Raghavachari, K.; Foresman, J. B.; Cioslowski, J.; Ortiz, J. V.; Baboul, A. G.; Stefanov, B. B.; Liu, G.; Liashenko, A.; Piskorz, P.; Komaromi, I.; Gomperts, R.; Martin, R. L.; Fox, D. J.; Keith, T.; Al-Laham, M. A.; Peng, C. Y.; Nanayakkara, A.; Challacombe, M.; Gill, P. M. W.; Johnson, B.; Chen, W.; Wong, M. W.; Andres, J. L.;

- Gonzalez, C.; Head-Gordon, M.; Replogle, E. S.; Pople, J. A. Gaussian, Inc., Pittsburgh PA, 1998.
37. Malkin, V. G.; Malkina, O. L.; Casida, M. E.; Salahub, D. R. *J. Am. Chem. Soc.* **1994**, *116*, 5898-5908.
38. Pipek, J.; Mezey, P. J. *J. Chem. Phys.* **1989**, *90*, 4916-4927.
39. Gamess (Version R5): Schmidt, M. W.; Baldridge, K. K.; Boatz, J. A.; Elbert, S. T.; Gordon, M. S.; Jensen, J. H.; Koseki, S.; Matsunaga, N.; Nguyen, K. A.; Su, S. J.; Windus, T. L.; Dupuis, M.; Montgomery, J. A. *J. Comput. Chem.* **1993**, *14*, 1347-1363.
40. Wu, J. I.; Dobrowolski, M. A.; Cyrański, M. K.; Merner, B. L.; Bodwell, G. J.; Schleyer P. v. R. *Mol. Phys.* **2009**, *107*, 1177-1186.

CHAPTER 8

CONCLUSIONS

Although much of our current view of even the simplest organic molecules and representative chemical debates continue to change, strategic applications of computational chemistry provide new chemical insight and can be used to critically examine chemical knowledge. Strain, hyperconjugation, conjugation, and aromaticity are highly *transferable* chemical properties that govern the structures and energies of hydrocarbons cooperatively.

The generality of our findings have broad chemical impact. For example, the lengths of typical C–C, C=C, and C–H bonds are the result of blends of electron delocalization effects, hybridization changes, strain, and other coexisting effects. Hence, Dewar’s early proposal that hybridization contributes to the shortening of C–C bonds, just as they do for C–H bonds, for sp^3 , sp^2 , and sp hybridized carbons, is only part of the story. While hyperconjugative and conjugative interactions across C–C single bonds (as well as C=C double bonds) favor bond shortening (π -bonds, in particular prefer shorter optimal bond distances), this is often offset by increased Pauli repulsion between vicinal groups and “ σ -bond length strain,” which results from compressed or elongated σ -bonds having less effective orbital overlap. Thus, compared to the 1.54 Å C–C bond of ethane, the C–C σ -bonds of ethylene, benzene, and butadiene (both the central C–C bond and σ -bonds involved in the two C \equiv C triple bonds) all suffer from “ σ -bond length strain”

While the understanding of molecular structure and energy still is overly “ π -focused,” we reinforce Mulliken’s early authoritative view, that, differences between π conjugation and hyperconjugation among saturated and unsaturated groups only are “quantitative rather than

qualitative.” Although π conjugative stabilizations generally have greater energetic impact, per interaction, hyperconjugative stabilization involving the σ -frameworks of molecules can have comparable overall net energetic contribution, due to their greater numbers of interactions in molecules. For example, cyclopropane benefits from substantial geminal CCC σ -hyperconjugative stabilization; this, instead of σ -aromaticity, contributes to its much lower strain energy in view of the other cycloalkanes. Cyclooctatetraene is far from a model for “unconjugated” cyclic olefins, as the twisted C–C bonds in the D_{2d} form promote “two-fold” double hyperconjugation. For the same reason, macromolecules with highly twisted geometries, as well as those with non-planar π surfaces, e.g. Möbius rings, fullerenes, nanotubes, and proteins, also are expected to benefit from considerable hyperconjugative stabilization. Both π - and σ -electron delocalization stabilize molecules effectively.

Aromaticity is a very robust electronic phenomenon that broadly describes “*the manifestation of electron delocalization in two or three dimensional closed circuits,*” and thus, is not easily quenched by structural (geometric and electronic) distortions. The Clar aromatic π -sextet rule governs the local aromaticity patterns of polycyclic systems; BLW and NICS computations provide quantitative energetic and magnetic evidence for Clar aromaticity. Our work also contributes to the increasing awareness that “aromaticity” is a ground state property, and thus cannot be evaluated by chemical reactivity as well as other two-state properties cannot be used as measures of aromaticity. Linear polycyclic benzenoids have more reactive but more aromatic central rings, while the outer rings are less reactive but less aromatic. We emphasize that aromaticity and antiaromaticity are only “relative” energetic properties that depend on comparisons to specific reference standards, and thus, their presence (or absence) are not always directly correlated to the thermochemical stabilities of organic compounds. Antiaromatic

molecules have net stabilizing π conjugation and are destabilized only “relatively” when their π systems are compared to those of acyclic π conjugated references. The high energy of cyclobutadiene is mostly due to unfavorable geometric features in its σ -framework.

I hope some of the findings presented in this dissertation will stimulate new ways of thinking and teaching about chemistry.

LIST OF PUBLICATIONS

1. Why Cyclooctatetraene is Highly Stabilized: The Importance of “Back and Forth” Double Hyperconjugation, J. I. Wu, Y. Mo, P. v. R. Schleyer, **2011** (Submitted to *Chemistry – A European Journal*).
2. [n]Imperilenes: Stacked [n]Trannulenes Separated by Planar Cycloalkane Rings, F. A. Shakib, M. R. Momeni, J. I. Wu, P. v. R. Schleyer, Z. Azizi, M. Ghambarian, **2011** (Submitted to *Organic Letters*)
3. Aromaticity in Group-14 Homologues of the Cyclopropenylum Cation, I. Fernandez, M. Duvall, J. I. Wu, QS Li, P. v. R. Schleyer, G. Frenking, *Chem. Eur. J.* **2011**, *17*, 2215-2224.
4. Star-Like Aluminium-Carbon Aromatic Species, YB Wu, JL Jiang, HG Lu, ZX Wang, N. Perez-Peralta, R. Islas, M. Contreras, G. Merino, J. I. Wu, P. v. R. Schleyer, *Chem. Eur. J.* **2011**, *17*, 714-719.
5. A Study of Aromatic Three Membered Rings, HJ Wang, P. v. R. Schleyer, J. I. Wu, Y. Wang, H. J. Wang, *Int. J. Quant. Chem.* **2011**, *111*, 1031-1038.
6. Consistent Evaluation of Aromaticity in Methylenecyclopropene Analogs, Y. Wang, I. Fernandez, M. Duvall, J. I. Wu, QS Li, P. v. R. Schleyer, G. Frenking, *J. Org. Chem.* **2010**, *75*, 8252-8257.
7. The Aromaticity and Relative Stabilities of Azines, Y. Wang, J. I. Wu, QS Li, P. v. R. Schleyer, *Org. Lett.* **2010**, *12*, 4824-4827.

8. Why are Perfluorocyclobutadiene and Some Other (CF)_n Rings Non-Planar? J. I. Wu, F. A. Evangelista, P. v. R. Schleyer, *Org. Lett.* **2010**, *12*, 768-771.
9. Why are Some (CH)₄X₆ and (CH₂)₆X₄ Polyheteroadamantanes So Stable? Y. Wang, J. I. Wu, QS Li, P. v. R. Schleyer, *Org. Lett.* **2010**, *12*, 1320-1323.
10. Direct Assessment of Electron Delocalization Using NMR Chemical Shifts, S. N. Steinmann, D. F. Jana, J. I. Wu, P. v. R. Schleyer, Y. Mo, C. Corminboeuf, *Angew. Chem. Int. Ed.* **2009** *121*, 10012-10017.
11. Electrophile Affinity: a Reactivity Measure for Aromatic Substitution, G. Koleva, B. Galabov, J. I. Wu, H. F. Schaefer III, P. v. R. Schleyer, *J. Am. Chem. Soc.* **2009**, *131*, 14722-14727.
12. Is Cyclopropane Really the sigma-Aromatic Paradigm? W. Wu, B. Ma, J. I. Wu, P. v. R. Schleyer, Y. Mo, *Chem. Eur. J.* **2009**, *15*, 9730-9736.
13. Ab initio Study of the Geometry, Stability and Aromaticity of Cyclic S₂N₃⁺ Cation Isomers and Their Isoelectronic Analogs, GH Zhang, YF Zhao, J. I. Wu, P. v. R. Schleyer, *Inorg. Chem.* **2009**, *48*, 6773-6780.
14. 4n π Electrons but Stable: N,N-Dihydrodiazapentacenes, J. I. Wu, C. S. Wannere, Y. Mo, P. v. R. Schleyer, U. H. F. Bunz, *J. Org. Chem.* **2009**, *74*, 4343-4349.
15. The Effect of Perfluorination on the Aromaticity of Benzene and Heterocyclic Six-Membered Rings, J. I. Wu, F. G. Pühlhofer, P. v. R. Schleyer, R. Puchta, B. Kiran, M. Mauksch, N. J. R. v. E. Hommes, I. Alkorta, J. Elguero, *J. Phys. Chem. A* **2009**, *113*, 6789-6794.
16. On the Aromatic Stabilization Energy of the 4N π Electron Pyrene, J. I. Wu, M. A. Dobrowolski, M. K. Cyrancki, B. L. Merner, G. J. Bodwell, Y. Mo, P. v. R. Schleyer,

- Mol. Phys.* **2009**, *107*, 1177-1186. (*Special Issue in Honor of Professor Henry F. Schaefer*)
17. Homobenzene: Homoaromaticity and Homoantiaromaticity in Cycloheptatrienes, ZF Chen, H. Jiao, J. I. Wu, R. Herges, S. B. Zhang, P. v. R. Schleyer, *J. Phys. Chem. A.* **2008**, *112*, 10586-10594.
 18. Interplay of π -Electron Delocalization and Strain in [n](2,7)Pyrenophanes, M. A. Dobrowolski, M. K. Cyranski, B. L. Merner, G. J. Bodwell, J. I. Wu, P. v. R. Schleyer, *J. Org. Chem.* **2008**, *27*, 8001-8009.
 19. Are N,N-Dihydrodiazatetracene Derivatives Antiaromatic? S. Miao, S. M. Brombosz, P. v. R. Schleyer, J. I. Wu, S. Barlow, S. R. Marder, K. I. Hardcastle, U. H. F. Bunz, *J. Am. Chem. Soc.* **2008**, *130*, 7339-7344.
 20. A Thiadiazole-Fused N,N-Dihydroquinoxaline: Antiaromatic but Isolable S. Miao, P. v. R. Schleyer, J. I. Wu, K. I. Hardcastle, U. H. F. Bunz, *Org. Lett.* **2007**, *9*, 1073-7076.